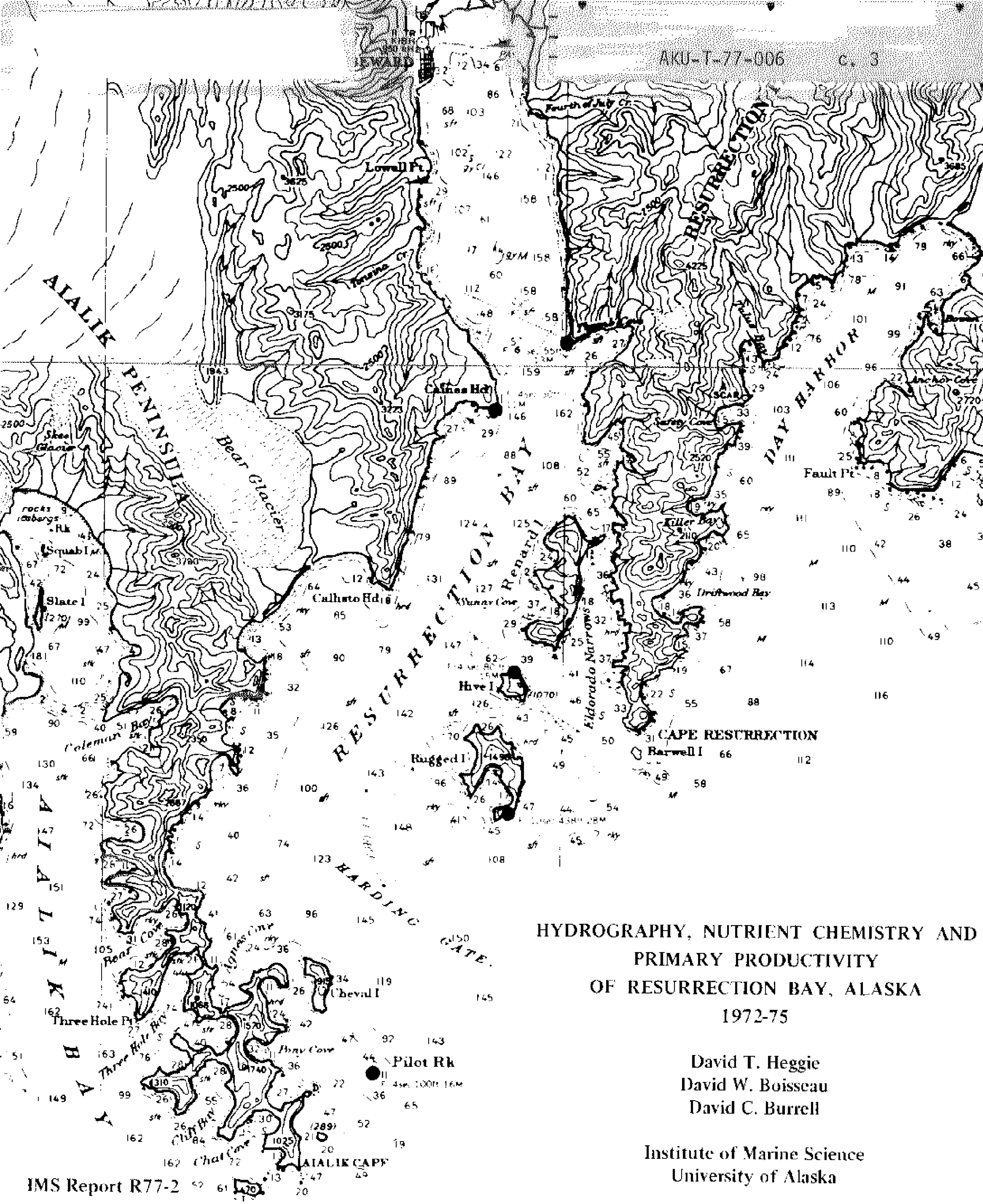

HYDROGRAPHY, NUTRIENT CHEMISTRY AND PRIMARY PRODUCTIVITY OF RESURRECTION BAY, ALASKA 1972-75

David T. Heggie
David W. Boisseau
David C. Burrell

Institute of Marine Science
University of Alaska

IMS Report R77-2
Alaska Sea Grant Report 77-9

Institute of Marine Science
University of Alaska
Fairbanks, Alaska 99701

HYDROGRAPHY, NUTRIENT CHEMISTRY AND PRIMARY PRODUCTIVITY OF RESURRECTION BAY, ALASKA

1972-75

David T. Heggie, David W. Boisseau, and David C. Burrell

IMS Report R77-2
Alaska Sea Grant Report 77-9

J. R. Moore, Director
July 1977

ABSTRACT

The waters of Resurrection Bay are most stratified during the summer months of June-September. Exchange of water between the fjord and the Gulf of Alaska takes place principally below 150-m depth, beginning about May or June and being complete by October. As a result of the relaxation of winter downwelling conditions at the coastline, dense (σ_t>26.00) water advected onto the adjacent continental shelf in summer, penetrates the inner fjord across the sill to displace the relict bottom waters upward and out of the fjord. During the winter (October-April) the dense water advected into the deep inner basin exchanges predominately by vertical eddy mixing with less dense waters above sill depth. During 1974-75 daily rates of primary productivity varied between 2978 mg C m^{-2} d^{-1} in summer (June) and 8 mg C m^{-2} d^{-1} in winter (January). Annual net productivity in the fjord was about 260 g C m^{-2}. Seasonal and spatial variations of nutrients (nitrogen, phosphorus and silicon) show removal from surface waters during the summer by plant growth. Phytoplankton productivity appears to be limited in the summer by NO_3-N supply. A flux of remineralized nutrients is evident year round across the sediment-seawater interface. The frequency of bottom water renewals is sufficient to prevent anoxic conditions developing in the water column of this fjord.

ACKNOWLEDGEMENTS

This publication is the result of research sponsored by the Energy Research and Development Administration (Contract No. E(45-1)-229, TA No. 1), the National Science Foundation (Grant No. G9 37963), the Alaska Sea Grant Program under Grant No. 04-6-158-44039 from NOAA Office of Sea Grant, Department of Commerce and by the University of Alaska with funds appropriated by the State of Alaska.

All cruises were conducted aboard the R/V *Acona* and the assistance of the ship's crew is acknowledged, especially Ken Turner, Robert Ashley, and Ray Braggington. E. R. (Dolly) Dieter participated in most of the cruises and her assistance in cruise preparation, and skill in the collection of much of the hydrographic data is gratefully acknowledged. The advice and direction of Dr. J. Goering and the assistance of Dr. D. Nelson are greatly appreciated. The facilities of the Institute of Marine Science, Seward Station, under the direction of Dr. R. Nevé were used extensively during cruises into Resurrection Bay. We wish to thank other investigators, who have worked in this fjord, especially Drs. T. Royer, C. Hoskins and R. Nevé who have provided some of their ship time to collect data from Resurrection Bay. Rosemary Hobson did much of the computer processing of these data, David Nebert assisted with the deployment of current meters, Robert Clasby (Seward Station) analysed the samples collected for nutrient concentrations. Jim Hendee assisted with the reduction of much of the nutrient data and original drafting of the figures. Judith Henshaw and Ana Lea Vincent drafted the final figures.

TABLE OF CONTENTS

TABLE OF CONTENTS (continued)

LIST OF FIGURES

LIST OF FIGURES (continued)

LIST OF FIGURES (continued)

LIST OF FIGURES (continued)

LIST OF APPENDIX FIGURES

LIST OF TABLES

INTRODUCTION

Alaskan subarctic fjords are relatively recent geologic features, formed by the carving and gouging actions of glaciers and the subsequent rise in sea level that accompanied thawing and glacial recession. Most Alaskan fjords are now glacier free, but several in Glacier Bay and Prince William Sound still have tidewater glaciers at the head of the fjord.

The hydrography, circulation patterns and biological productivity of estuaries are not well understood. The seasonal and spatial variations of salinity and temperature (which determine the density of water) and circulation patterns within fjords would be expected to be dependent upon the relative access of the fjord to the marine source waters, local topography, regional climate and differences in freshwater inputs. The biological productivity of these regions is believed to be controlled principally by available light conditions and the seasonal and spatial variations in concentrations, hence supply, of the major nutrient elements (nitrogen, phosphorus and silicon) to the euphotic zone where plant growth occurs.

Port Valdez, the terminus of the Trans-Alaskan Oil Pipeline, is to date the most comprehensively studied Alaskan fjord (Hood *et al.*, 1973). Other, more specific studies, directed principally at an understanding of circulation patterns, have been presented by McAllister *et al.* (1959). Nebert (1972), Reeburgh *et al.* (1976), Muench and Schmidt (1975) and Schmidt (1977). Muench and Heggie (1977) have discussed the general characteristics, timing, frequency and extent of the deep water exchange of several Alaskan fjords, with respect to the seasonal variations of the fjord source waters, and the fjord sill depth.

Cruises were conducted to Resurrection Bay at approximately monthly intervals between November 1972 and May 1975. Inclusion here of all the data from these 24 cruises would be too voluminous, therefore only general representations of the hydrography, nutrient chemistry, and phytoplankton productivity are presented and discussed. Some of these data were of specific interest to one of us (Heggie, 1977), who has examined the exchange of deep water between the fjord and the Gulf of Alaska. Because of the latter's significance as a control on the circulation within the fjord, and on the supply of nutrients (nitrogen, phosphorus and silicon) to the fjord, the exchange (noted above) is discussed in some detail.

A key index to the data collected from Resurrection Bay is given in Tables 1 and 2. These data are on file at the Institute of Marine Science, University of Alaska, Fairbanks, Alaska, and the National Oceanographic Data Center, Washington, D.C.

STUDY AREA

Resurrection Bay is a fjord estuary located on the Kenai Peninsula of southcentral Alaska (Fig. 1). The fjord is approximately 30 km long, 6 to 8 km wide, and oriented in a north-south direction. An inner basin, 290 m deep, is separated from the outer reaches of the fjord by a sill at approximately 185 m depth located south of Caines Head. The outer fjord is approximately 250 m deep and opens directly onto the Gulf of Alaska. A longitudinal bathymetry profile is shown in Figure 2. Cross-channel profiles of the bathymetry at several stations in the fjord are shown in Figures 3 and 4.

The continental shelf area in the north-western Gulf of Alaska varies between about 50 km and 110 km in width and shoals to about 175 m approximately 70 km offshore. The fjord is bounded on both sides by mountains of around 1000 m in height. The weather within Resurrection Bay is governed principally by the regional meteorological conditions that exist over the Gulf of Alaska. A low pressure system dominates during the winter months, and longshore winds over the adjacent coastline regions are channelled by the steep mountains axially within the fjord. The predominant wind directions in Resurrection Bay during the winter months are northerly (Fig. 5). (The dominant Aleutian low pressure system in the Gulf of Alaska results in predominating strong east winds over the adjacent continental shelf.) Conversely, during the summer months, because of weak and variable west winds over the adjacent continental shelf, winds within Resurrection Bay are predominantly southerly.

TABLE 1

Resurrection Bay Station Locations

Station	Latitude	Longitude
RES-1	60°06.5'	149°23.8'
RES-2A	60°03.5'	149°24.6'
RES-2	60°03.5'	149°22.3'
RES-2B	60°03.5'	149°21.2'
RES-2.5	60°01.2'	149°21.5'
RES-3	59°58.9'	149°20.5'
RES-4A	59°55.1'	149°26.5'
RES-4	59°54.7'	149°24.5'
RES-4B	59°54.5'	149°23.2'
RES-5	59°50.7'	149°28.0'

TABLE 2

Resurrection Bay Survey: Data Index

ACONA CRUISE	DATE	STATION	STD	HYDRO	OXY	NH_3	PO_4	NO_3	SiO_4	COMMENTS
146	Nov 21-22, 1972	RES-1	X	X	X	-	-	-	-	-
		RES-2	X	X	X	-	X	X	X	No nutrient
		RES-3	X	X	X	-	X	X	X	Data below 250 m
		RES-4	X	X	X	-	X	X	X	-
		RES-5	X	X	X	-	-	X	X	-
148	Dec 4-9, 1972	RES-1	X	X	X	-	-	-	-	-
		RES-2	X	X	X	-	X	X	X	No nutrient
		RES-3	X	X	X	-	X	X	X	Data below 250 m
		RES-4	X	X	X	-	X	X	X	-
		RES-5	X	X	X	-	X	X	X	-
154	Jan 30 & Feb 3, 1972	RES-1	X	X	X	-	-	-	-	-
		RES-2	X	X	X	-	X	X	X	No nutrient
		RES-3	X	X	X	-	X	X	X	Data below 250 m
		RES-4	X	X	X	-	X	X	X	-
		RES-5	X	X	X	-	X	X	X	-
160	Mar 12-13, 1973	RES-1	X	X	X	-	-	-	-	-
		RES-2	X	X	X	-	X	X	X	-
		RES-2.5	X	X	X	-	X	X	X	-
		RES-3	X	X	X	-	X	X	X	-
		RES-4	X	X	X	-	X	X	X	-
		RES-5	X	X	X	-	X	X	X	-
		RES-Nev6	X	X	X	-	-	-	-	60°5.9'149°26.0'
		RES-Nev6	X	X	X	-	-	-	-	60°5.9'149°26.2'
161	Apr 3, 1973	RES-1	-	X	X	-	-	-	-	-
		RES-2	-	X	X	X	X	X	X	-
		RES-2.5	-	X	X	X	X	X	X	-
		RES-3	-	X	X	X	X	X	X	-
		RES-4	-	X	X	X	X	X	X	-
		RES-5	-	X	X	X	X	X	X	-

TABLE 2

Continued

ACONA CRUISE	DATE	STATION	STD	HYDRO	OXY	NH_3	PO_4	NO_3	SiO_4	COMMENTS
163	May 7, 1973	RES-2.5	-	X	X	X	X	X	X	-
		RES-4	-	X	X	X	X	X	X	-
		RES-Nevé	X	X	X	X	X	X	X	60°5.9'149°28.2'
166	May 17-26, 1973	RES-2	-	X	X	X	X	X	X	-
		RES-2.5	X	X	X	X	X	X	X	Hydrographic time series ∿16 hr
		RES-3	-	X	X	-	-	-	-	-
		RES-4	X	X	X	X	X	X	X	-
		RES-5	-	X	X	X	X	X	X	-
		RES-Nevé	X	X	X	X	X	X	X	60°5.9'149°28.2'
171	July 6, 1973	RES-2.5	X	-	-	-	-	-	-	-
		RES-4	X	-	-	-	-	-	-	-
		RES-5	X	-	-	-	-	-	-	-
176	Sept 6-9, 1973	RES-1	X	X	X	X	X	X	X	-
		RES-2	X	X	X	X	X	X	X	-
		RES-2.5	X	X	X	X	X	X	X	Hydrographic time series ∿16 hr
		RES-3	X	X	X	X	X	X	X	N,S. Data incomplete above 150m
		RES-4	X	X	X	X	X	-	-	-
		RES-5	X	X	X	X	X	-	-	-
		RES-Nevé	X	X	X	X	X	X	X	60°5.2'149°26.2'
		RES-Nevé	X	X	-	-	-	-	-	60°5.2'149°26.1'
178	Sept 19-21, 1973	RES-1	-	X	X	X	X	-	-	-
		RES-2	-	X	X	X	X	-	-	-
		RES-2.5	X	X	X	X	X	X	X	-
		RES-3	-	X	X	-	-	-	-	-
		RES-4	X	X	X	X	X	X	X	-
		RES-5	-	X	X	X	-	-	-	-

TABLE 2

Continued

ACONA CRUISE	DATE	STATION	STD	HYDRO	OXY	NH_3	PO_4	NO_3	SiO_4	COMMENTS
180	Oct 9-10, 1973	RES-1	X	X	X	X	X	X	X	-
		RES-2	-	-	X	X	X	X	X	-
		RES-3	X	X	X	X	X	X	X	-
		RES-4	X	X	X	X	X	X	X	-
		RES-5	X	X	X	X	X	X	X	-
		RES-Nevé	X	X	X	X	X	X	X	60°5.8'149°26.0'
182	Nov 16-17, 1973	RES-1	X	X	X	-	X	X	X	-
		RES-2	X	X	X	-	X	X	X	-
		RES-2.5	X	X	X	-	-	X	X	-
		RES-3	X	X	X	-	X	X	X	-
		RES-4	X	X	X	-	-	X	X	-
		RES-5	X	X	X	-	-	-	-	-
		RES-Nevé	X	X	X	-	-	-	-	60°5.8'149°26.0'
183	Dec 14-17, 1973	RES-1	X	X	X	-	X	X	X	-
		RES-2	X	X	X	-	X	X	X	-
		RES-2.5	X	X	X	-	X	X	X	-
		RES-3	X	X	X	-	X	X	X	-
		RES-4	X	X	X	-	X	X	X	-
		RES-5	X	X	X	-	X	X	X	-
		RES-Nevé	X	X	X	-	X	X	X	60°5.8'149°26.0'
186	Mar 27-28, 1974	RES-2.5	-	X	X	X	X	X	X	-
		RES-4	-	X	X	X	X	X	X	-
		RES-5	-	X	X	-	-	-	-	-
187	Apr 20-21, 1974	RES-1	-	X	X	-	-	-	-	-
		RES-2	-	X	X	-	-	-	-	-
		RES-2.5	-	X	X	-	-	-	-	-
		RES-3	-	X	X	-	-	-	-	-
		RES-4	-	X	X	-	-	-	-	-
		RES-5	-	X	X	-	-	-	-	-

TABLE 2

Continued

ACONA CRUISE	DATE	STATION	STD	HYDRO	OXY	NH_3	PO_4	NO_3	SiO_4	COMMENTS
190	June 10, 1974	RES-1	X	X	X	-	-	-	-	-
		RES-2	X	X	X	-	-	-	-	-
		RES-2.5	X	X	X	-	-	-	-	-
		RES-3	X	X	X	-	-	-	-	-
		RES-4	X	X	X	-	-	-	-	-
		RES-5	X	X	X	-	-	-	-	-
192	June 26-28, 1974	RES-4	-	X	X	X	X	X	X	-
		RES-2.5	-	X	X	X	X	X	X	-
195	Jul 24-26, 1974	RES-2	X	-	-	-	-	-	-	-
		RES-2.5	X	X	X	X	X	X	X	-
		RES-3	X	-	-	-	-	-	-	-
		RES-4	X	X	X	X	X	X	X	-
201	Oct 18-20, 1974	RES-2	X	-	-	-	-	-	-	-
		RES-2.5	X	X	X	X	X	X	X	-
		RES-3	X	-	-	-	-	-	-	-
		RES-4	X	X	X	X	X	X	X	-
		RES-Nevé	X	X	X	X	X	X	X	60°5.9'149°26.2'
		RES-Nevé	X	X	X	X	X	X	X	60°5.8'149°24.2'
		RES-Nevé	X	X	X	X	X	X	X	60°5.8'149°22.2'
203	Nov 22-26, 1974	RES-2.5	X	X	X	X	X	X	X	-
		RES-4	X	X	X	X	X	X	X	-
		RES-Nevé	-	-	-	-	-	-	-	60°5.8'149°26.3'
		RES-Nevé	-	-	-	-	-	-	-	60°5.8'149°24.2'
204	Jan 21-23, 1975	RES-1	X	X	X	X	X	X	X	-
		RES-2	X	X	X	X	X	X	X	Nutrient data below 200 m is incomplete
		RES-2.5	X	X	X	X	X	X	X	
		RES-3	X	X	X	X	X	X	X	-
		RES-4	X	X	X	X	X	X	X	-
		RES-5	X	X	X	X	X	X	X	-

TABLE 2

Continued

ACONA CRUISE	DATE	STATION	STD	HYDRO	OXY	NH_3	PO_4	NO_3	SiO_4	COMMENTS
206	Feb 25-28, 1975	RES-2	X	-	-	-	-	-	-	-
		RES-2.5	X	X	X	X	X	X	X	Nutrient data below 200 m is incomplete
		RES-3	X	-	-	-	-	-	-	
		RES-4	X	X	X	-	X	X	X	-
		RES-5	-	-	-	-	-	-	-	-
208	Apr 9-11, 1975	RES-2	X	-	-	-	-	-	-	-
		RES-2.5	X	X	X	X	X	-	X	Hydrographic time series ∿16 hr
		RES-3	X	-	-	-	-	-	-	-
		RES-4	X	X	X	X	X	-	X	-
		RES-5	X	X	X	X	X	-	X	-
210	May 13-15, 1975	RES-2	X	-	-	-	-	-	-	-
		RES-2.5	X	X	X	X	X	-	X	-
		RES-3	X	-	-	-	-	-	-	-
		RES-4	X	X	X	X	X	-	X	-

* Dates given indicate hydrographic data collection only.

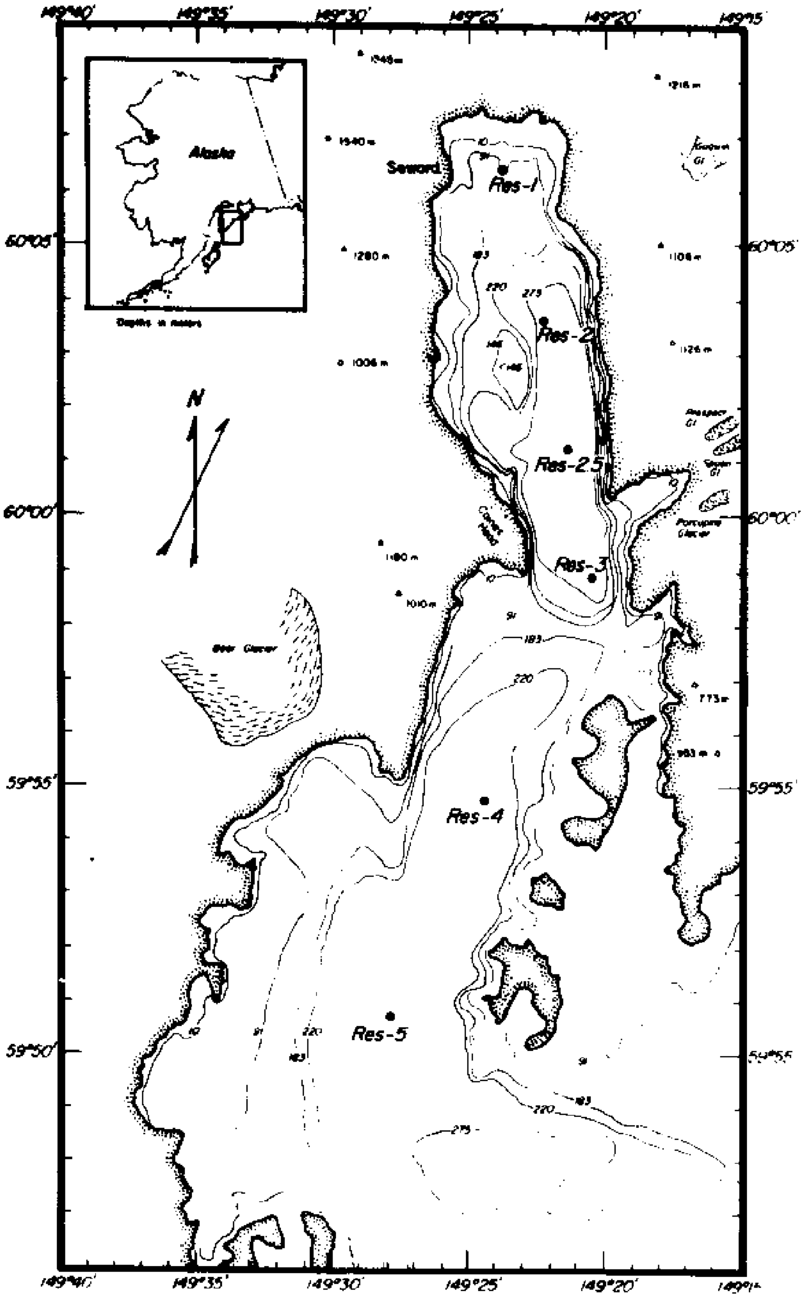

Figure 1. Map of Resurrection Bay showing station locations and depth contours.

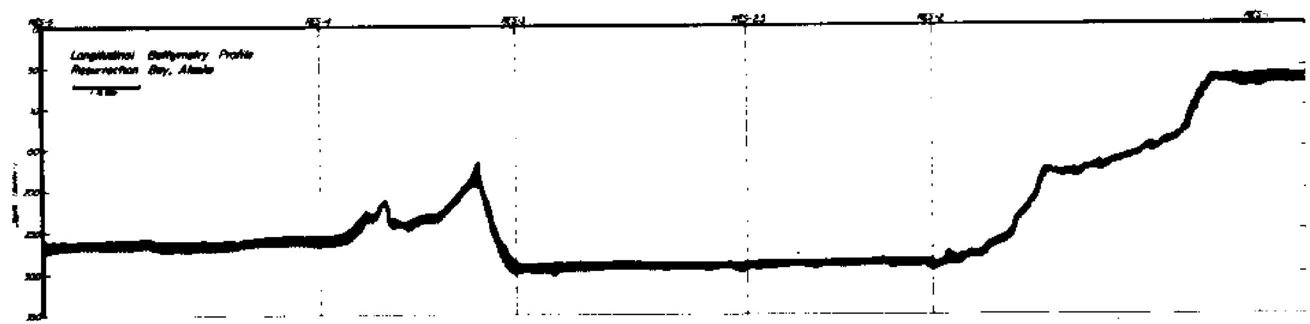

Figure 2. Longitudinal bathymetry.

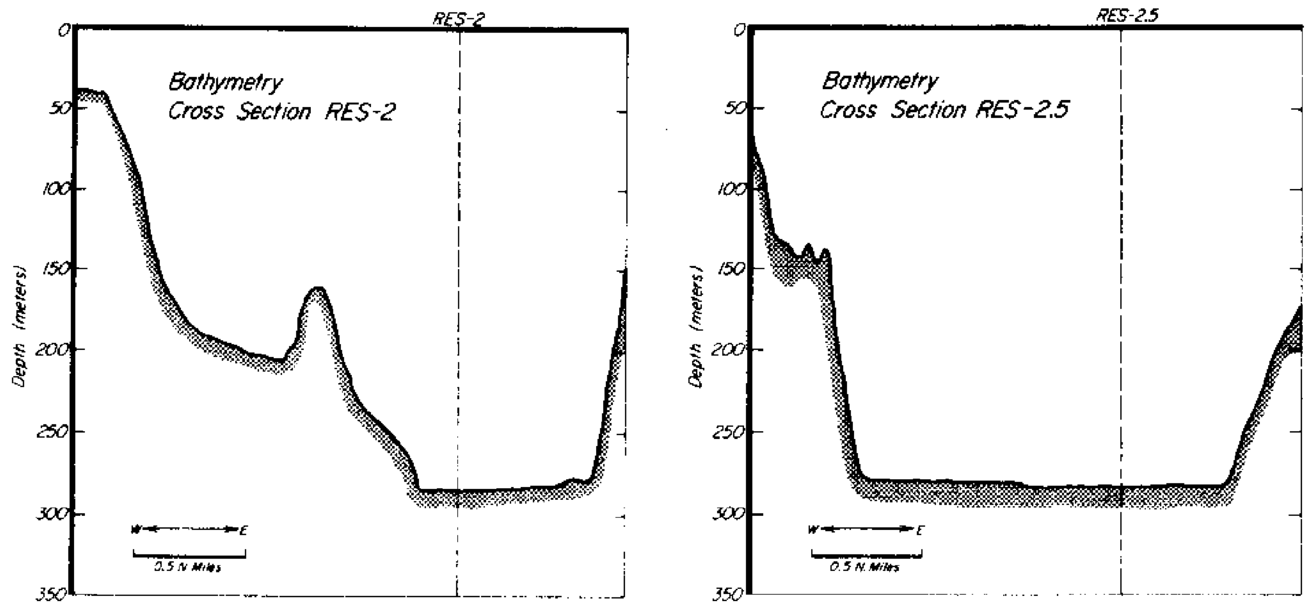

Figure 3. Cross channel bathymetry RES-2, and RES-2.5.

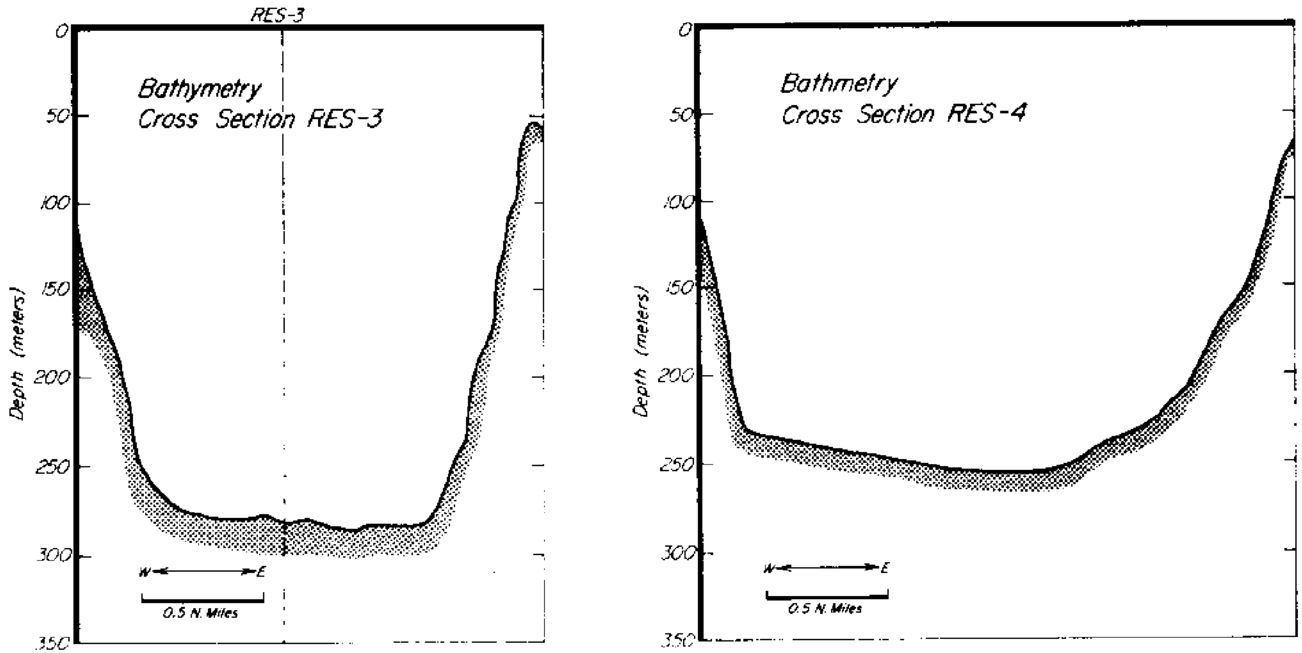

Figure 4. Cross channel bathymetry RES-3, and RES-4.

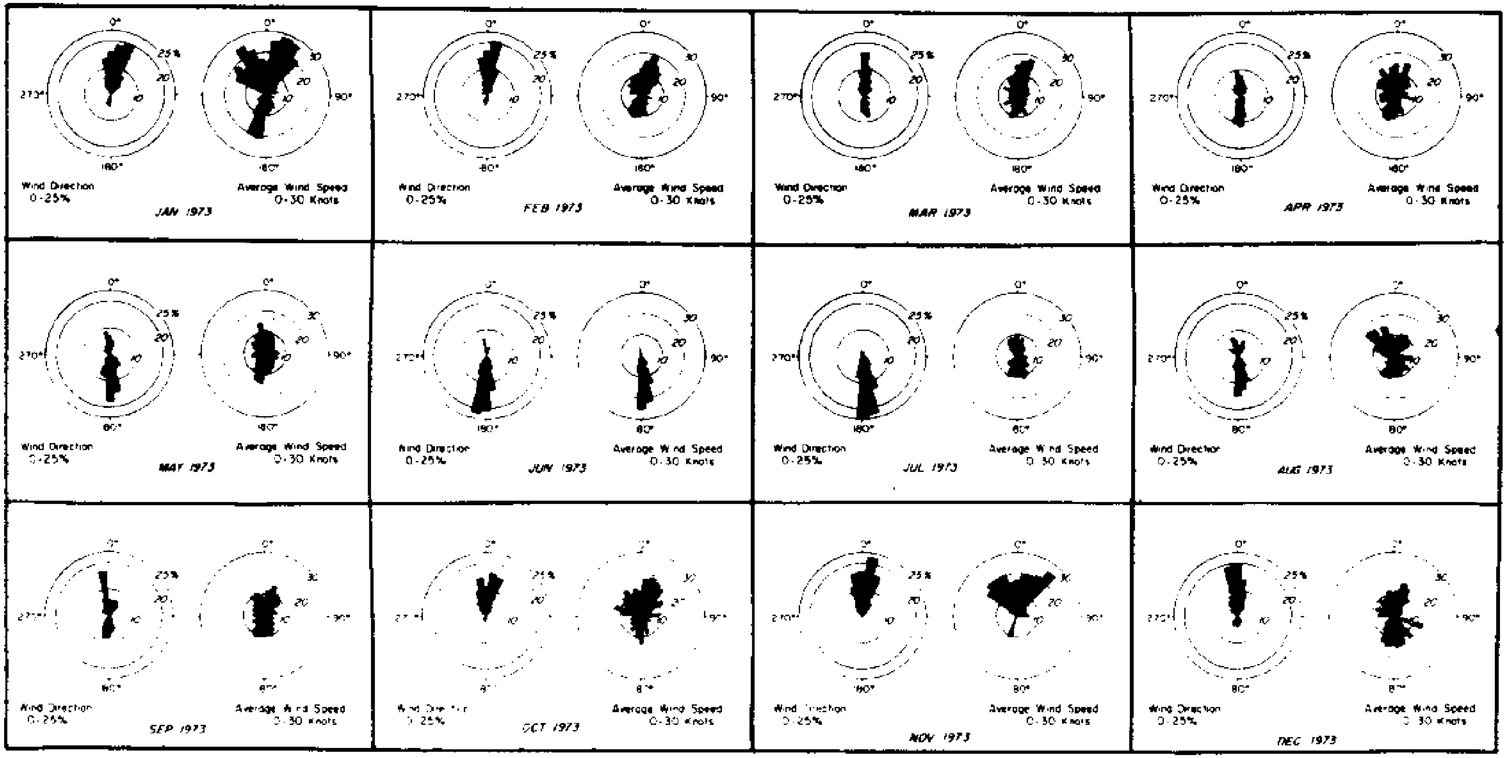

Figure 5. Histogram analysis of wind data from Resurrection Bay during 1973 (U.S. Weather Bureau, unpublished data).

Freshwater is added to the outer reaches of the fjord from Bear Glacier, and at the head of the fjord from the Resurrection River. Data are not available for runoff from Bear Glacier but the principal source of freshwater to the fjord is probably the Resurrection River. U.S.G.S. records, summarized in Figure 6, show that most runoff occurs between July and September and varies between about 500 m^3 sec^{-1} and 75 m^3 sec^{-1}; the average being about 110 m^3 sec^{-1}. During the winter, freshwater input drops to below 50 m^3 sec^{-1}, and may be as low as about 10 m^3 sec^{-1}, between January and March.

MEASUREMENTS

Five stations (Fig. 1) have been occupied since November 1972 on an approximately monthly basis to obtain samples for T (temperature), S (salinity), O_2 (oxygen), and nutrient (nitrogen, phosphorus, silicon) determinations. Nansen bottles and a Bissett Berman STD were used to collect the hydrographic data. Discrete Nansen bottle sampling was conducted below 150 m at approximately 20-m intervals to the basin floor (290 m). The STD data obtained were calibrated using Nansen T and S data. The latter were selected by visual inspection of the STD chart trace where temperature and salinity gradients were minimal (to minimize depth error effects), and differences between the discrete Nansen data and the STD data at that depth were computed. An average difference was determined over the entire cruise and this offset applied to all stations to produce a final STD printout. The accuracy and precision of the final data are considered to be ± 0.02°C and ± 0.02°/₀₀ in temperature and salinity respectively.

Measurements of current speed and direction were obtained at station RES-2.5, with Aanderra recording current meters installed at depths of 42, 93, 185 and 286 m. These data were obtained during the oceanographic winter months of March through May of 1973, and again during the late summer, September through October of 1973.

Samples for dissolved oxygen content were analyzed by the Carpenter modification of the Winkler titration. Analyses were carried out, using standard techniques, for nitrate and nitrite, phosphate, silicate and ammonia at the Seward Station of the Institute of Marine Science. The

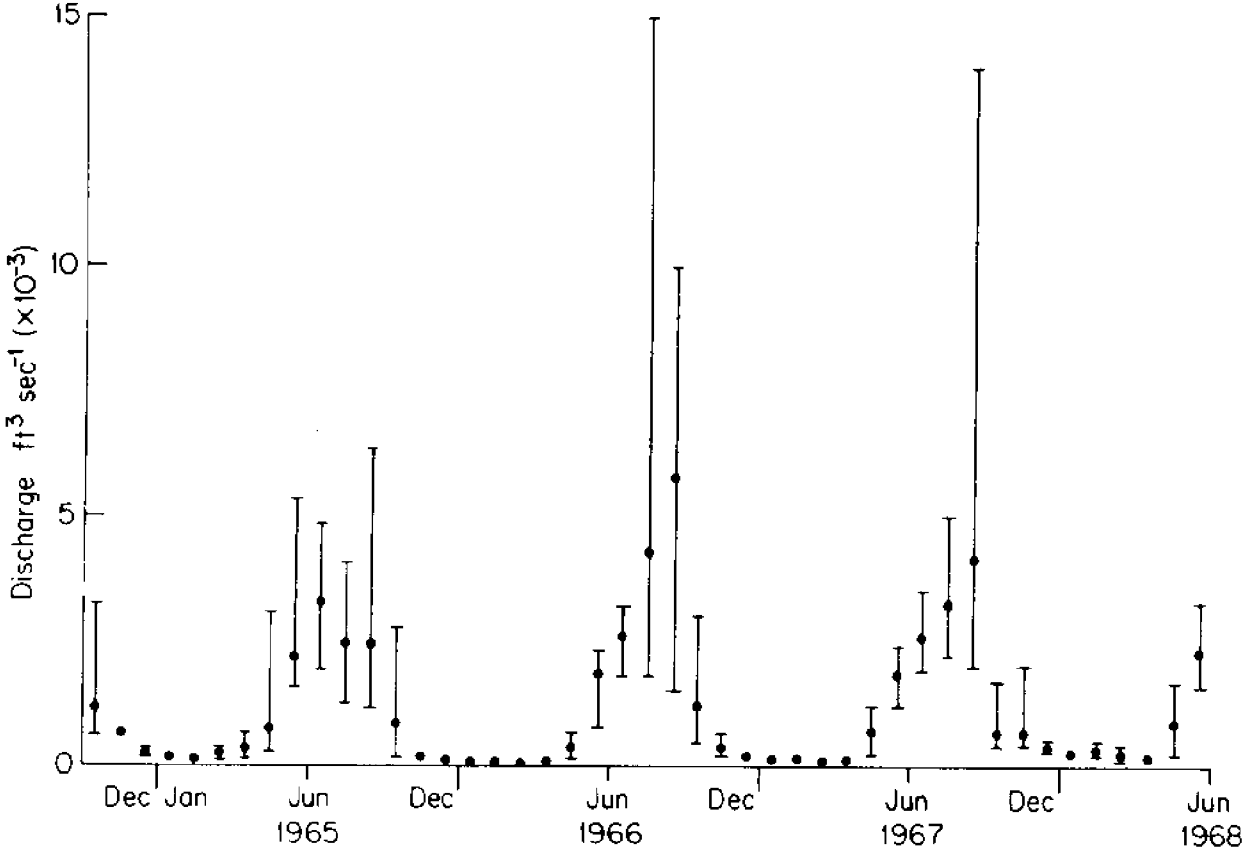

Figure 6. Variations of Resurrection River runoff (U.S.G.S., unpublished data).

above constituents were also determined in interstitial waters squeezed from sediments taken from station RES-2.5. The sediment samples were collected with a Benthos gravity corer, extruded into Reeburgh (1967) type squeezers, and the interstitial water was collected by squeezing the sediments at about 20-30 psi with nitrogen gas. All samples for nutrient analyses were filtered through glass filters and stored frozen prior to analysis.

Primary productivity measurements employing ^{14}C labelled bicarbonate (Steeman-Nielson, 1962) were conducted on the natural phytoplankton populations at stations RES-2.5 and RES-4 between April 1974 and April 1975. Five liter PVC Niskin bottles were used to collect water samples at depths corresponding to 100%, 50%, 25%, 10% and 1% ambient light penetration measured with a Secchi disk. Samples for carbon uptake were drawn, innoculated with the labelled bicarbonate solution and incubated in natural light at sea surface temperatures under neutral density screens calibrated to the approximate light conditions at sample depth. At all stations samples were drawn and incubation begun between 0830 and 0930 hours and continued for approximately 6 hours. The samples were then filtered, the filters placed in Aquasol liquid scintillation flor and returned to Fairbanks for counting.

Primary productivity values reported are in mg carbon m^{-2} h^{-1} for hourly rates integrated over the 1% light depth and mg carbon m^{-2} d^{-1} for daily rates, assuming the rate of production remained constant from one hour after sunrise to one hour before sunset. Production periods at the latitude of Resurrection Bay ranged from 17 hours in mid summer to 4 hours in mid winter.

In addition to the above parameters, water was drawn for carbonate alkalinity, nutrient chemistry and chlorophyll *a* concentrations. The samples for Chl *a* were filtered immediately, the filters frozen and returned to Fairbanks for analysis. The biomass values reported are in mg Chl *a* m^{-2} for standing stock integrated over the 1% light depth. The concentration of Chl *a* was calculated according to the equation of Parsons and Strickland, given in Strickland and Parsons (1968). Pheopigment concentrations were not determined.

HYDROGRAPHY

BACKGROUND

Circulation in Fjord Basins

Fjords are estuarine systems, characterized morphologically by steep sides, deep basins, and often a sill that inhibits the direct exchange of fjord water with adjoining marine coastal water (Pritchard, 1967). Surface water circulations are determined by the relative importance of driving forces such as freshwater river runoff, tides, and winds. Fjords are generally, but not always, stratified in salinity, hence density. Such stratification is at a maximum during the summer and fall months, when fresh water due to snow melt and rains is added to the fjord, and minimal during mid-winter months (February-March) when most precipitation, because of below freezing air temperatures, is stored as snow. The less dense freshwater overlays the more dense marine water and flows seaward out of the fjord. The seaward flow of freshwater at the surface entrains more dense marine water from below and this process results in a longitudinal salinity gradient and an up-estuary flow, to maintain volume continuity, beneath the surface outflow. This generalized flow pattern, commonly known as the "estuarine circulation" is confined to relatively shallow depths within fjords. Observational and theoretical treatments of this type of circulation have been presented, e.g., McAllister *et al.* (1959), Hansen and Rattray (1966), and Winter (1973).

As freshwater input patterns change the relative importances of driving forces for the circulation also change and sub-Arctic Alaskan fjords, particularly during the winter, and compared to fjords in more temperate climates (e.g., Pickard, 1967), would be expected to behave more like embayments than estuarine systems. Hence, circulations driven by winds, atmospheric pressure differences, tides and thermohaline convection might become more important.

Deep-water circulations (and here the term is used loosely merely to indicate water removed from the direct influence of driving forces for the surface water circulations), are generally determined by processes that cause the density of the adjacent marine source water to vary and to be advected into the fjord, often across a sill, and by *in situ* processes such as thermohaline convection and turbulent exchange. In the absence of a strong freshwater-induced seaward pressure gradient, density differences between marine source water and resident fjord water should be critical in controlling flow patterns in fjord deep waters.

The general hydrography of Resurrection Bay is presented in the following text and exchange of water between the fjord and the adjacent Gulf of Alaska is emphasized.

Seasonal Variations in Marine Source Water: Gulf of Alaska

Royer (1975), in a two year (1970 to 1972) study of the northwestern continental shelf waters of the Gulf of Alaska, found that the seasonal variations were governed primarily by the predominating atmospheric conditions. During the winter months (October through April) the Aleutian low dominated and the associated strong easterly winds in the northern Gulf resulted in onshore (north) Ekman transport and accumulation of surface water along the coast. The resulting coastal convergence depressed the deep waters off the shelf (downwelling) and low salinity 32.00°/₀₀ to 32.50°/₀₀ cold, 2.0 to 3.0°C water persisted there during the winter. The North Pacific high dominated in the summer and associated with this were weak and variable westerly winds in the northern Gulf. A weak offshore (south) component of Ekman transport (essentially a relaxation of the intense winter downwelling), permitted more dense (σ_t>26.00), saline S >33.00°/₀₀ and warmer T ∿5.0°C water which had been depressed off the shelf during the winter to be advected up onto the shelf. Further work by Royer (personal communication) has shown a similar seasonal variation in the water masses on the shelf during the years 1973 to 1976.

RESULTS

Variations in Salinity, Temperature and Oxygen

The following data are intended to demonstrate the seasonal and inter-basin differences and similarities in the water structure of Resurrection Bay. The discussion is centered about data principally from two stations (Table 1): RES-2.5 which is representative of the inner deep basin and

RES-4, representative of the outer fjord reaches. Data from other stations in the fjord are included for completeness.

The hydrography of the surface waters of the fjord is dominated by the relative importance of freshwater runoff. This is highest during the summer months resulting in minimum surface salinities and maximum temperatures. Conversely, minimal runoff in winter and the cold air temperatures results in maximum salinities and minimum temperatures at the surface.

The character of the deep waters of the fjord in the summer is determined by the advection of dense (σ_t>26.00) water (upwelling) onto the adjacent continental shelf. However, in the winter, the deep water behind the sill of the inner basin is relatively isolated from the flushing of the outer reaches of the fjord that occurs as a result of the downwelling at the coastline. This latter results in less dense (σ_t<26.00) water being found in the outer fjord and the adjacent shelf regions during the winter.

Surface Waters

Salinity and temperature stratification was most evident in the water column between April and November. This condition coincided with spring and summer warming, snow melt and freshwater runoff. The stratification was intensified between August and October because of increased rainfall. Surface salinities generally varied between 23°/₀₀ and 29°/₀₀, during the summer months, but were found as low as 16°/₀₀ and 26°/₀₀ (September 1973) in the inner and outer reaches of the fjord respectively. Surface temperatures as high as 14°C were measured throughout the fjord during July months. The average summer freshwater runoff ($\sim$110 m^3) amounts to only about 1% of the tidal prism (semi-diurnal tide, mean range 3 to 4 m, surface area of fjord $\sim 10^8$ m^2). Peak runoffs observed - $\sim$500 m^3 sec^{-1} - represent about 5% of the tidal prism.

Maximum surface water salinities of approximately 31.5°/₀₀, and minimum temperatures, <3.0°C, were found throughout the fjord during March and April, and resulted respectively from decreased freshwater runoff and surface heat loss to the cold dry winter air masses. Because of thermohaline convection and other energy sources for mixing such as winds and tides, the water column exhibited minimum stability about this time.

The relative influences of melt water and runoff in the surface waters of the fjord are reflected in the LANDSAT satellite images of this region taken during July (summer; Fig. 7) and February (winter; Fig. 8). The light imagery of the surface waters during July represents water turbidity due to freshwater runoff and sediment discharge; this is completely absent during February.

Deep Waters

Maximum salinities were found through the entire fjord deep water region during September and October. Figures 9 through 13 give time series plots for stations RES-2 through RES-5. Salinities >33.00°/₀₀ (σ_t>26.00), temperatures of ∿5.0°C, and oxygen concentrations of around 4.0 ml ℓ^{-1}, were measured below about 150 m.

Minimum salinities were found in the deep waters during March through May. There was, however, a significant difference between the minimum salinities observed in the inner and outer basins (Figs. 10 and 12). For example, at 250 m, at the outer station (RES-4), salinities were found as low as 32.21°/₀₀ (σ_t = 25.56; February, 1975), 32.53°/₀₀ (σ_t = 25.84; April, 1974), 32.27°/₀₀ (σ_t = 25.64; April, 1973). However, at the corresponding depth and times at the inner station (RES-2.5) the salinities observed were 32.79°/₀₀ (σ_t = 25.88), 32.69°/₀₀ (σ_t = 25.93), and 32.8°/₀₀ (σ_t = 25.98). Similarly, minimum temperatures were observed at these times. Temperatures ranged between 3.5 and 4.5°C, below about 200 m at RES-4, while at RES-2.5 they ranged between 4.00 and 5.00°C.

A deep pycnocline persisted at the inner station during the fall and winter months (October to April) between about 180 and 220 m (RES-2.5; Figs. 14 through 17). This was not however, a persistent feature at the outer station (RES-4; Figs. 18 through 21). Over the period March-April the outer station exhibited minimum stability with differences in temperature and salinity from 100 m to 250 m of around 1.0°C and 0.75°/₀₀ (σ_t∿0.40). However, at the inner station differences of this order persisted over only about a 60 m depth interval encompassing the sill (185 m). These disparities reflect the more stratified nature of the deep waters around the sill at the inner station.

Erratic vertical excursions of around 10 to 50 m/month were observed in isohaline and isothermal surfaces below about 150 m at the outer station RES-4 (Fig. 12; Figs. 22 through 27 show longitudinal profiles). At the inner station RES-2.5, however, the vertical excursions of the isohaline and isothermal surfaces were only about 10 to 20 m/month (Figs. 10, and 22 through 27) and varied quasi-uniformly between October and May. The contrast between the two stations was most marked below about 150 m. At 250 m depth the overall seasonal range in salinities and temperatures were about 1.3°/₀₀ ($33.3 > S > 32.0$), and 2.0°C ($6.00 > T > 4.0$) at RES-4, while at RES-2.5 it was less: about 0.4°/₀₀ ($33.2 > S > 32.6$) and 1.1°C ($5.7 > T > 4.6$).

The seasonal ranges and vertical structures in oxygen contents below about 150 m were markedly different between the two stations RES-4 and RES-2.5 (Figs. 14 through 21). Oxygen concentrations at RES-4 varied between 3.5 and 7.5 ml ℓ^{-1} and, while concentrations generally decreased with depth, both maxima and minima were found throughout the water column. The seasonal variations at depth were erratic, as was the case with the temperature and salinity variations noted previously. At RES-2.5 concentrations varied between about 1.0 ml ℓ^{-1} and 7.5 ml ℓ^{-1} and always decreased with depth. Concentrations at the sill depth (185 m) generally increased throughout the winter months to about 7.0 ml ℓ^{-1}, but toward the bottom (290 m) decreased to about 1.0 ml ℓ^{-1}. An oxygen gradient, directed into the deep basin developed and intensified between October and April (Figs. 14 through 17).

Current Meter Observations

The current meter data are presented briefly here to complement the hydrographic observations. Recorded directions and average speeds are shown in Table 3. The winter records indicate a net inflow between 93 and 185 m. The persistence of northerly (down estuary) winds during these months probably resulted in a net outflow at the surface. At 185 m an average speed of 1.13 cm sec^{-1} at 35° (inward) was computed; at 286 m an outward (147°) "drift" of 0.25 cm sec^{-1} was recorded. The latter record did not reproduce any features of the record at the sill depth (185 m), but appeared

Figure 7. LANDSAT satellite imagery of Resurrection Bay and Environs, July 1975.

Figure 8. LANDSAT satellite imagery of Resurrection Bay and environs; February 1976.

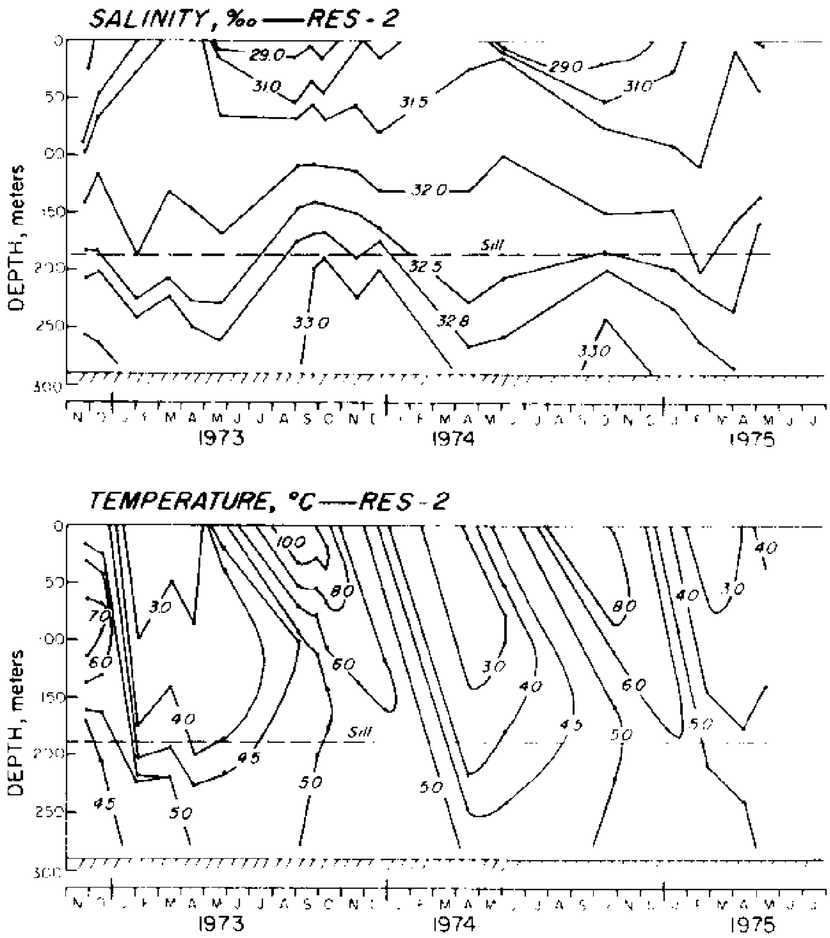

Figure 9. Seasonal variations of temperature and salinity, RES-2.

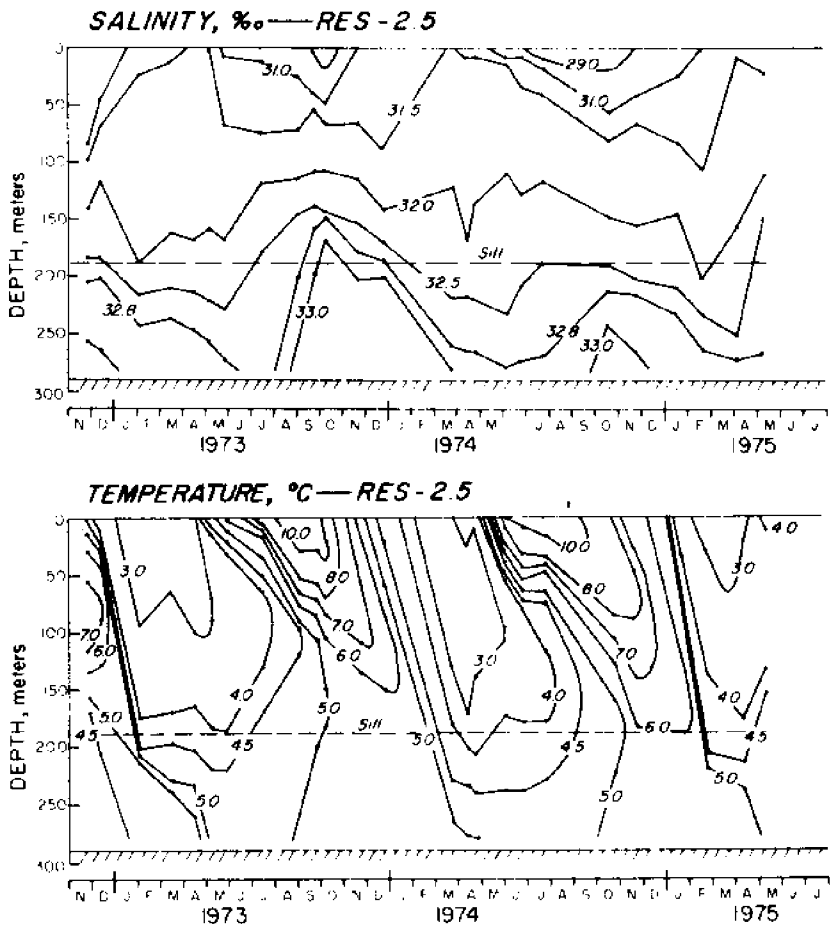

Figure 10. Seasonal variations of temperature and salinity, RES-2.5.

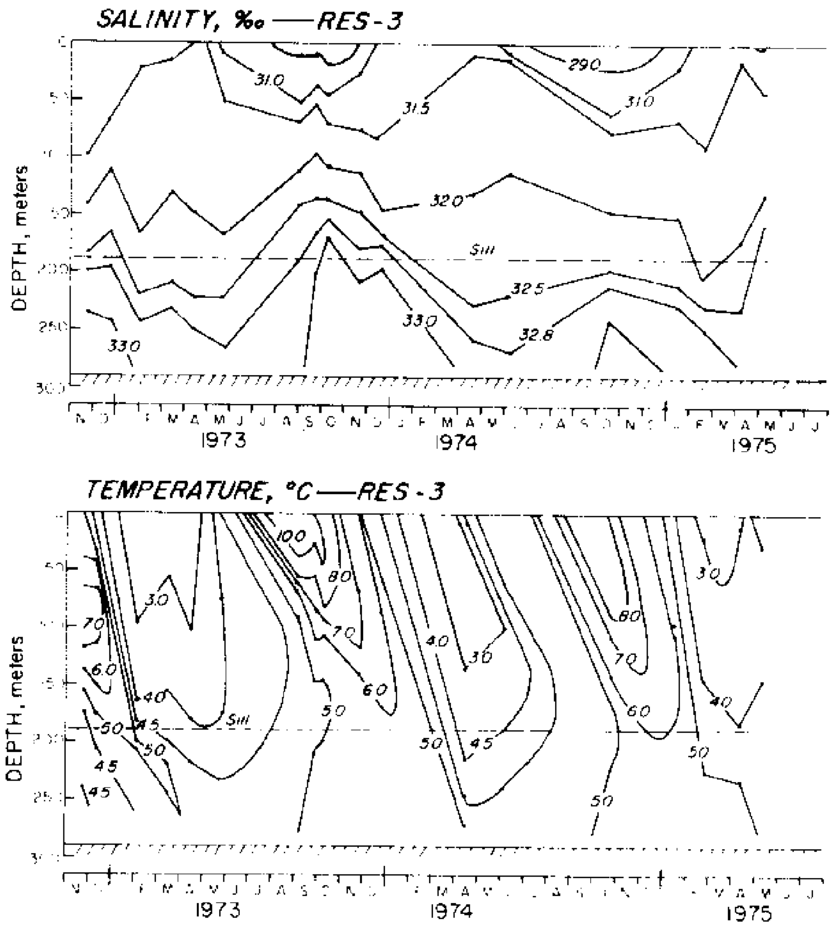

Figure 11. Seasonal variations of temperature and salinity, RES-3.

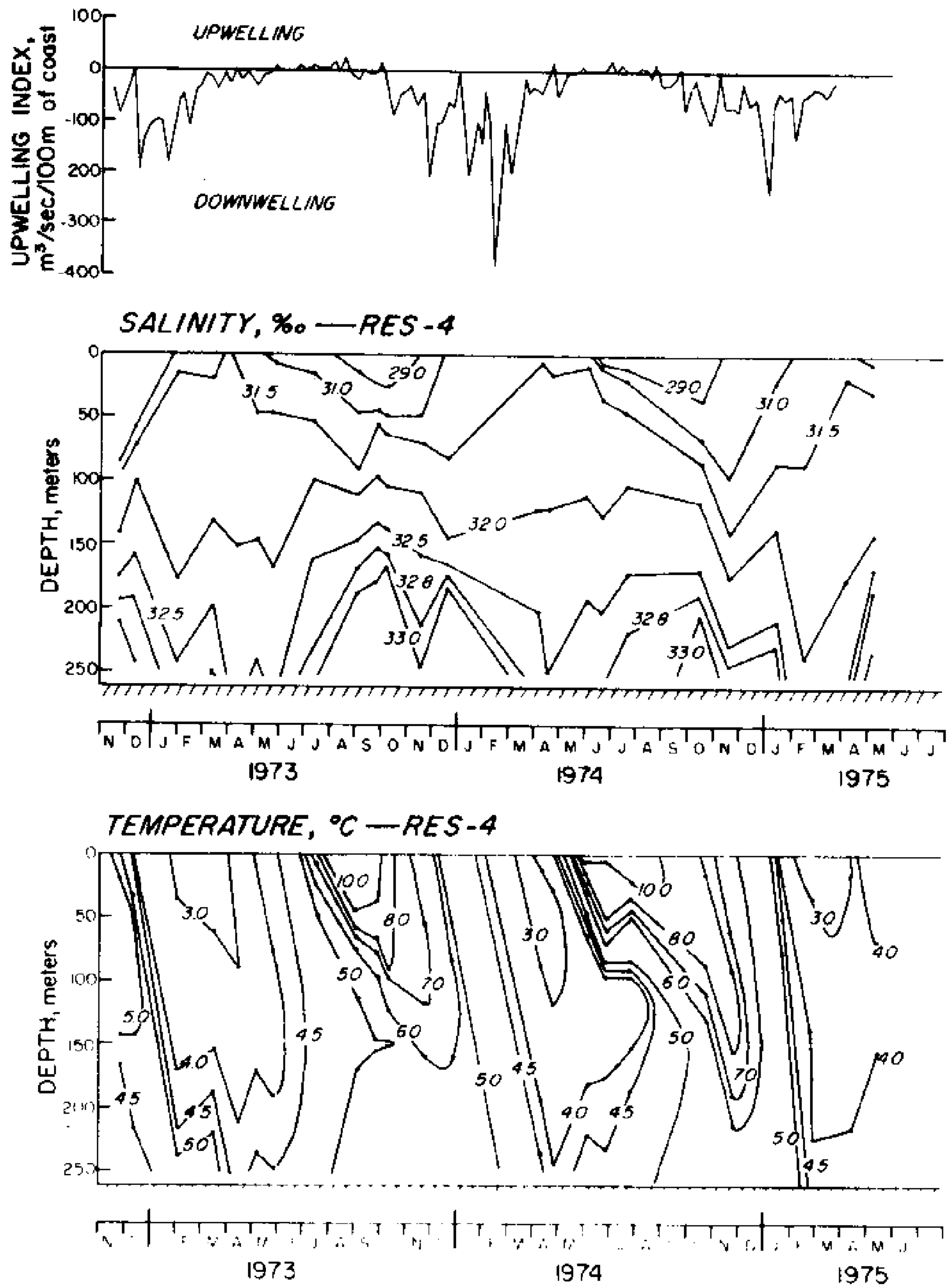

Figure 12. Seasonal variations of temperature, salinity, RES-4, and upwelling index at the coastline.

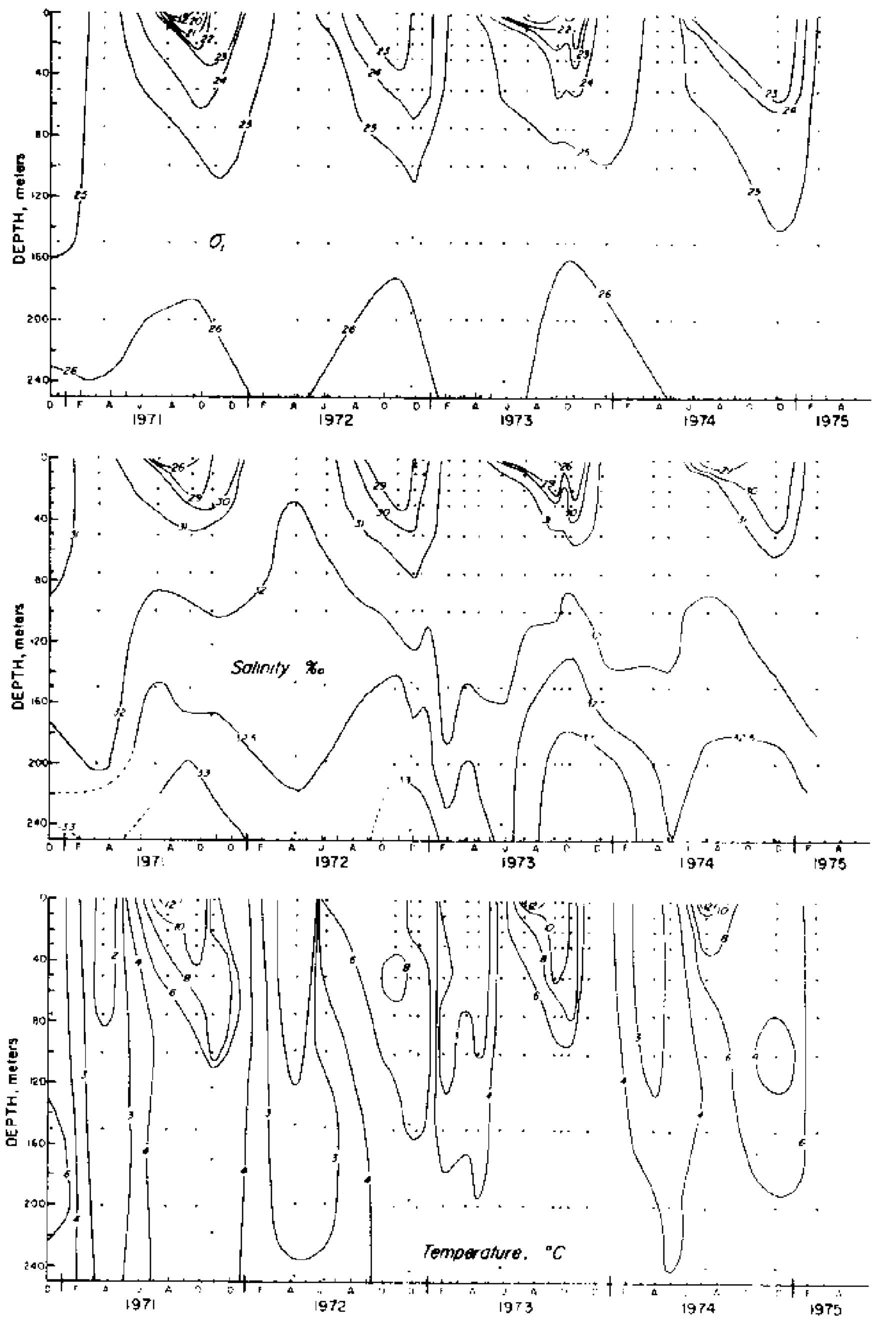

Figure 13. Seasonal variations of temperature, salinity and density, RES-5. (Courtesy of T. C. Royer; station GAK-1).

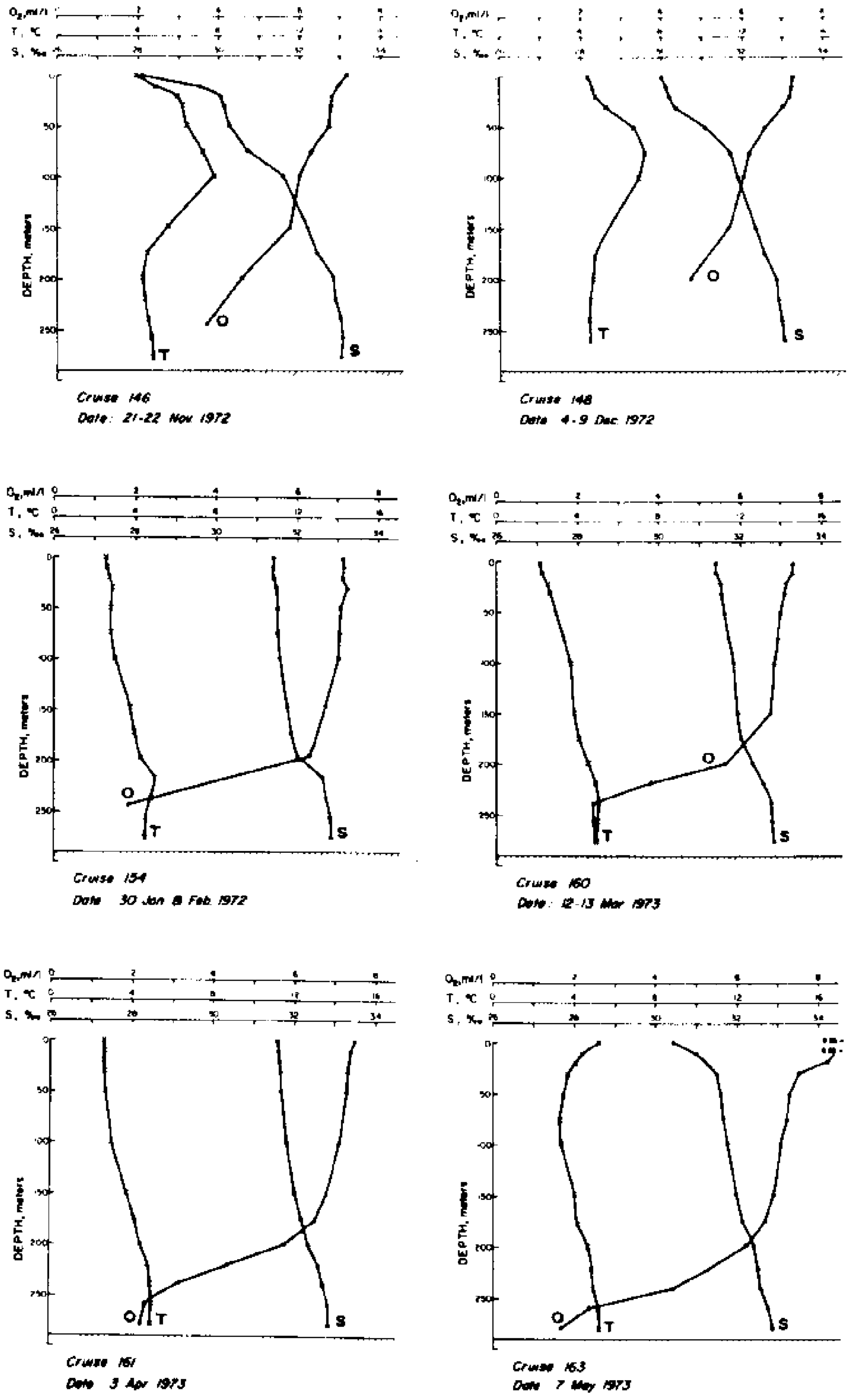

Figure 14. Vertical profiles of temperature (T), salinity (S), and oxygen (O), RES-2.5. November 1972 - May 1973.

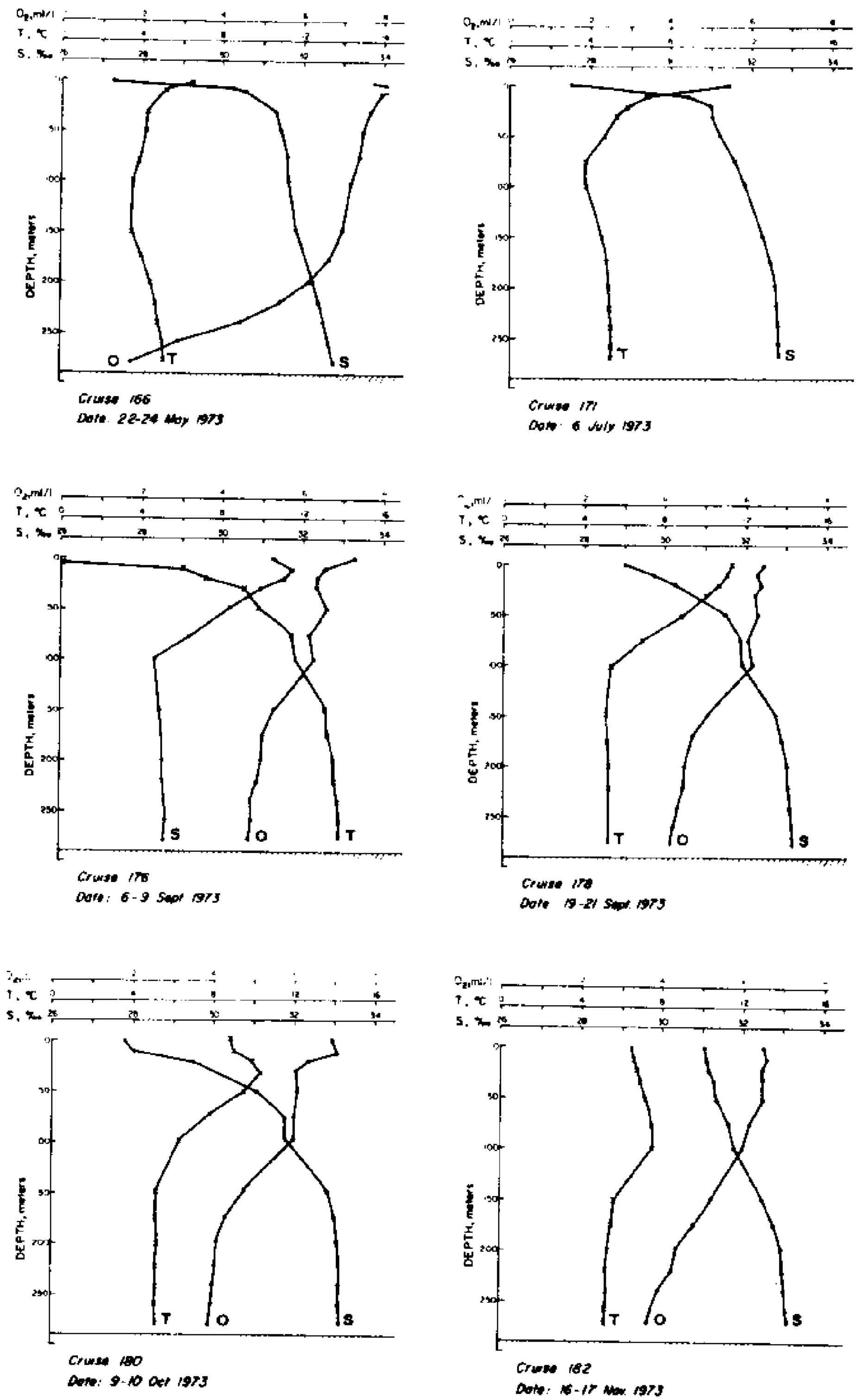

Figure 15. Vertical profiles of temperature (T), salinity (S), and oxygen (O), RES-2.5. May 1973 - November 1973.

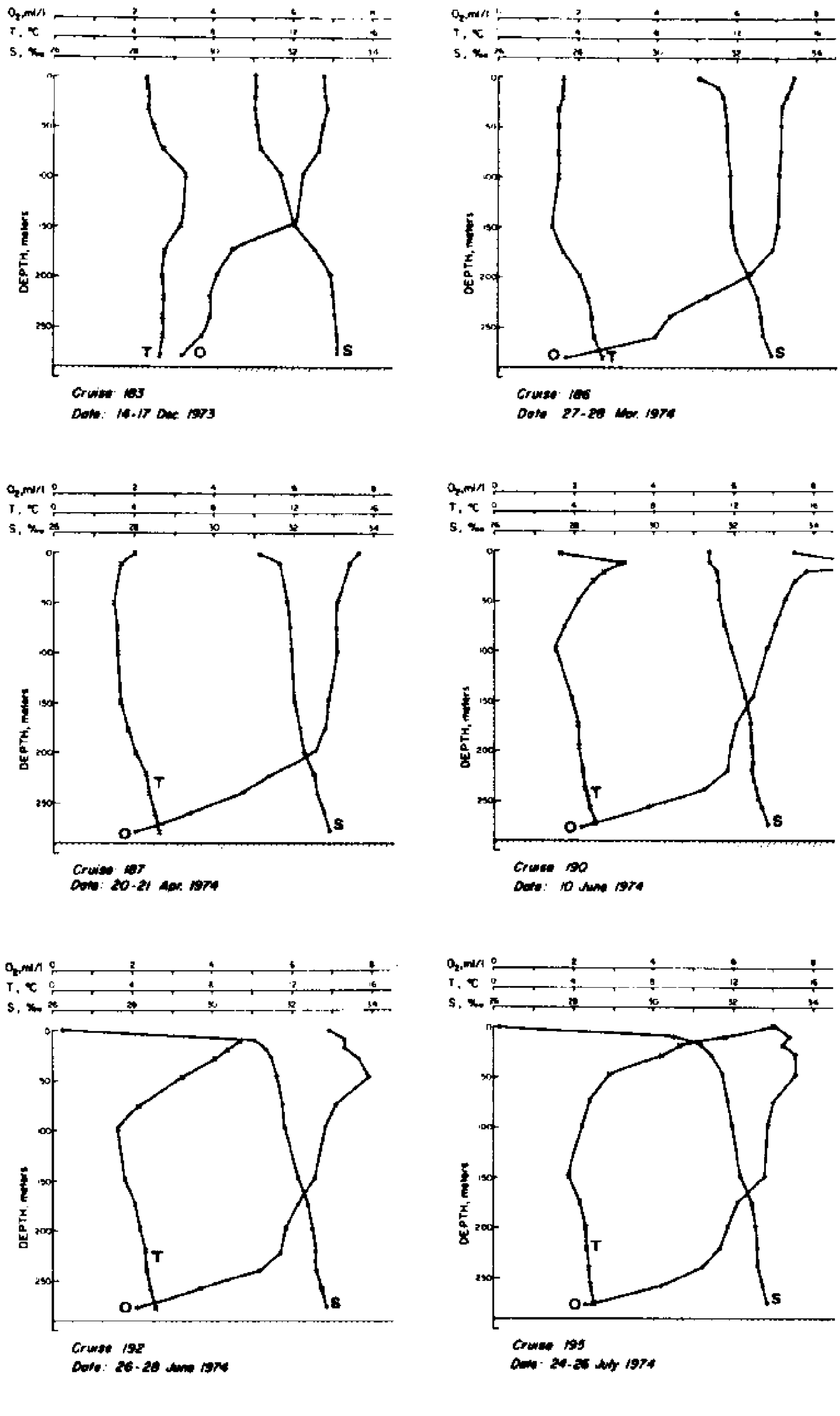

Figure 16. Vertical profiles of temperature (T), salinity (S), and oxygen (O), RES-2.5. December 1973 - July 1974.

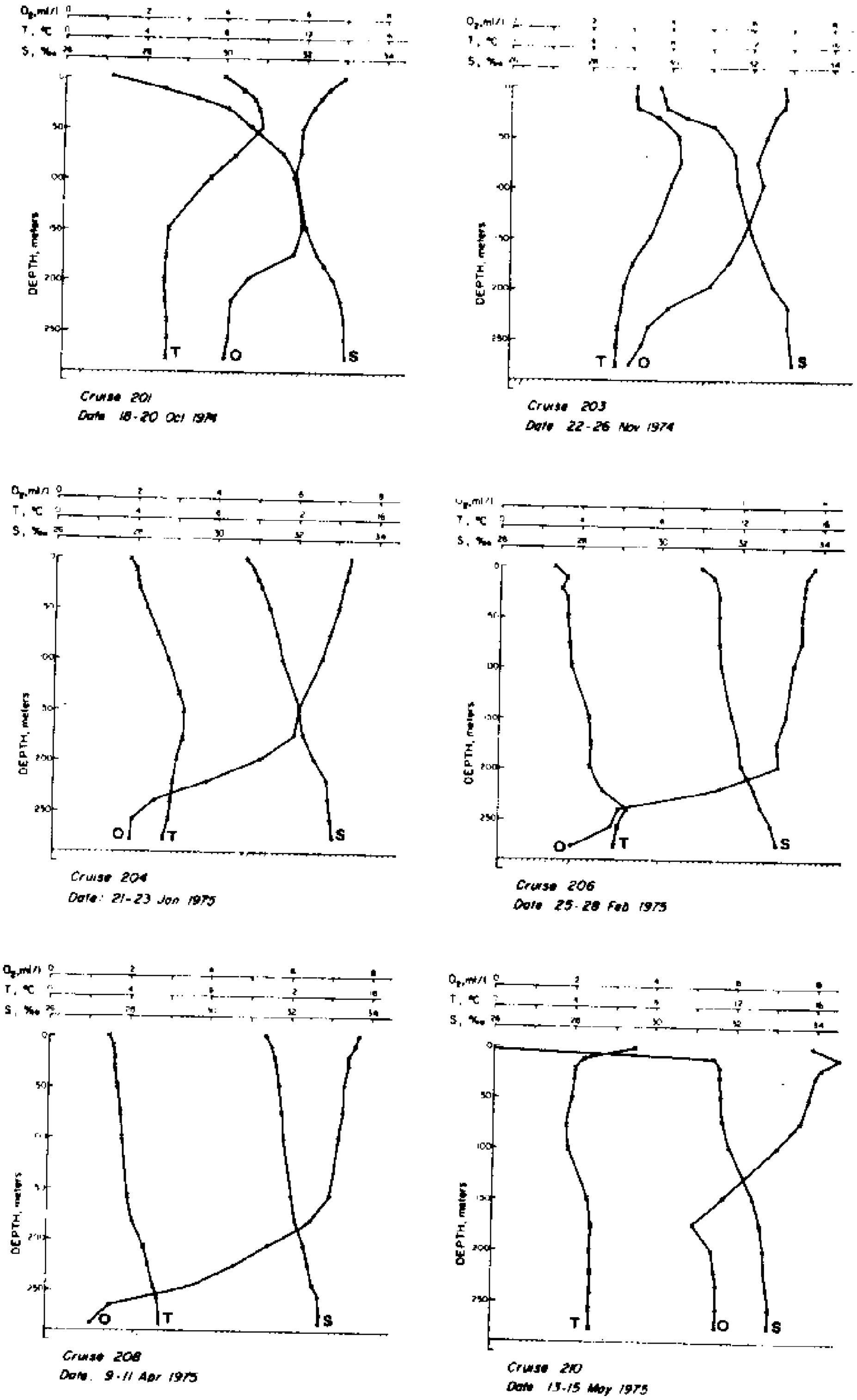

Figure 17. Vertical profiles of temperature (T), salinity (S), and oxygen (O), RES-2.5. October 1974 - May 1975.

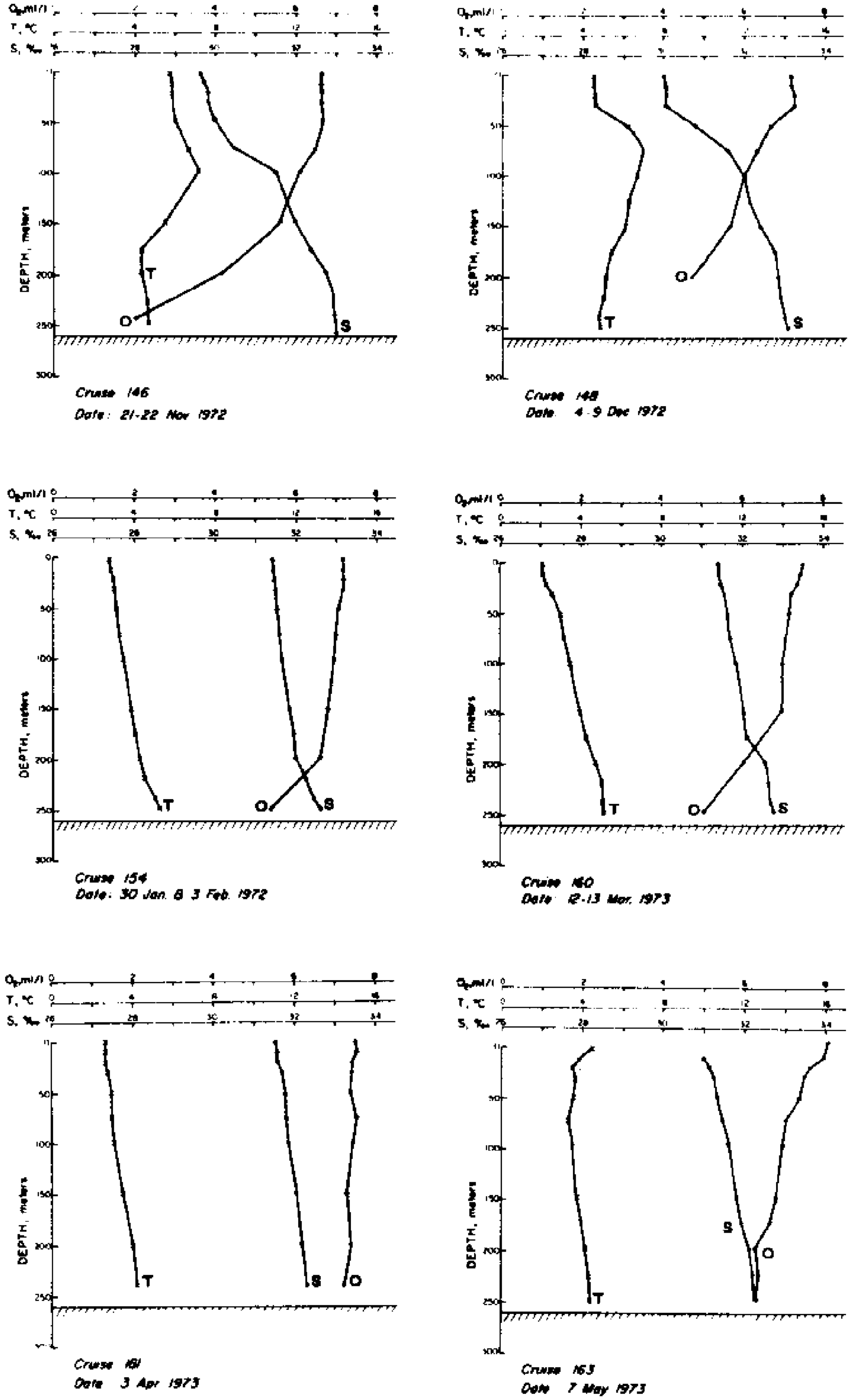

Figure 18. Vertical profiles of temperature (T), salinity (S), and oxygen (O), RES-4. November 1972 - May 1973.

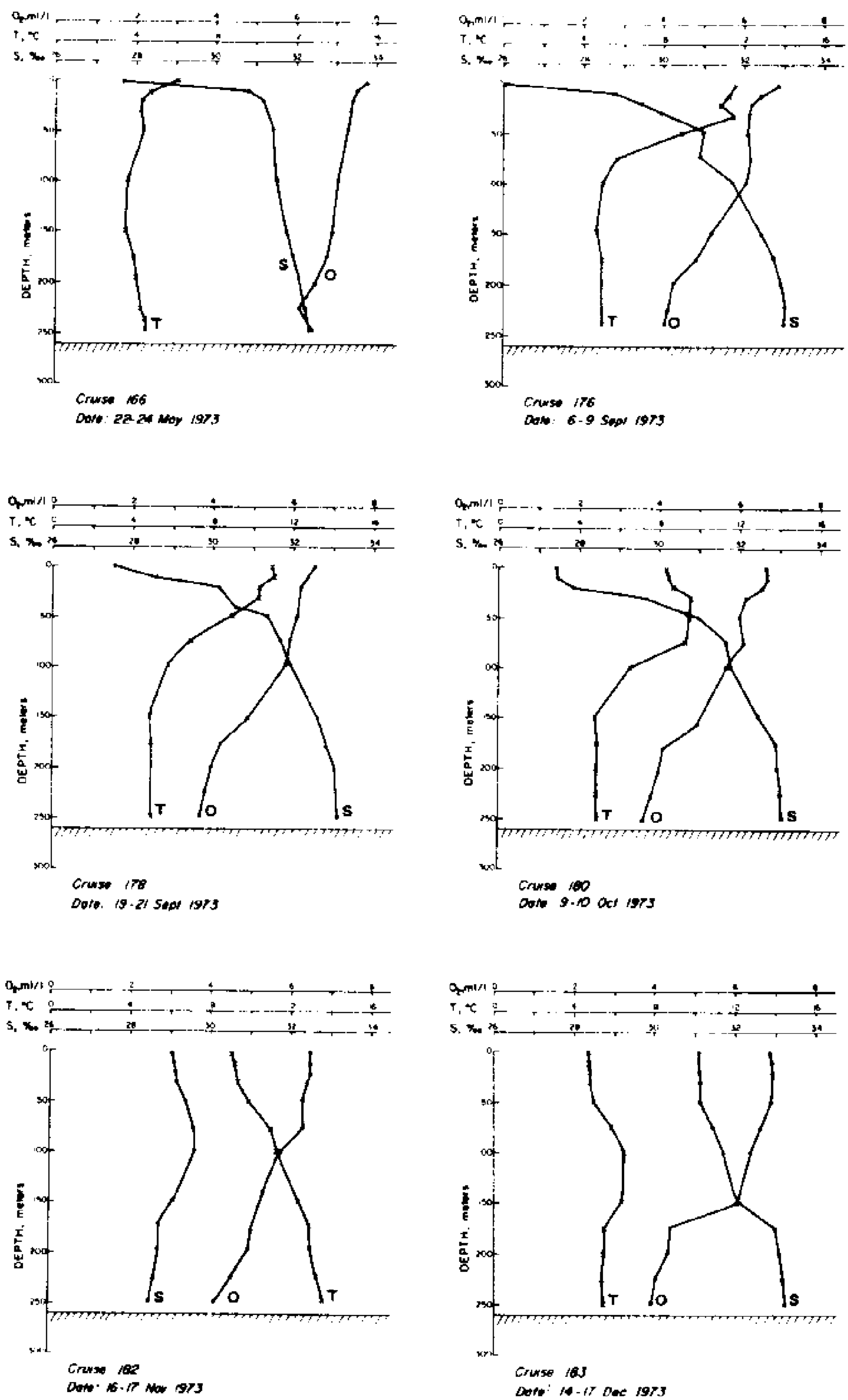

Figure 19. Vertical profiles of temperature (T), salinity (S), and oxygen (O), RES-4. May 1973 - December 1973.

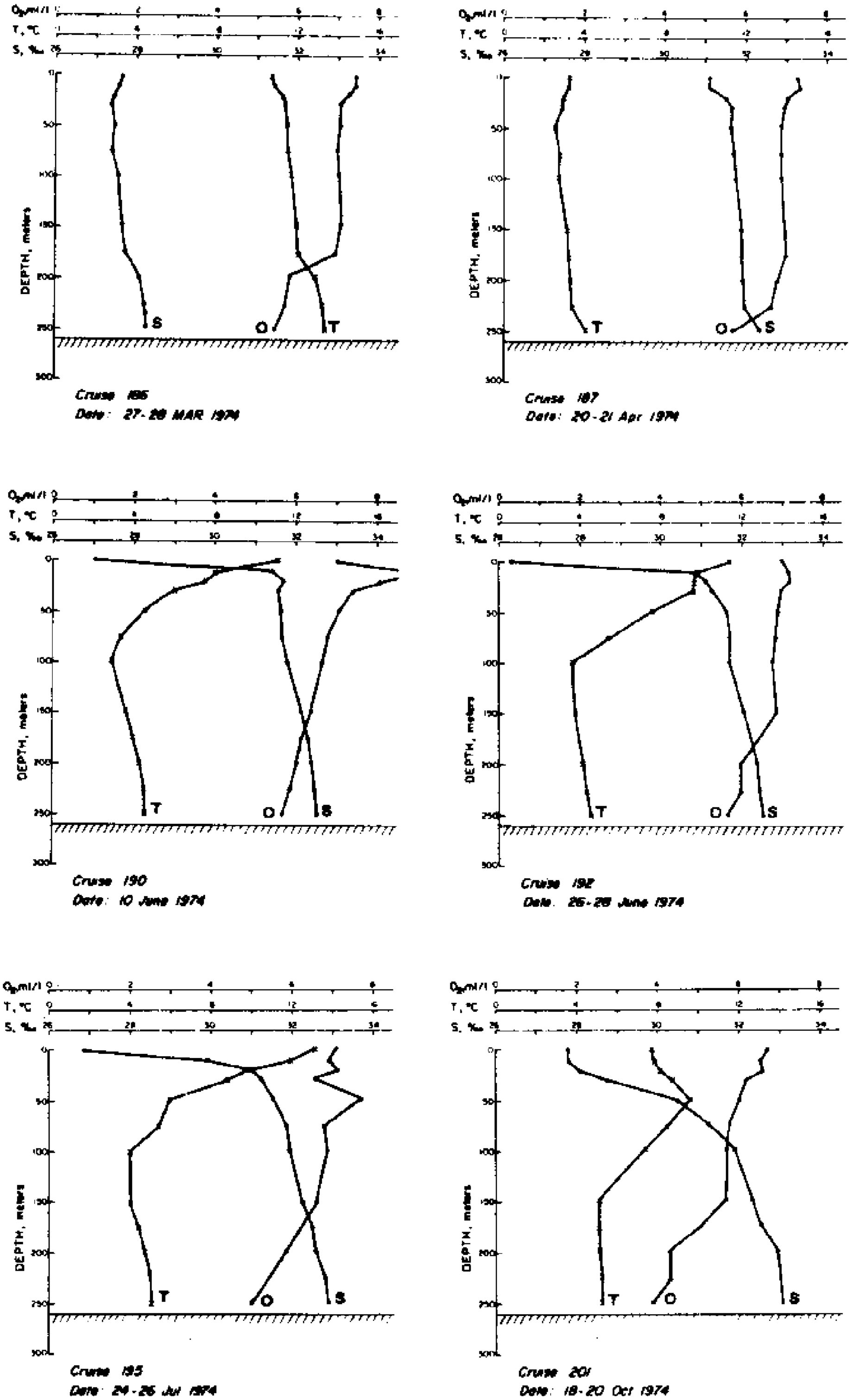

Figure 20. Vertical profiles of temperature (T), salinity (S), and oxygen (O), RES-4. March 1974 - October 1974.

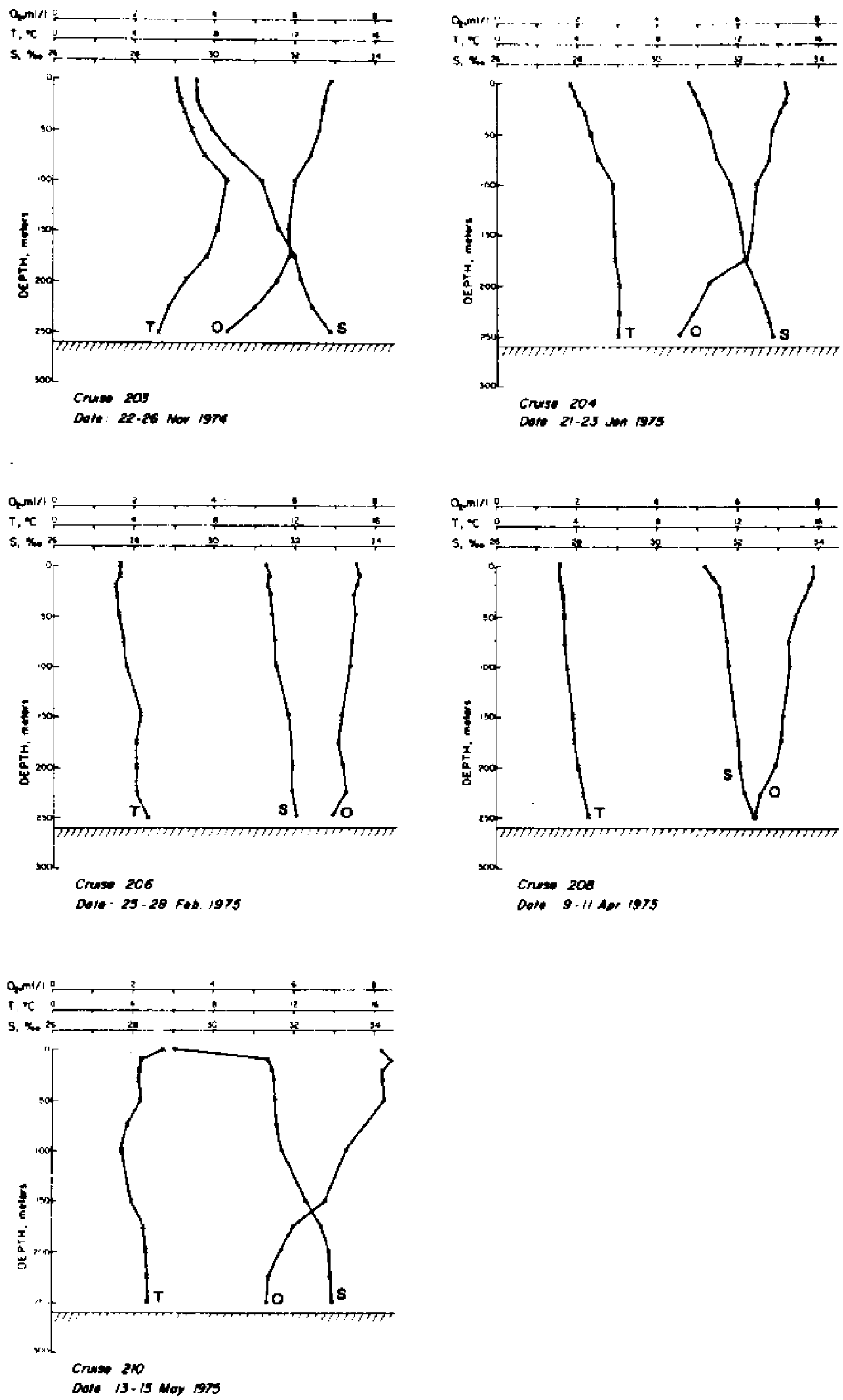

Figure 21. Vertical profiles of temperature (T), salinity (S), and oxygen (O), RES-4. November 1974 - May 1975.

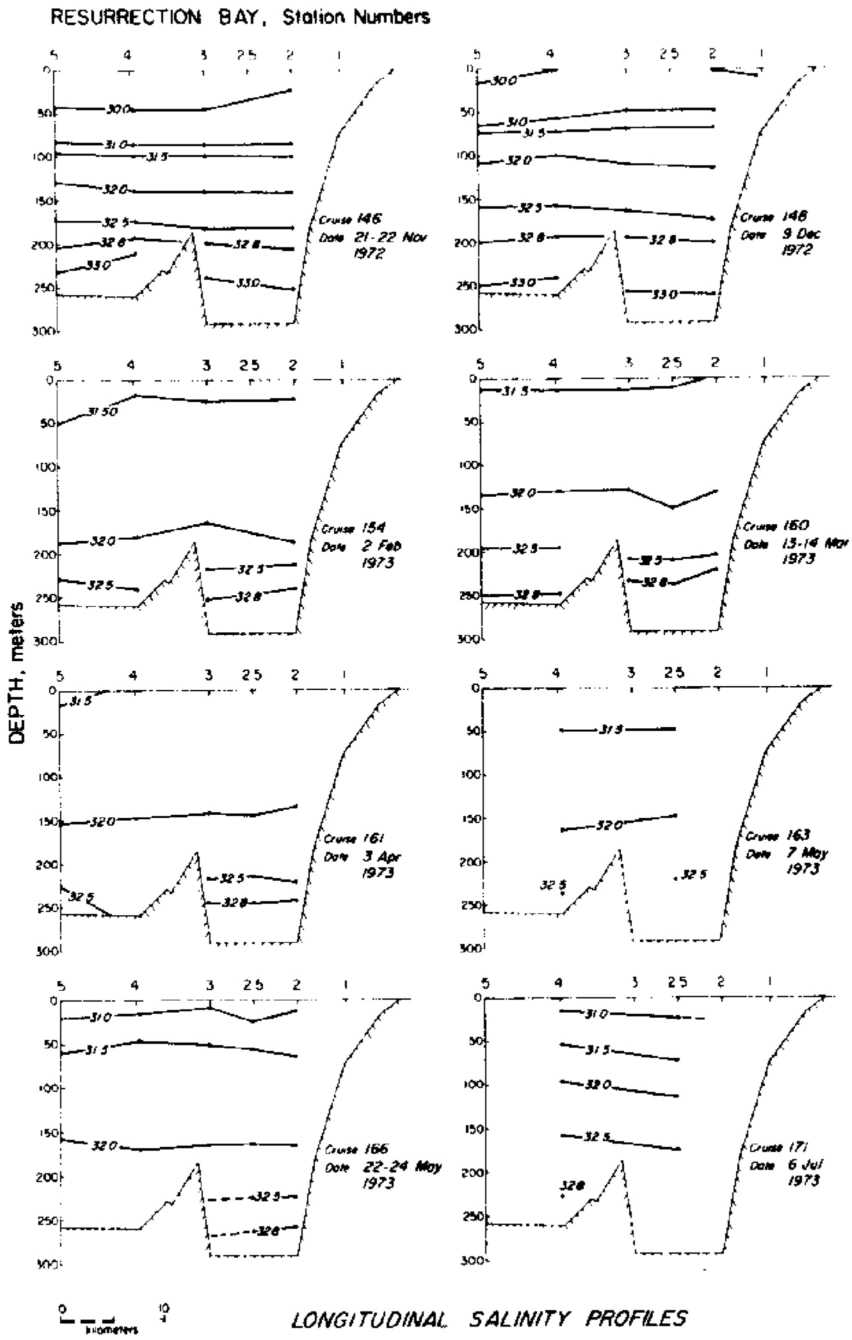

Figure 22. Longitudinal salinity profiles: November 1972 - July 1973.

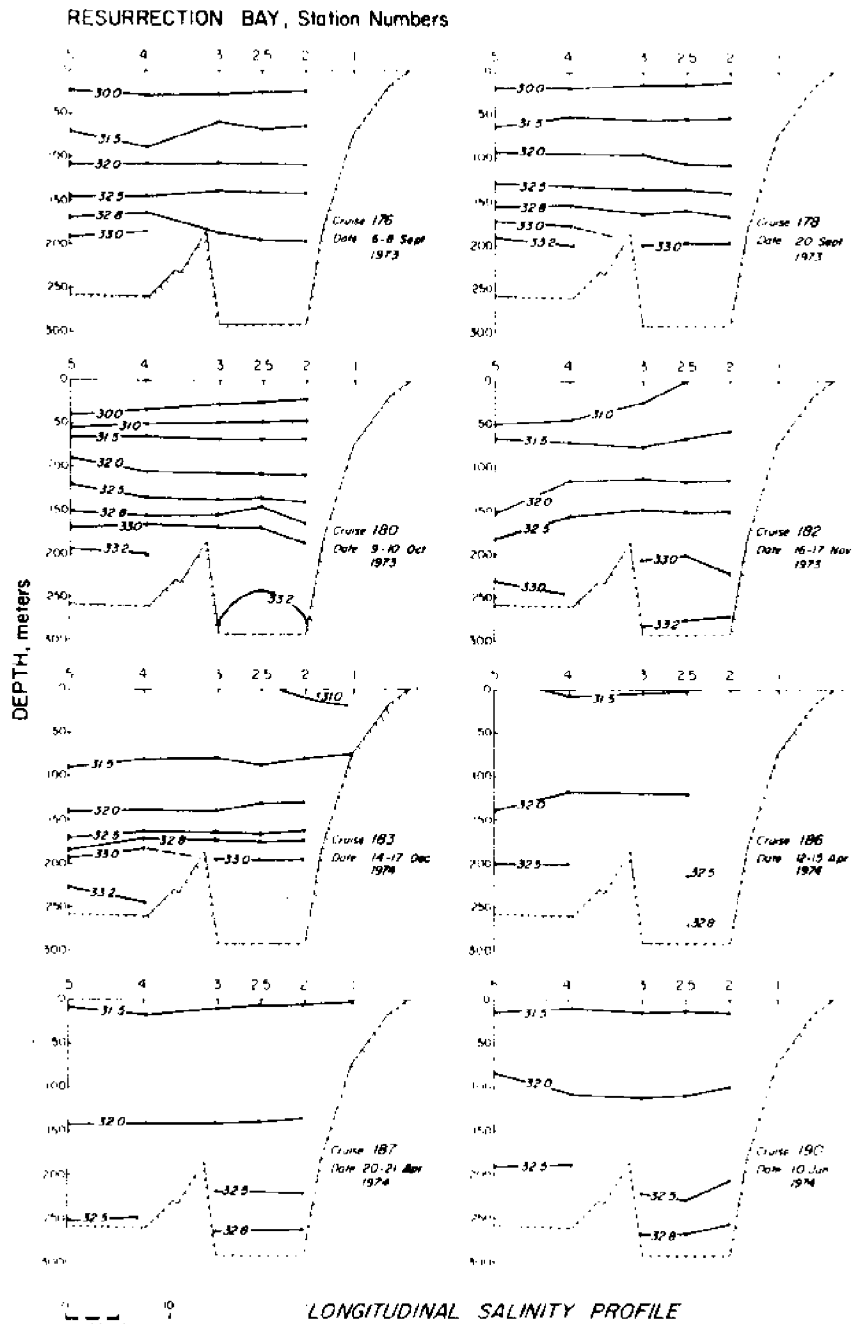

Figure 23. Longitudinal salinity profiles: September 1973 - June 1974.

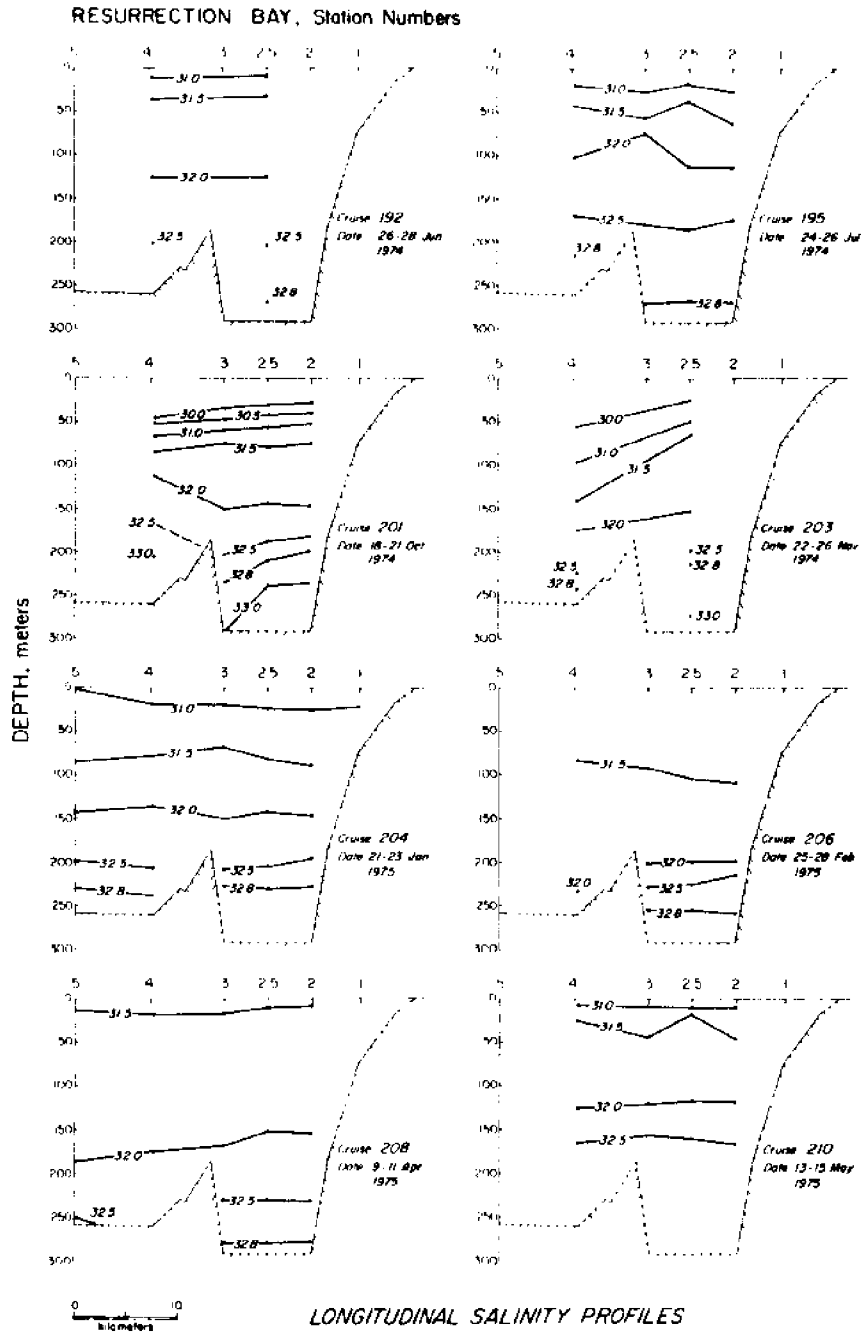

Figure 24. Longitudinal salinity profiles: June 1974 - May 1975.

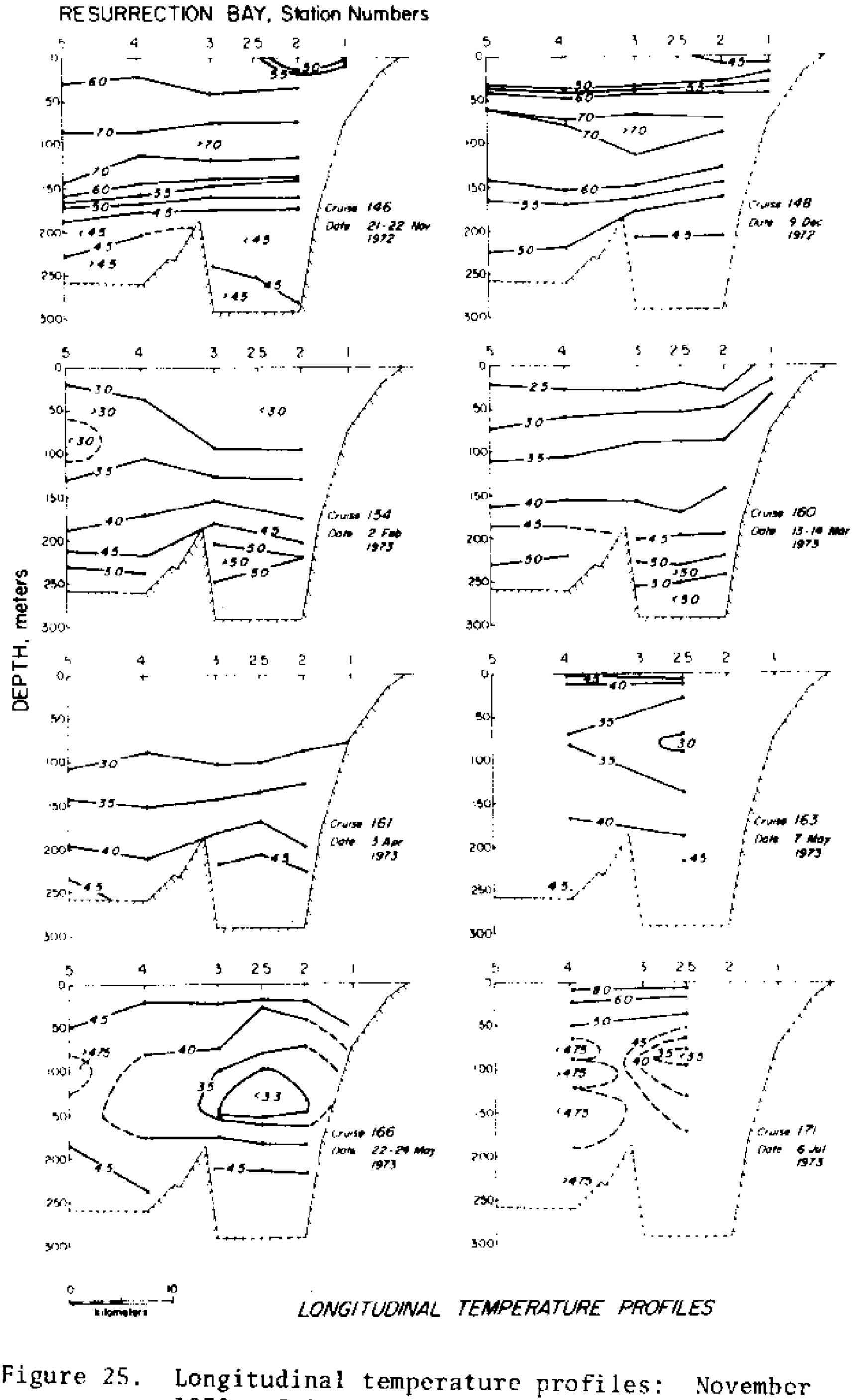

Figure 25. Longitudinal temperature profiles: November 1972 - July 1973.

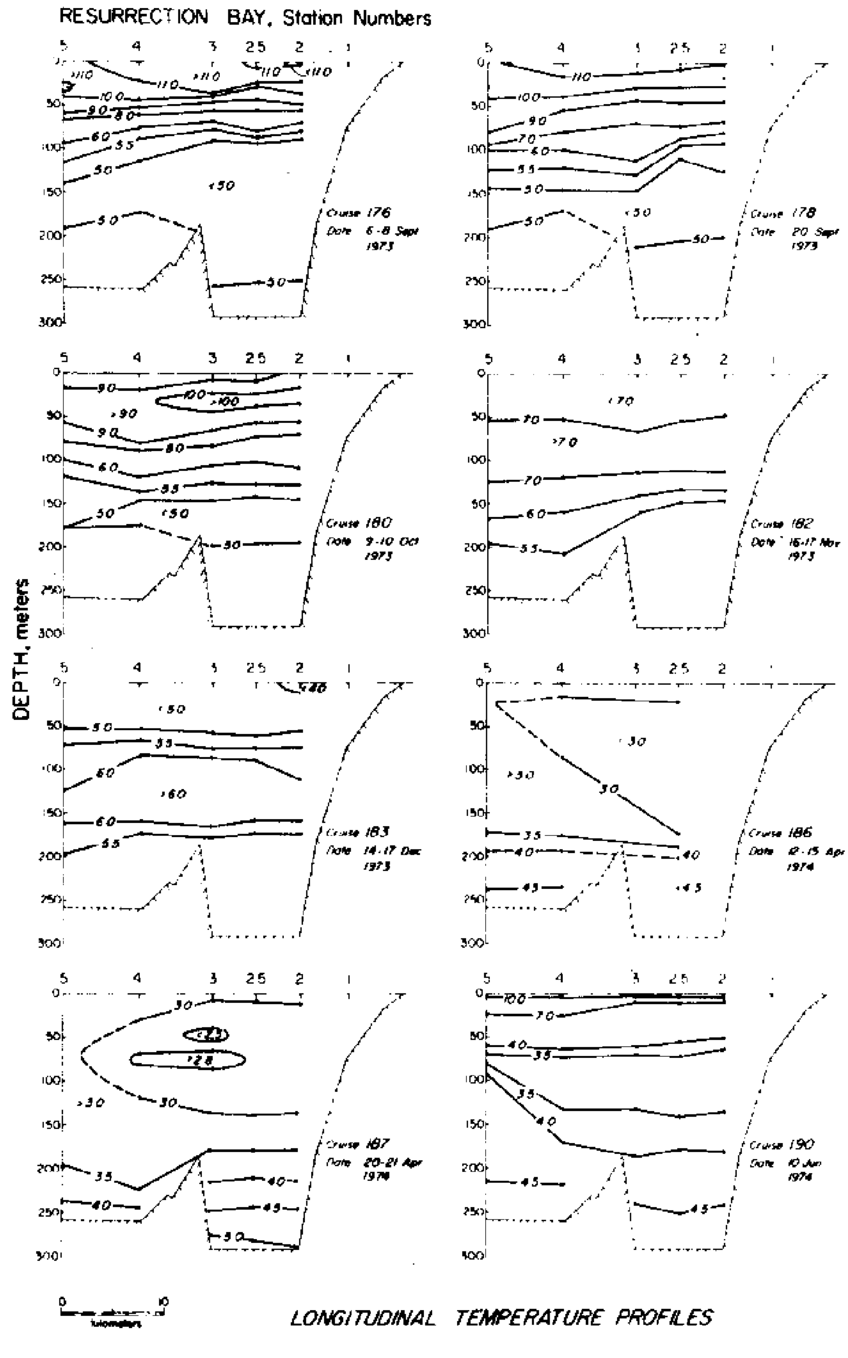

Figure 26. Longitudinal temperature profiles: September 1973 - June 1974.

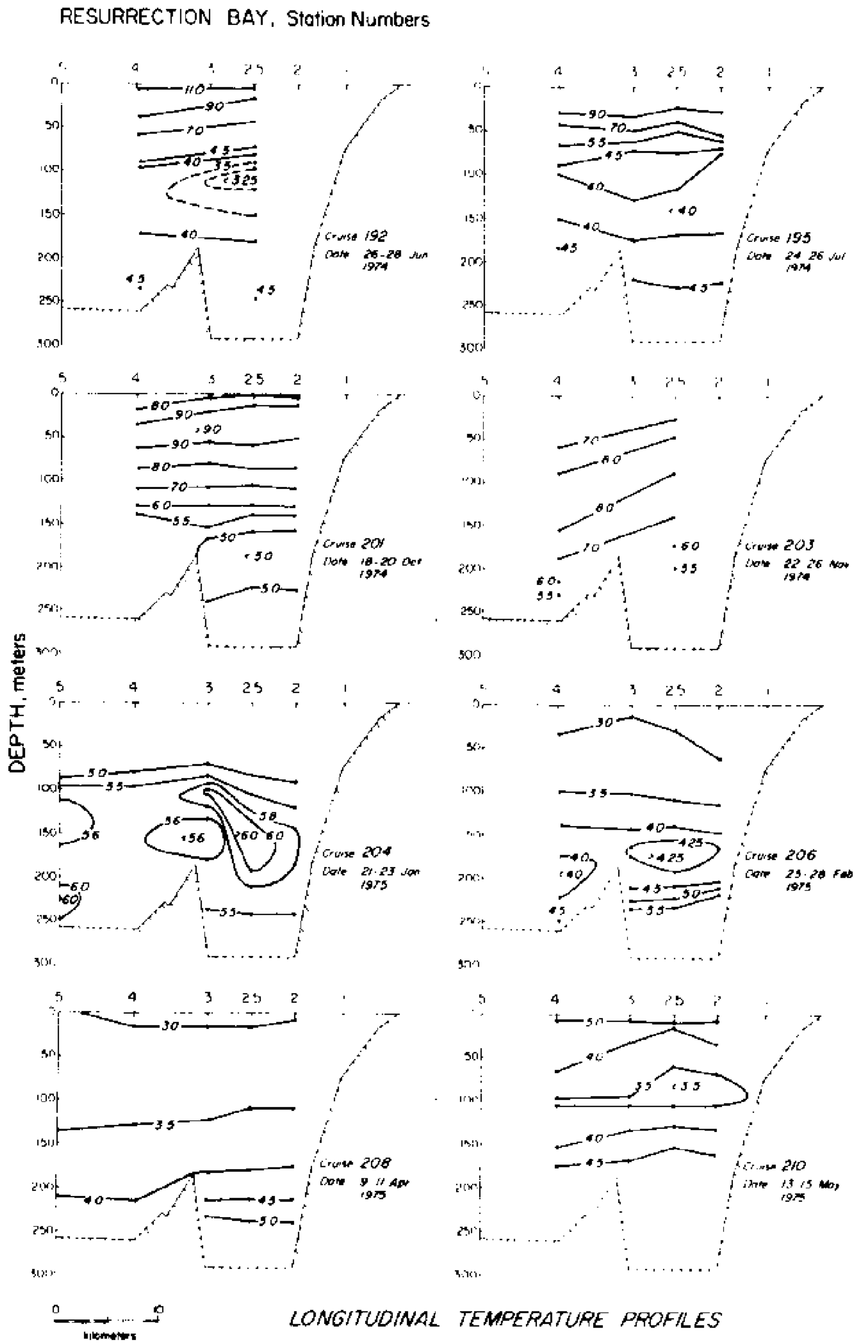

Figure 27. Longitudinal temperature profiles: June 1974 - May 1975.

TABLE 3

Current Meter Data

	March 13-May 8 1973		September 5-October 9 1973	
Z (meters)	Average Speed cm/sec	Direction degrees	Average Speed cm/sec	Direction degrees
42	Meter	Flooded	3.69	8 (I)
93	0.77	11 (I)*	0.88	119 (0)
185	1.13	35 (I)	1.13	179 (0)
286	0.25	147 (0)	3.11	28 (I)

*
I inflow
0 outflow

dominated by semi-diurnal tidal fluctuations only. During the time period of this record, there was a net loss of salt out of the basin and a consequent decrease in density.

The summer current meter records showed a circulation pattern very different from that of winter. At 285 m an almost continuous inflow (northerly) was recorded with an average speed of 3.1 cm sec^{-1} and net outflow was measured at the sill (185 m) and at 93 m. While these meters were in place successive increases in salinity (hence density) in the basin were observed during three observation periods (Fig. 28).

DISCUSSION

Summer Conditions

Time series representations of salinity in the outer basin and weekly means of the coastal upwelling indices, computed for a 3° grid centered about 60°N, 149°W located off the entrance to Resurrection Bay in the Gulf of Alaska, are shown in Figure 12. The indices were computed from distributions of the surface atmospheric pressure (Bakun, 1973). A negative index indicates onshore transport (coastal convergence and downwelling) and a positive value offshore transport (coastal divergence and upwelling).

The general features of this plot are similar to Royer's (1975) data and show the divergence of the isolines during the winter months (October through April), with decreasing salinities in deep water, and the convergence of the isolines during the summer when maximum salinities were found below 150 m. The appearance of more dense (σ_t>26.00) water on the continental shelf during the summer resulted from a relaxation of the coastal convergence and the downwelling conditions (Royer, 1975). The relatively dense water (σ_t>26.00, S > 33.00°/₀₀ and T ~5°C) was evident throughout the outer and inner reaches of Resurrection Bay during September and October (e.g., Figs. 9 through 13). The successive density increases observed (Fig. 28) together with inflow at 286 m (Table 3), in the inner basin, can be explained by the advection of more dense water across the sill which sinks to the basin floor and displaces the less dense resident basin water upward. The outflow (south) between 185 m and 92 m probably represents the displaced water.

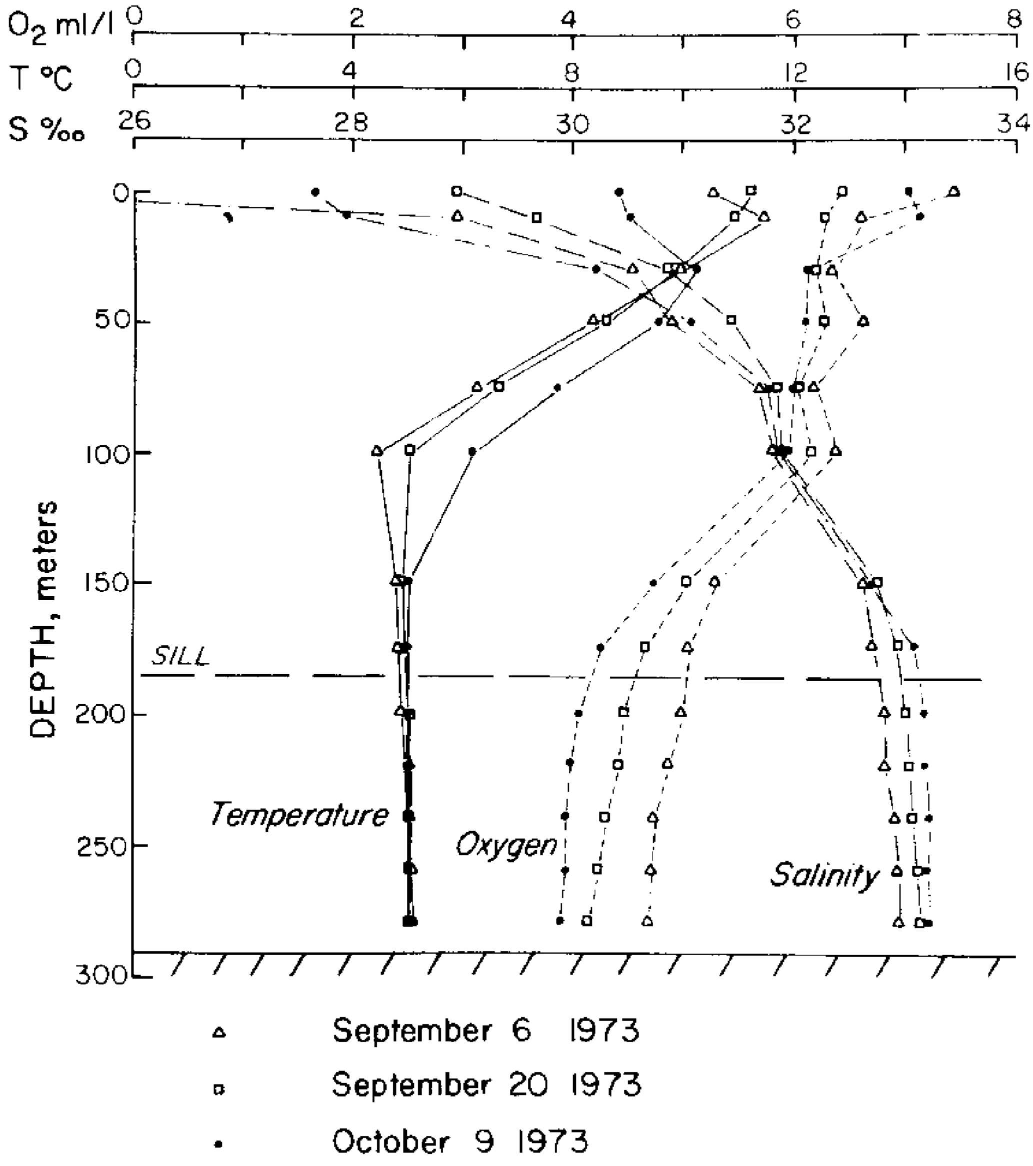

Figure 28. Detailed vertical profiles of temperature, salinity and oxygen during September - October 1973, RES-2.5

Winter Conditions

Outer Fjord

The winter data indicate that different processes control the temperature and salinity distributions of the inner and outer regions of the fjord. Royer (1975) assessed the importance of convection with vertical mixing as a control on the water structure on the shelf and found that mixing to 250 m *via* this mechanism was improbable. Although vertical isopycnal conditions were not observed at the outer station (RES-4) the water column was least stable between February and April. Convective cooling with vertical mixing would result in an increase in density, but this was not observed in the deep water during the winter months. The latter process appears to be limited to the upper 100 m in Resurrection Bay and the general depression of the isohaline (Fig. 12) - and therefore the isopycnal - lines below about 100 m between October and April, must result from the downwelling of less dense surface water. The more dense (σ_t>26.00, S > 33.00°/₀₀, T ∿5.0°C) water present in the outer reaches of the fjord during October has been swept down and out of the fjord by the downwelling of surface water. The densities (σ_t∿25.5) at 250 m at this station (RES-4) between February and April were similar to those on the adjacent continental shelf.

The erratic vertical excursions in the salinity and temperature isolines in the outer reaches of the fjord (RES-4) below 150 m during the winter months can be explained by advective processes. Although the sampling frequencies of the two data sets are different, a comparison of the salinity (density) and upwelling index variations as given in Figure 12 suggests that depressions in isohaline lines are preceeded by or coincide with downwelling (coastal convergence) conditions and, conversely, that elevations in isohaline lines follow or coincide with relaxations of downwelling conditions. The erratic vertical excursions of the isopleths appear to reflect the relative intensities of the coastal convergences. The accumulation of surface water at the coastline drives the dense bottom water out of the fjord; conversely relaxations of the coastal convergence permit more dense water to flow into the fjord from the adjacent Gulf.

Inner Fjord

At the inner station (RES-2.5), both the temperature and salinity time-series plots below about 150 m differ from those observed at the outer station discussed above. The only similarities are in the variations of the 32.00°/₀₀ isoline, which fluctuates between about 100 and 200 m. This implies that, between these depths, the same processes control the time distributions of salinity and density at these stations. The water masses advected through the outer fjord from the Gulf of Alaska penetrate the inner fjord across, and above, the sill (185 m). However, the more uniform decrease in salinities in the inner fjord basin (Figs. 9-11), suggests that water below the sill is generally not subjected to advective influxes. Although the probability of influxes into the inner basin is low during the oceanographic winter and spring months (because of less dense water on the adjacent shelf) occasional influxes have been observed. However, at these times, only some fraction of the basin water behind the sill was exchanged, in contrast to the complete advective replacement that takes place during September and October. Such "anomalous" influxes were observed during early winter (for example in December 1972 and 1973), when remnants of the summer upwelled water still existed on the adjacent shelf, and during spring (March 1973, April 1974, April and May 1975), when the density of the resident basin water had decreased, winter downwelling at the coastline had relaxed, and relatively more dense water appeared in the outer fjord.

The changes in temperature and salinity below the sill vary in a quasi-uniform fashion during the winter (October through April). The temperature distributions reflect warming of the deep water due to the downward penetration of heat from the temperature maximum created during the summer. Temperatures around the sill depth range between about 5.0 and 6.0°C by January. The rapid erosion of the warm water core throughout the winter by surface heat loss results in a decrease of the temperature around the sill to 3.5 to 4.5°C by mid-March. Temperatures at 280 m vary over a more narrow range ∿0.5°C compared to an ∿2.5°C range at the sill, over the approximate seven month winter period. Salinities decrease during the winter, and as with the temperatures, vary at the bottom of the basin over a narrow range ∿0.35°/₀₀ compared to an ∿0.70°/₀₀ variation around the sill over the same time period. The distributions of temperature and salinity in the deep waters of the inner basin during the winter (October through April; Figs. 29 through 31) result predominantly from a vertical turbulent exchange across the sill by mixing of the more dense (S ∿33.00°/₀₀ T ∿5.0°C) water advected into the basin during the summer with the less dense (S ∿32.00°/₀₀ to 32.50°/₀₀) (T ∿3.0 to 5.0°C) water found on the shelf during the winter.

Advective exchange of the deep water of the inner basin appears to begin again around May or June when the density of the resident basin water has decreased during the previous winter months by vertical mixing. Influxes were observed to penetrate to about 270 m in June and July of 1974, but amounted to only about 20% of the basin volume, although in May of 1975 approximately 90% of the basin water was replaced. The density of the marine source waters has increased sufficiently (σ_t>26.00) by September or possibly earlier to lead to the complete renewal of the deep and bottom waters of this basin.

This cycle of advective renewal of the deep water in the summer and fall followed by vertical eddy exchange throughout the winter months has been observed in the inner basin over a period of three years. The exchange processes are examined quantitatively below.

Vertical Turbulent Exchange Across the Sill

The rates of transfer of heat and salt are characterized by coefficients of eddy conductivity and eddy diffusion respectively. For any parcel of water, the determination of mixing coefficients from budget considerations depends upon the quantitative evaluation of all export and input terms (Sverdrup *et al.*, 1942). Salinity and temperature are conservative properties, i.e., they are changed by external processes only at boundaries and in the bulk of a fluid are affected by advection and diffusion only. Distributions of temperature and salinity have commonly been used to determine turbulent mixing coefficients. Rattray (1967) found, using similarity methods, that the rate of change of salinity in the deep water of fjords could be represented as a balance between horizontal advection and vertical diffusion. Unfortunately the contribution to the salt and heat budgets, in the deep water below the sill, from horizontal advection has been difficult to evaluate in Resurrection Bay. The stations in the inner basin reflected

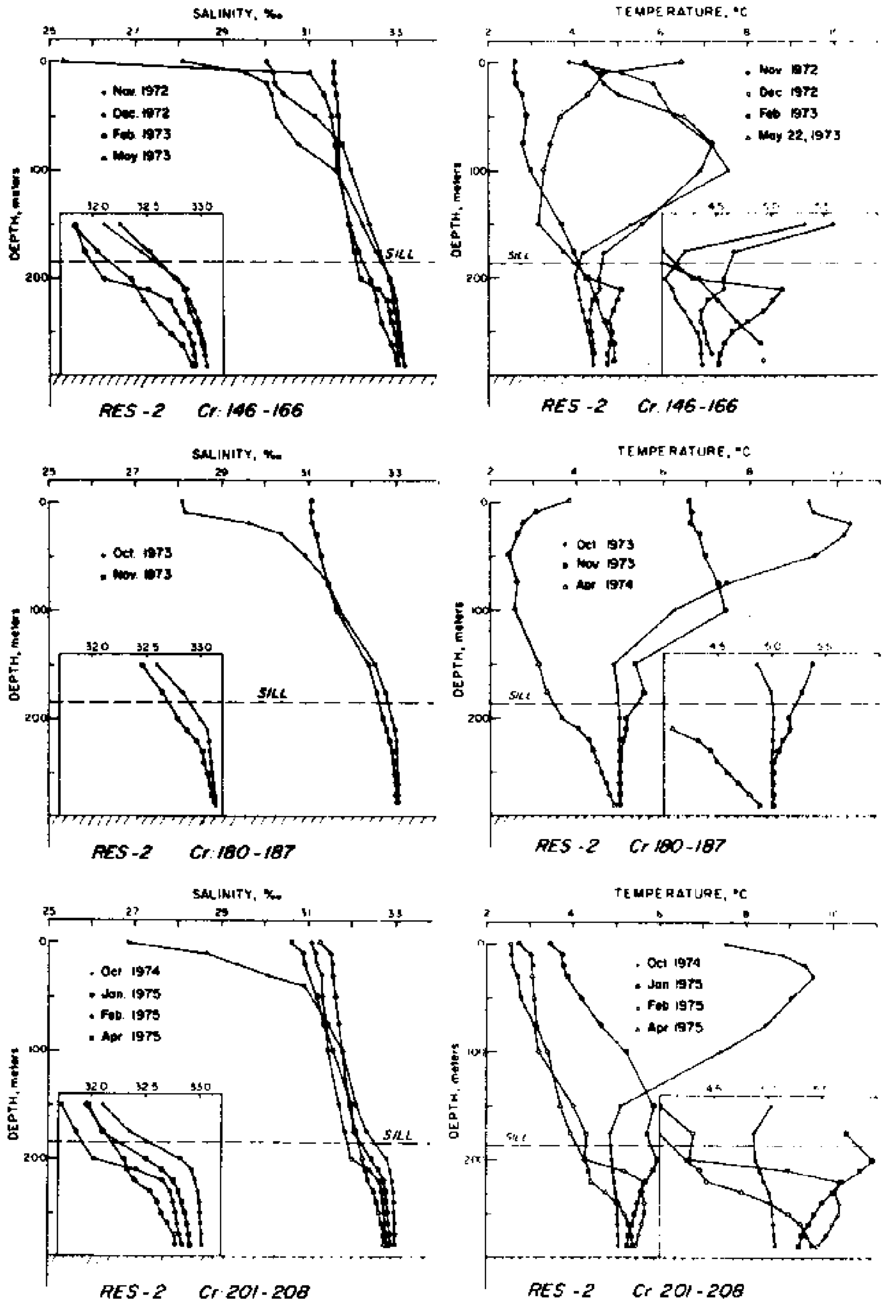

Figure 29. Detailed vertical profiles of temperature and salinity, RES-2, during oceanographic winter months.

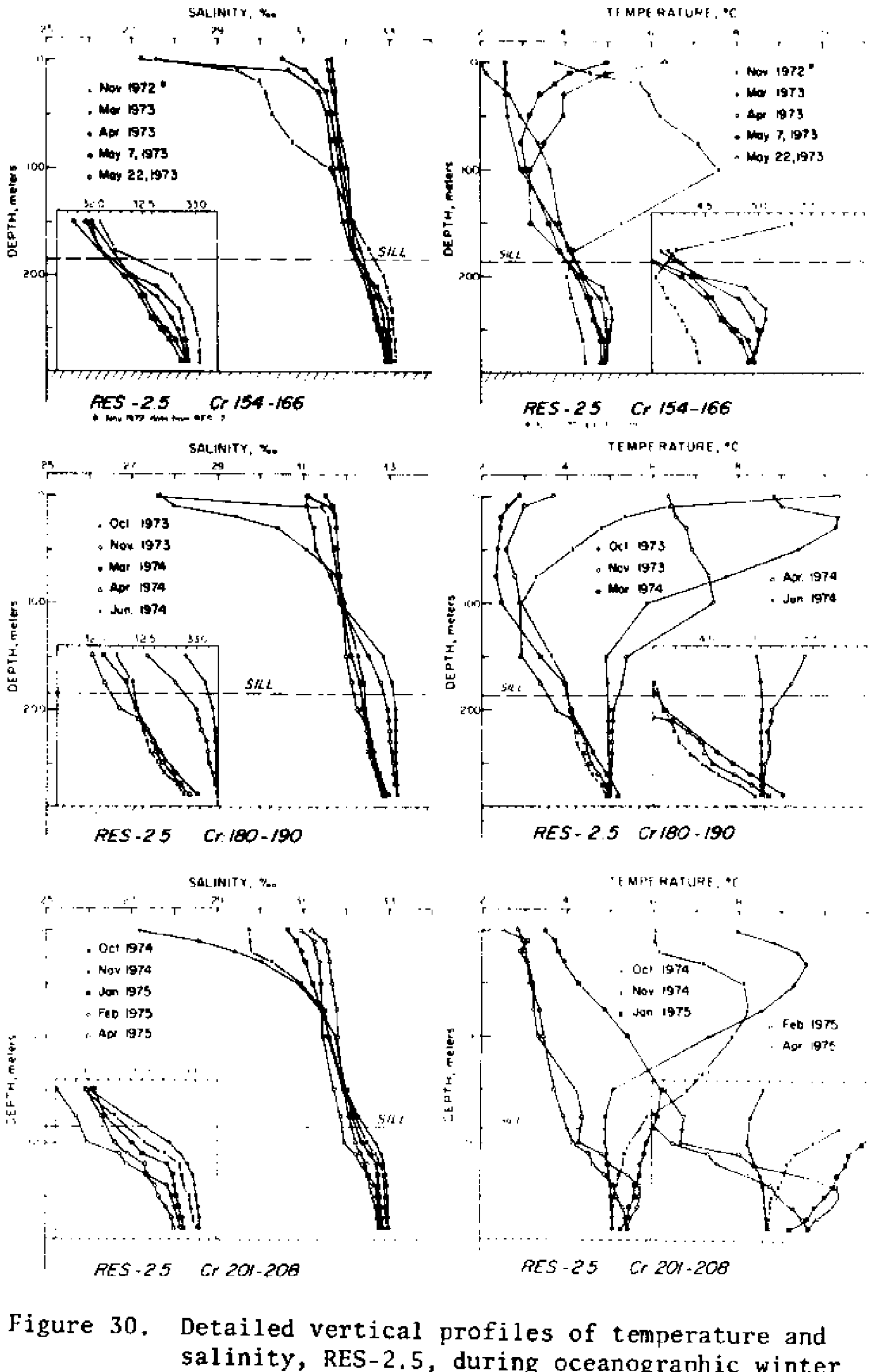

Figure 30. Detailed vertical profiles of temperature and salinity, RES-2.5, during oceanographic winter months.

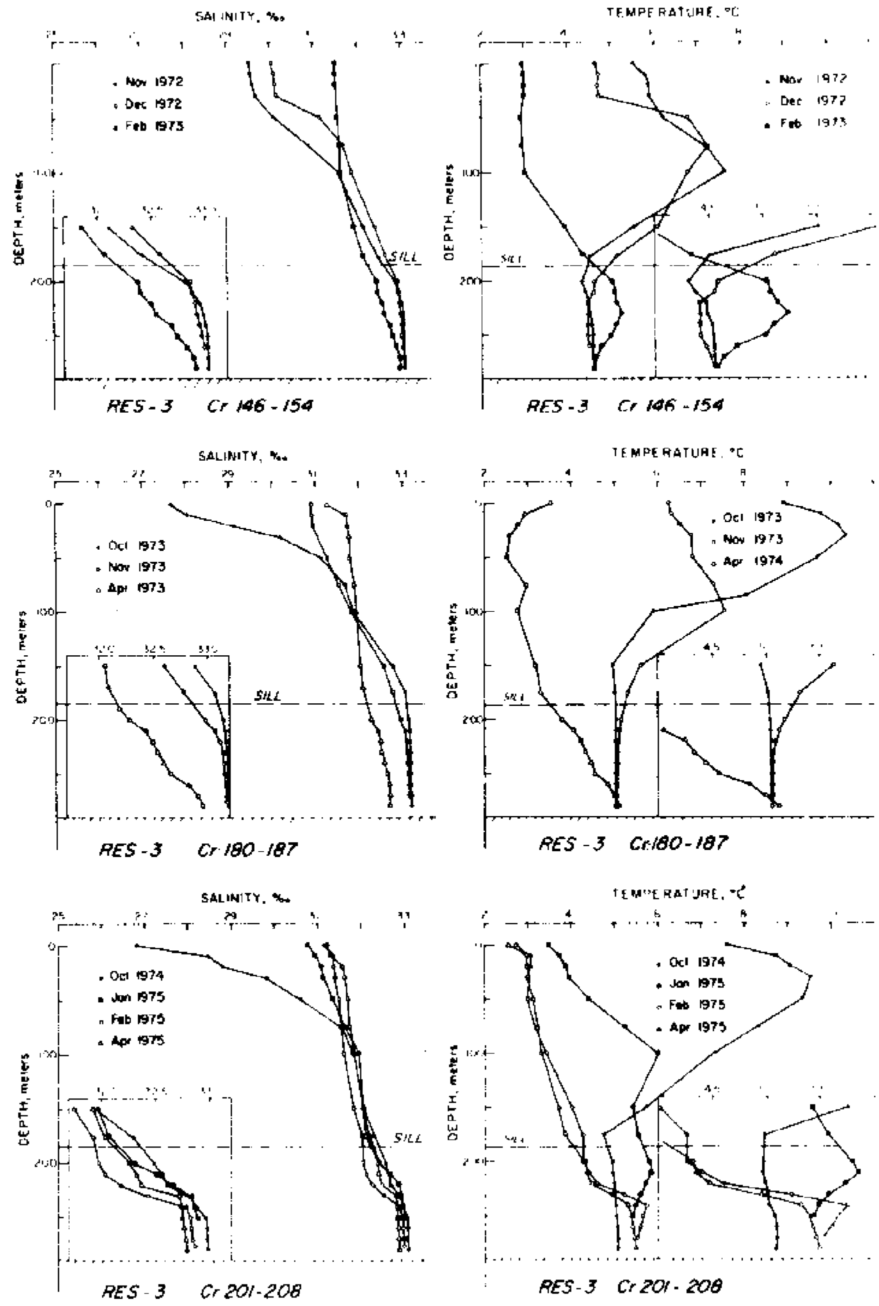

Figure 31. Detailed vertical profiles of temperature and salinity, RES-3, during oceanographic winter months.

reasonable homogeneity in temperature and salinity, although occasional analytically significant differences have been observed (see Appendix). There is no evidence for consistent longitudinal gradients in temperature or salinity and, in the absence of these, the horizontal advection term in the budget equation becomes insignificant. There is however, certainly some motion in this basin as evidenced by the varying slopes in the salinity (density) profiles below the sill, e.g., October 1974 (Fig. 24). The latter period however, was at the time of (or shortly after) extensive advective renewal of the deep water and it might be expected that dense water once advected into the basin would undergo some oscillatory motion until damped by friction. Mean flow at and above the sill depth during the winter months, may have also induced some compensating flow below the sill. However, the persistence of a vertical pycnocline through the sill depth region would tend to dampen any such flow, and part of the energy associated with horizontal flow, above the sill, would be redistributed into energy for vertical turbulent mixing across the pycnocline. Horizontal motion in the basin (excluding direct influxes of dense water across the sill) may be convective in nature, resulting from longitudinal temperature and salinity differences, or be of a seiche-type generated by intermittent surges in horizontal flow above the sill. The distributions of salinity and temperature during the winter months may be expressed as one-dimension diffusion equations, where lateral and horizontal advection and diffusion terms and vertical advection may be neglected.

The simplified salt balance equation is:

$$\frac{\delta \bar{S}}{\delta t} = -\frac{\delta}{\delta Z} (K_z \frac{\delta \bar{S}}{\delta Z})$$

where Z is depth, $\frac{\delta \bar{S}}{\delta t}$ the rate of change of salinity, K_z the vertical mixing coefficient and $\frac{\delta \bar{S}}{\delta z}$ the salinity gradient. The heat budget equation is similar but, S (salinity) is replaced by the product of Cp (specific heat) and T (temperature). The rate of loss of salt from a parcel of water bounded by the sill depth and the basin floor is then given (assuming no salt flux across the basin floor) by:

$$\int_{\text{bottom}}^{\text{sill}} \frac{\delta(\rho\bar{S})}{\delta t} \cdot dZ = K_z \frac{\delta S}{\delta Z} \text{ (sill)}$$

i.e., the rate of salt loss is the product of the vertical diffusion coefficient at the sill and the average gradient of salinity across the sill between the time periods of the observations. Equations of this type have been used to compute coefficients $K_z(S)$ and $K_z(T)$ at the sill depth (Table 4). As it was difficult to define exactly where the transition between the advective and diffusive regimes occurs, gradients have generally been determined over about a 40-m depth interval (180 to 220 m) encompassing the actual sill depth (185 m), and are subject to about a 20% error.

The calculated coefficients of Table 4 are within the general range of vertical eddy mixing coefficients determined by Craig (1969) of 0.1 to 10 $cm^2\ sec^{-1}$. They are consistent with coefficients determined in similar deep-silled basins, e.g., Sholkovitz and Gieskes (1971), of 4 to 6 $cm^2\ sec^{-1}$, but are higher than those determined in basins where vertical diffusional exchange is suppressed by a pycnocline. Spencer and Brewer (1971), found $K_Z = 0.14\ cm^2\ sec^{-1}$, in the main halocline of the Black Sea, and Fanning and Pilson (1972) determined a minimum $K_Z = 0.06\ cm^2\ sec^{-1}$, in the upper 700 m of the Cariaco Trench.

Vertical Advective Exchange Across the Sill

It was noted earlier that occasionally during the winter months the density of the water in the basin behind the sill increases. This can only be explained by the advective input of water located beyond the sill having a density greater than the density of the resident basin water. Advected horizontally across the sill, the dense water can then sink to a level of equal density within the basin. This section examines the volumes of water involved, and the vertical advective velocities associated with this type of exchange.

Advective exchanges of this type, other than the complete replacement of the basin water between September and October, are intermittent in character. Often, between two time periods when the density of the basin water had

TABLE 4

Coefficients of Eddy Diffusion and Conductivity at 200m, RES-2.5

Cruise	and Date	$K_z(S)$ $cm^2\ sec^{-1}$	$K_z(T)$ $cm^2\ sec^{-1}$
146	November 21, 1972		
		1.2	9.2*
148	December 9, 1972		
		3.1	-11.1**
154	February 3, 1973		
160	March 14, 1973		
		2.5	2.2
161	April 3, 1973		
		2.2	2.9
163	May 7, 1973		
		4.5	3.1
166	May 22, 1973		
180	October 9, 1973		
		6.7	6.1
182	November 17, 1973		
183	December 17, 1973		
		7.3	-29.9**
186	March 27, 1974		
		4.2	6.3
186#	April 15, 1974		
187	April 21, 1974		
		1.9	2.5
190	June 10, 1974		
201	October 18, 1974		
		2.1	7.2
203	November 26, 1974		
		1.6	6.4
204	January 21, 1975		
		4.4	-24.6**
206	February 27, 1975		

* Significant longitudinal temperature differences suggest a contribution from horizontal advection.

** Gradients in the temperature distributions change sign which introduces large uncertainties into the time average.

Single lines indicate partial advective replacement of deep basin water.

Double lines indicate complete advective replacement of deep basin water.

increased, there was no evidence of water at the outer station (RES-4) around the sill depth of a density high enough to penetrate into the basin (e.g., Cruise No. 160, March, 1973; Cruise No. 192, June, 1974; Cruise No. 8, April, 1975). This means that the dense water has, at some time between the two measurement periods, been advected across the sill to penetrate into the basin and has then been rapidly removed from the outer fjord. Such reasoning is consistent with the erratic and rapid changes in the isohaline and isothermal surfaces (Fig. 12), and density changes observed at RES-4 as discussed earlier.

The following computations have utilized data from RES-2.5 and are believed to be representative of the inner basin. Two approaches have been adopted which differ only in the form of the advection term. Equations may be written for the salt budget which state that the observed salt change between any two time periods is a contribution from an increase by advection across the sill, and a loss across the sill by diffusion. Each of the terms in the following expressions are explained in detail and examples of the computations given in Heggie (1977). The effect on the temperature and salinity profiles of the advective influx of more dense water into the fjord is illustrated in Figure 32.

The advective contribution in the first approach is expressed as a product of the difference between the average salinities of the influxed and the effluxed basin water, and a transport (volume/time). For a unit horizontal cross-sectional area the budget equation is:

$$\int_{\text{bottom}}^{\text{sill}} \frac{\delta S}{\delta t}\, dZ = (\bar{S}_I - \bar{S}_E)\, \frac{1}{\Delta t} \int_{o}^{h} dZ - K_z \int_{\text{bottom}}^{\text{sill}} \frac{\delta^2 S}{\delta Z^2}\, dZ$$

The time change and diffusive terms and both S_I and S_E were evaluated from the observed salinity distributions. Solution of the equation yields a volume of water influxed into the basin and an average vertical velocity.

The second approach expresses the advection term as a product of a vertical velocity W_z and a salinity gradient, $\frac{\delta S}{\delta Z}$:

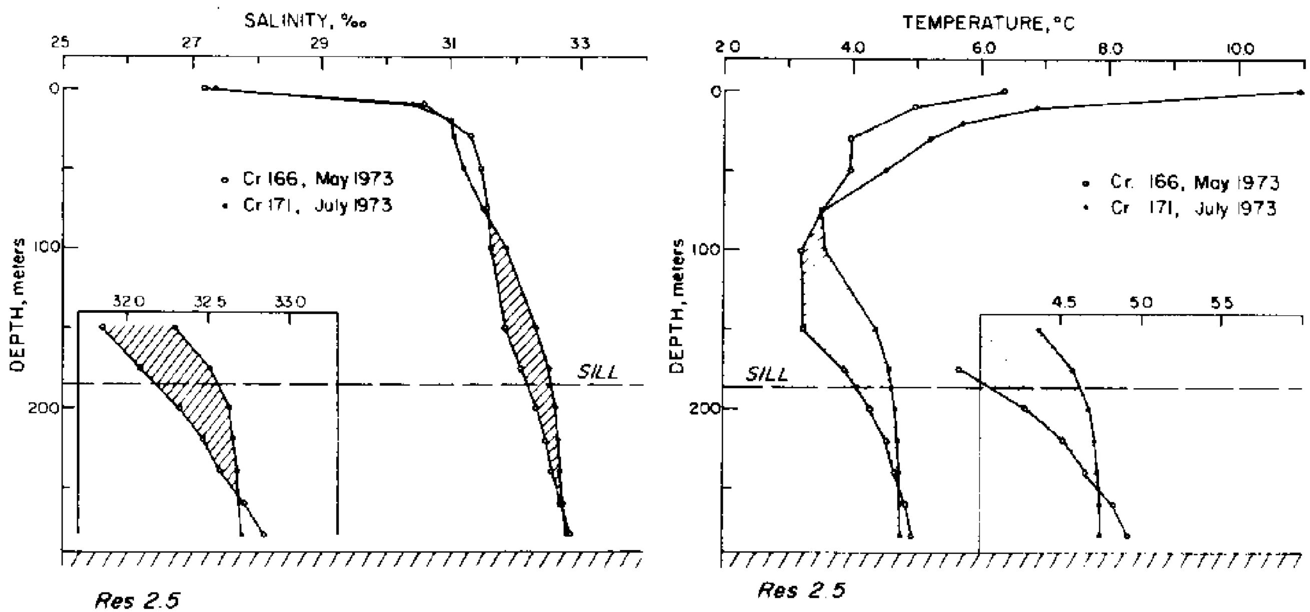

Figure 32. Vertical salinity temperature profiles May and July 1973 at RES-2.5 showing effects of advective influx.

$$\int_{Z^*}^{\text{sill}} \frac{\delta S}{\delta t}\, dZ = W_z \int_{Z^*}^{\text{sill}} \frac{\delta S}{\delta Z}\, dZ - K_z \int_{Z^*}^{\text{sill}} \frac{\delta^2 S}{\delta Z^2}\, dZ.$$

Z^* is the depth to which the influx penetrates, identified as the depth at which there is no density change between the two time periods. The equation is solved first for W_z, and the volume of water influxed into the basin is then $W_z \times \Delta t \times$ horizontal cross-sectional area.

Some assumptions and boundary conditions common to both approaches are:

1. The influx continues for the total time period between observations. This assumption, however, does not represent a realistic physical situation. The consequences of this are discussed later.
2. W_z and K_z are constant between the sill depth and depth of penetration of the influx over the time period of the influx.
3. Horizontal and lateral advection and diffusion terms are small compared to the vertical terms.
4. There is no salt or heat exchange across the basin floor.

The volumes of water and the vertical velocities associated with the advective exchanges are listed in Tables 5 and 6.

The current meter data (Table 3) were used to compute the volume and the vertical velocity of the water advected through the basin during the advective exchange of 1973. The cross-sectional area of the inner basin between the sill depth and basin floor is about 2.5×10^5 m^2 and this, combined with an average north (inward) speed of 2.52×10^{-2} m sec^{-1}, results in a transport of about 6×10^3 m^3 sec^{-1}. Over 35 days (length of current meter record) this is equivalent to a volume of about 2×10^{10} m^3; sufficient to replace the topographic basin volume ($\sim 3.5 \times 10^9$ m^3) about five times over. If it is assumed that the transport (6×10^3 m^3 sec^{-1}) falls vertically through a horizontal cross-sectional area encompassed by the sill depth contour ($\sim 5 \times 10^7$ m^2), the vertical velocity is:

$$\frac{6 \times 10^3 \text{ m}^3 \text{ sec}^{-1}}{5 \times 10^7 \text{ m}^2}$$

TABLE 5

Percent Volumes of Water Displaced During an Advective Influx to The Inner Fjord Basin

Cruise and Date			Method 1		Method 2	
			Salt	Heat	Salt	Heat
154	February	3, 1973	50%	74%	40%	50%
160	March	14, 1973				
166	May	22, 1973	60%	62%	82%	82%
171	July	6, 1973				
182	November	17, 1973	†—	45%	50%	—*
183	December	17, 1973				
187	April	21, 1973	22%	17%	30%	33%
190	June	10, 1974	17%	18%	12%	14%
192	June	28, 1974	20%	22%	15%	32%
195	July	25, 1974				
206	February	27, 1975	41%	34%	27%	29%
208	April	9, 1975	95%	83%	-ξ	-ξ
210	May	13, 1975				

*Computations break down as ΔT sill/Z^* $\rightarrow$ limit of precision of measurements.

†Computations break down as $(\overline{S}_I - \overline{S}_E) \rightarrow$ limit of precision of measurements.

ξComputations break down as ΔT sill/Z^* and ΔS sill/Z^* $\rightarrow$ limit of precision of measurements.

Single lines indicate extensive summer renewal of the deep water.

TABLE 6

Vertical Advection Velocities Associated with Influxes to the Deep Basin

	Method 1.				Method 2.			
	Salt Budget		Heat Budget		Salt Budget		Heat Budget	
CRUISE	$cm\ s^{-1}$ ($x\ 10^{-3}$)	$m\ yr^{-1}$	$cm\ s^{-1}$ ($x10^{-3}$)	$m\ yr^{-1}$	$cm\ s^{-1}$ ($x10^{-3}$)	$m\ yr^{-1}$	$cm\ s^{-1}$ ($x10^{-3}$)	$m\ yr^{-1}$
154								
	1.5	477	2.2	703	1.2	380	1.5	464
160								
166								
	1.6	491	1.6	491	2.1	657	2.1	657
171								
182								
	---		1.8	599	1.9	599	---	
183								
187								
	0.5	158	0.4	119	0.7	233	0.8	241
190								
	1.1	333	1.1	333	0.8	234	0.9	281
192								
	0.8	254	0.9	292	0.6	190	1.3	420
195								
206								
	1.2	377	0.9	272	0.8	234	0.8	234
208								
	2.6	806	3.0	947	---		---	
210								

which is numerically equal to 1.2 10^{-2} cm sec^{-1} or approximately 4000 m/yr.

A comparison of this computed vertical velocity with those listed in Table 6 shows it to be about an order of magnitude higher. It should be noted however, that the velocities listed in the table were computed assuming the influx took place over the total time period between observations and this is unrealistic. The record show that influxes were not continuous, but the time period over which each influx occurred was impossible to determine precisely. This probably depends upon the relative intensity of the driving force responsible for elevating the more dense water above the sill and maintaining it there so that inflow into the basin can occur. Some clues to the time scale of these sporadic influxes however were obtained from the March to May current meter record at the sill (185 m), which showed horizontal excursions across the sill into the inner basin that persisted for one to two days only. Assuming that when more dense water appeared at the sill it was advected into the basin over similar time periods, the velocities reported in Table 6, would have to be increased about one order of magnitude. Velocities adjusted this way agree reasonably well with that computed directly from the September through October current meter records.

Biological Oxygen Consumption Rates

Organic carbon either produced *in situ* in surface waters by photosynthesis or introduced as terrestrial runoff in coastal waters becomes a source of food for heterotrophic organisms. If the organic carbon supply rate is greater than the rate of supply of molecular oxygen, the activities of the heterotrophs may rapidly reduce the oxygen levels, and anoxic conditions can result. The latter are rarely found in the water column, except in deep basins with restricted circulation, e.g., Cariaco Trench, Black Sea, and Lake Nitinat, but often develop in near surface sediments. Oxygen consumption rates are important in controlling the flux of carbon through the hydrosphere. The following analyses present average oxygen consumption rates in the water column of the inner basin of this Alaskan fjord.

Figures 14 through 17 show that immediately after the advective replacement of the basin water in September and October, the oxygen levels were around 4.0 ml ℓ^{-1}. Throughout the following winter months oxygen levels at the sill increased to about 7.0 ml ℓ^{-1}, but deep in the basin (280 m) they decreased to about 1.0 ml ℓ^{-1} by March or April. A gradient directed into the basin developed and intensified between October and April. It should be noted that the total quantity of oxygen in the basin during September and October was approximately equal to that in the basin during March and April. However, the marked changes in the vertical distribution with time reflect contributions from input and export processes. It is proposed that such distributions are a balance between input across the sill by vertical eddy mixing and losses due to biological consumption in the basin. The following equation expresses this:

$$\int_{\text{bottom}}^{\text{sill}} \frac{\delta O_2}{\delta t}\, dZ = -\int_{\text{bottom}}^{\text{sill}} \frac{\delta}{\delta Z}\left(K_Z \frac{\delta O_2}{\delta Z}\right) dZ + \int_{\text{bottom}}^{\text{sill}} R\, dZ$$

If the diffusive input is greater than the time change term, R is negative and represents a net consumption. The general depth distributions of oxygen at the three stations in this basin were all similar. Some longitudinal differences, however, were observed which may be the result of spatial differences in consumption rates related to sources of supply of organic carbon.

Oxygen budgets have also been considered during the time periods when advective replacements of water across the sill occurred. The budget can be written in the following form, again assuming no longitudinal or lateral contributions:

$$\int_{\text{bottom}}^{\text{sill}} \frac{\delta O_2}{\delta t}\, dZ = \{\bar{O}_{2(I)} - \bar{O}_{2(E)}\} \frac{1}{\Delta t} \int_{o}^{h} dZ - K_z \int_{\text{bottom}}^{\text{sill}} \frac{\delta}{\delta Z}\left(\frac{\delta O_2}{\delta Z}\right) dZ + \int_{\text{bottom}}^{\text{sill}} R\, dZ$$

The advective contribution to the oxygen budget has been computed by comparing the oxygen concentration of the water advected ($O_{2(I)}$) into the basin with the average oxygen concentration of water effluxed ($O_{2(E)}$) from the basin. Average water column oxygen consumption rates are listed in Table 7. The consumption rates determined for periods of advective exchange, are consistent with the one-dimension diffusion model and are marked with an asterisk in this table. These data are compatible with average consumption rates determined from other fjords. For example, Barnes and Collias (1958) found rates varying between 1.8 and 7.3 ml ℓ^{-1} yr^{-1} in Tofino Inlet, British Columbia. The rates determined in this study vary between 1.1 and 7.6 ml ℓ^{-1} yr^{-1}. There appears to be no significant seasonal variations in oxygen consumption rates, but these latter would be expected to be highest during summer months when surface primary productivities, hence particulate organic carbon fluxes through the water column are highest.

Calculations based upon a simplistic model of the degradation of particulate organic matter in seawater, indicated that approximately 60% of the mean summers primary productivity was oxidized in the water column and about 40% therefore escaped degradation to settle onto the sediment surface (Heggie, 1977).

TABLE 7

Deep Water Biological Oxygen Consumption Rates

Resurrection Bay Station 2.5

Cruise and Date			Consumption Rate $ml\ cm^{-2}\ yr^{-1}$	Consumption Rate $ml\ \ell^{-1}\ yr^{-1}$
160	March	14, 1973	15.	1.5
161	April	3, 1973	17.	1.7
163	May	7, 1973	11.	1.1
166	May	22, 1973		
180	October	9, 1973		
			15.	1.5
182	November	17, 1973		
*			42.	4.2
183	December	17, 1973		
			39.	3.9
186	March	27, 1974		
			55.	5.5
186#	April	15, 1974		
187	April	21, 1974		
			23.	2.3
190	June	10, 1974		
*			52.	5.2
192	June	28, 1974		
*			26.	2.6
195	July	25, 1974		
201	October	18, 1974		
			69.	6.9
203	November	26, 1974		
			69.	6.9
204	January	21, 1975		
			18.	1.8
206	February	27, 1975		
*			76.	7.6
208	April	9, 1975		
*			28.	2.8
210	May	13, 1975		

*Advective contribution to the oxygen budget accounted for.

NUTRIENT CHEMISTRY

BACKGROUND

Over the period November 1972 through May 1975, analysis of seawater samples for nutrients, nitrate, ammonia, phosphate and silicate, have been carried out from many of the cruises as listed in the key index (Table 2).

Oxidized forms of nitrogen, phosphorus and silicon are found in the sea at the micromolar concentration level. These elements are an essential requirement for phytoplankton growth, and together with carbon dioxide extracted from seawater, carbon, nitrogen and phosphorus are incorporated into living cells. The composition of "average" organic matter in plants has these elements existing in the approximate ratios; C:N:P::106:15:1 (Redfield *et al.*, 1963).

The nutrients are depleted from seawater during periods of rapid phytoplankton growth, transferred to higher trophic levels by the activities of grazing zooplankton and other animals, recycled in the euphotic zone by excretion from plants and grazers, and removed from this zone to the deep sea by sinking of dead plants and animals, fecal pellets, and actively migrating zooplankton (Raymont, 1963). Dead plants and animals, and fecal pellets sinking out of the euphotic zone are subject to bacterial oxidation throughout the water column. As long as oxygen is available as the preferred electron acceptor the oxidation of organic matter proceeds according to the scheme outlined by Richards (1965) and, together with carbon dioxide, remineralized (oxidized) forms of nitrogen, phosphorus, and silicon are returned to the deep water. This continuous cycle of uptake and regeneration between the surface water and deep waters of the world's oceans and estuaries explains the widespread observation of generally lower concentrations of these elements in surface compared with deep waters.

This section describes the major features of the distributions of nitrate, ammonia, phosphate and silicate in Resurrection Bay. Nutrient data were not collected as extensively as the hydrographic data and the nature of these data are such that only the most general description of the processes controlling concentrations and distributions are possible. As with the hydrography, the data assembled are principally from two stations: RES-4, representative of the outer reaches, and RES-2.5, representative of the inner fjord basin. Depth distributions of nitrate, phosphate, silicate, and ammonia at station RES-4 are shown in Figures 33 through 37, and for RES-2.5 in Figures 38 through 42. The seasonal variations of nitrate, phosphate, and silicate at RES-2.5 are given in Figure 43, and at RES-4 in Figure 44. Longitudinal profiles for these nutrients have also been prepared for those periods when data was obtained from all stations. Such profiles for nitrate are given as Figures 45 and 46, for phosphate, Figures 47 and 48, and for silicate, Figures 49 and 50.

RESULTS

Water Column

Nitrate

The concentrations of nitrate (NO_3^-) reported include nitrite (NO_2^-), and these varied between <1.0μ M in surface waters during spring and summer months to greater than 60μ M in bottom waters of the inner basin during the winter months. Surface waters <50 m were depleted to concentrations generally less than about 5μ M during the summer months throughout the fjord. Nitrate began to increase in the surface water during the fall and early winter months when phytoplankton uptake was diminished. The highest concentrations, 15 to 20μ M of nitrate in the fjord surface waters were found during mid-winter and early spring months (January-March). Concentrations of nitrate in the deep waters, >150 m, varied between about 15μ M and 60μ M. Minimum concentrations were found during the winter months at the outer station (RES-4) but, conversely, maximum concentrations occurred during the winter months in the bottom waters of the inner basin.

Silicate

Silicon in seawater, occurs as orthosilicic acid H_4SiO_4. Silicate concentrations in Resurrection Bay varied between about 2μ M in the surface water during the summer months to greater than 55μ M in bottom waters during the winter months. Surface waters along the length of the fjord had highest silicate concentrations during the winter and early spring

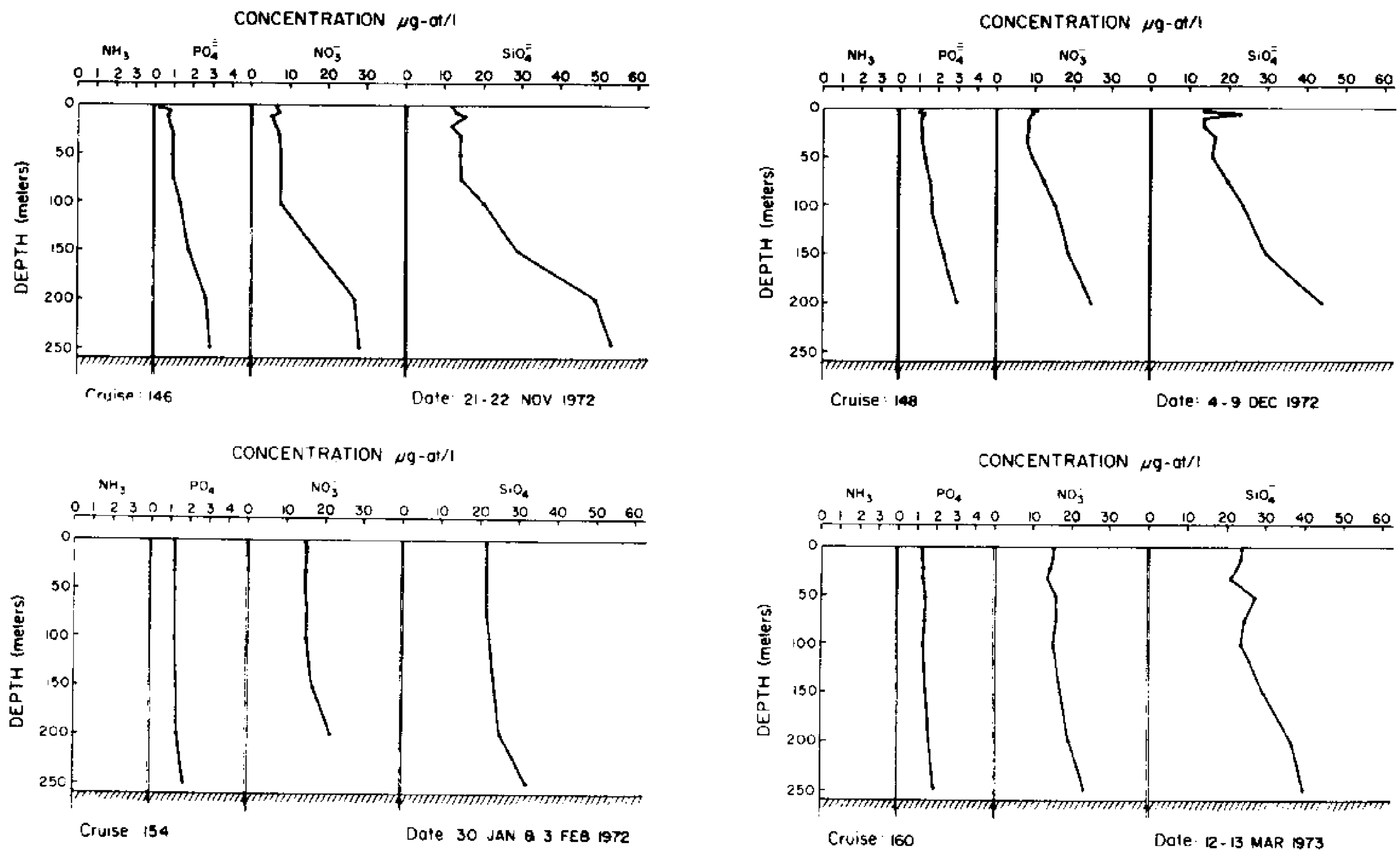

Figure 33. Vertical profiles of ammonia, phosphate, nitrate, and silicate, RES-4, November 1972 - March 1973.

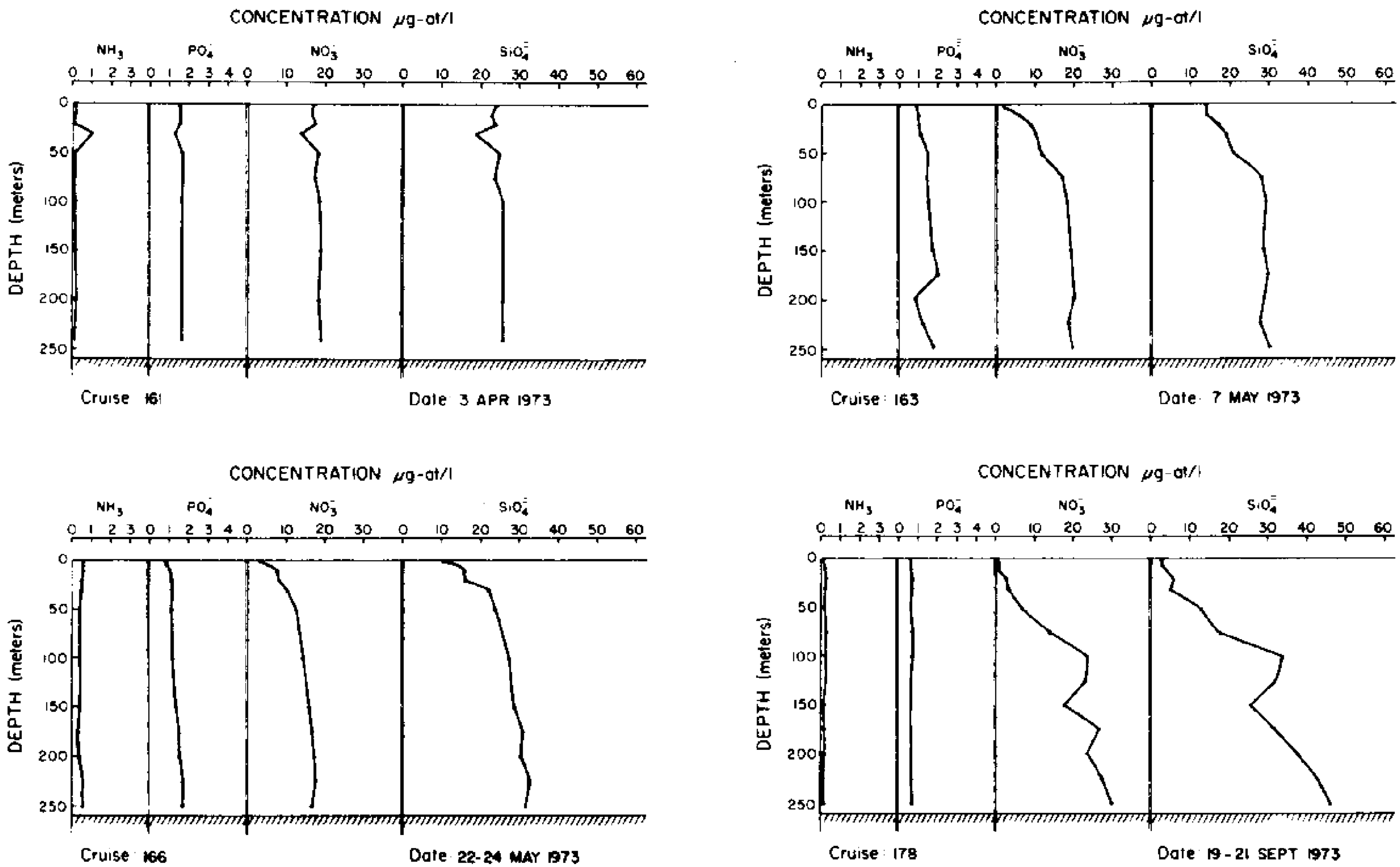

Figure 34. Vertical profiles of ammonia, phosphate, nitrate, and silicate, RES-4, April 1973 - September 1973.

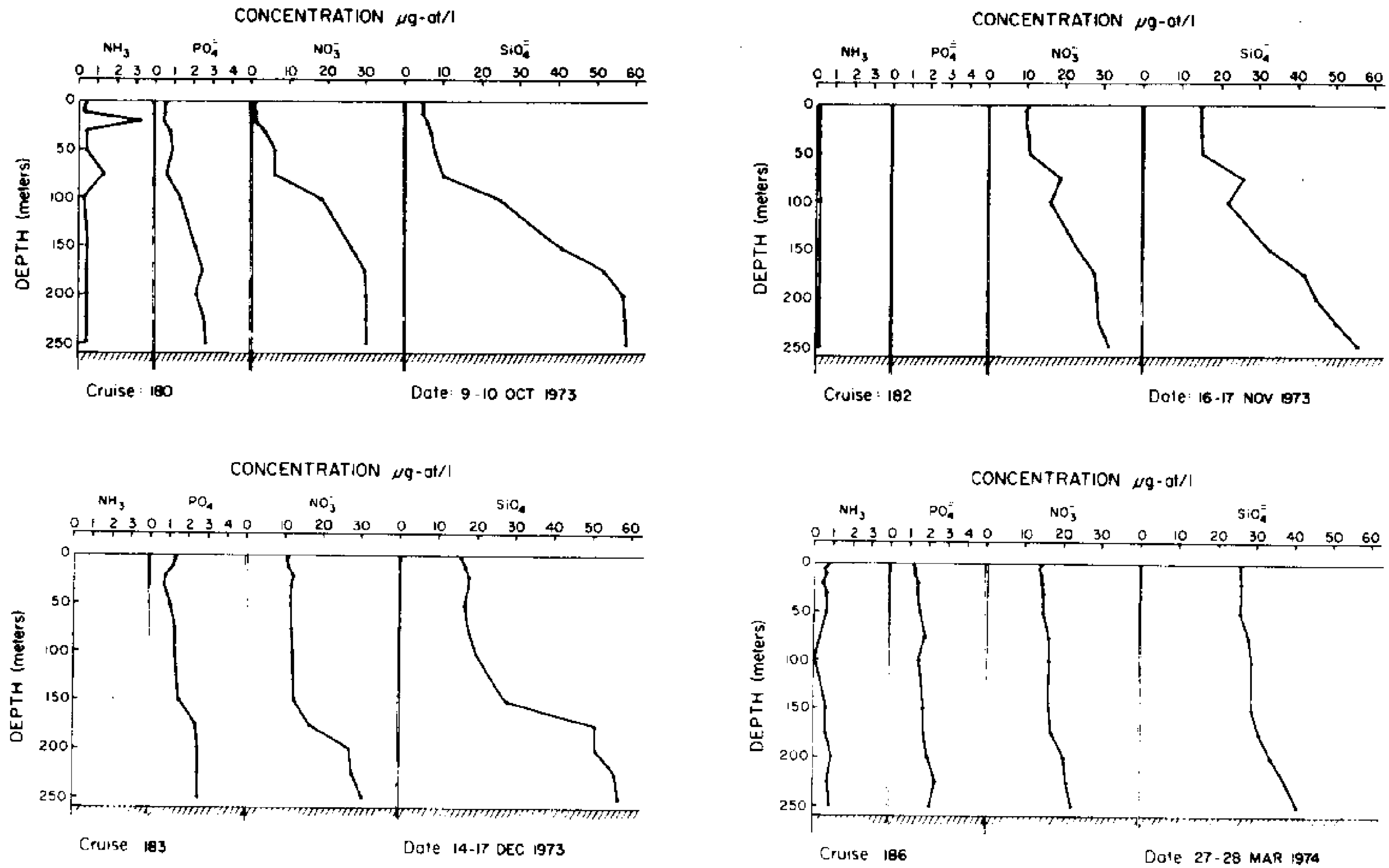

Figure 35. Vertical profiles of ammonia, phosphate, nitrate, and silicate, RES-4, October 1973 - March 1974.

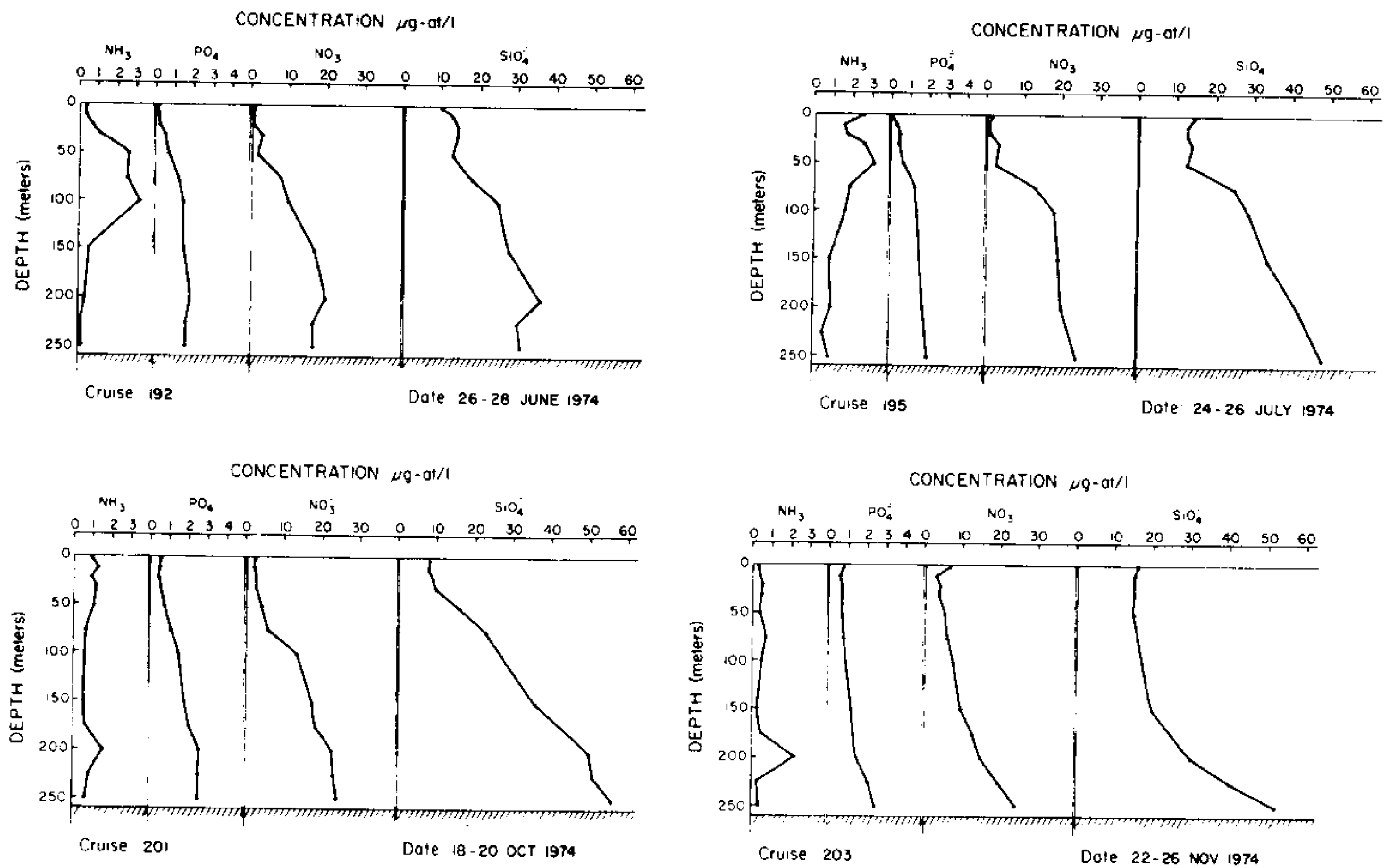

Figure 36. Vertical profiles of ammonia, phosphate, nitrate, and silicate, RES-4, June 1974 - November 1974.

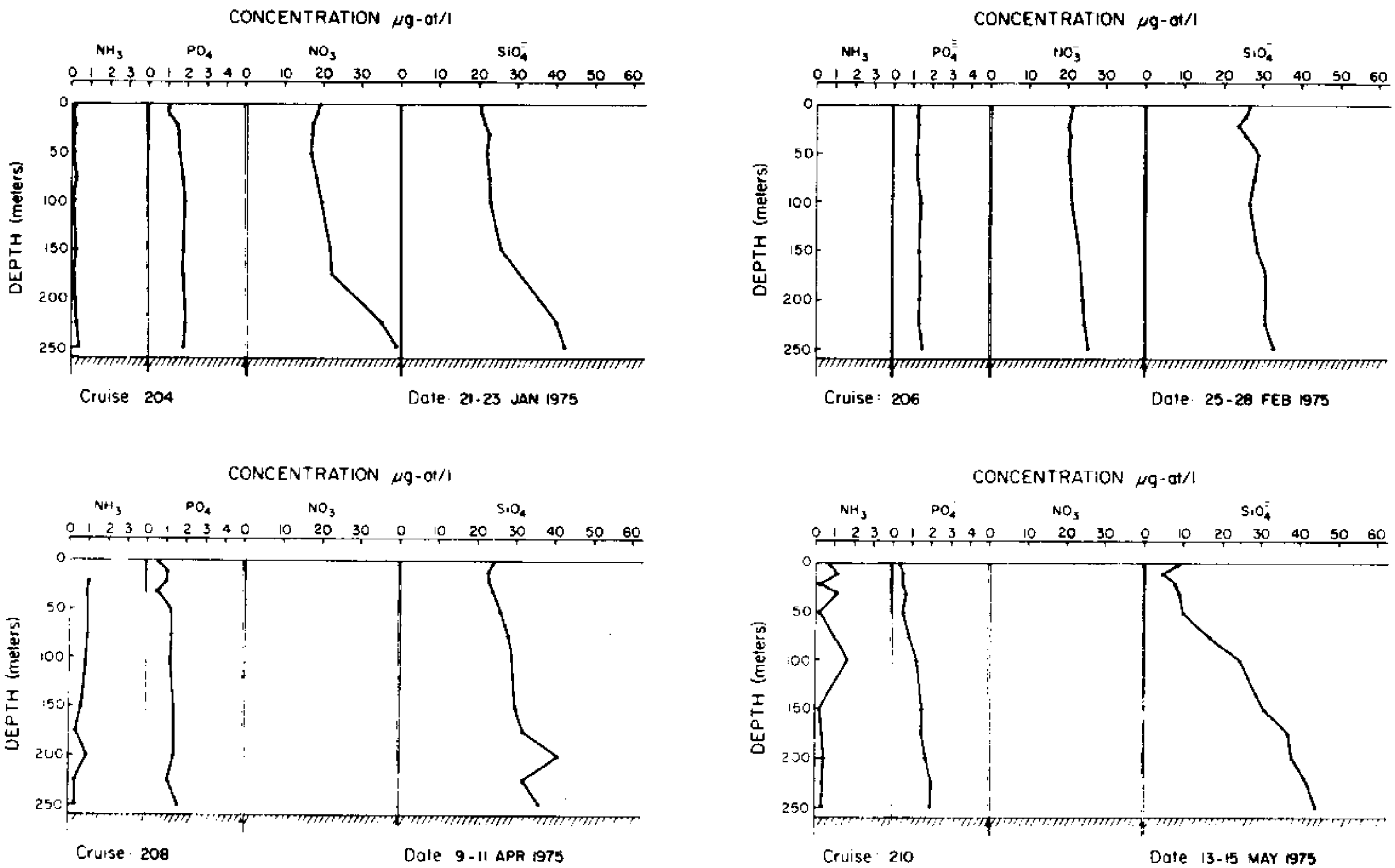

Figure 37. Vertical profiles of ammonia, phosphate, nitrate, and silicate, RES-4, January 1975 - May 1975.

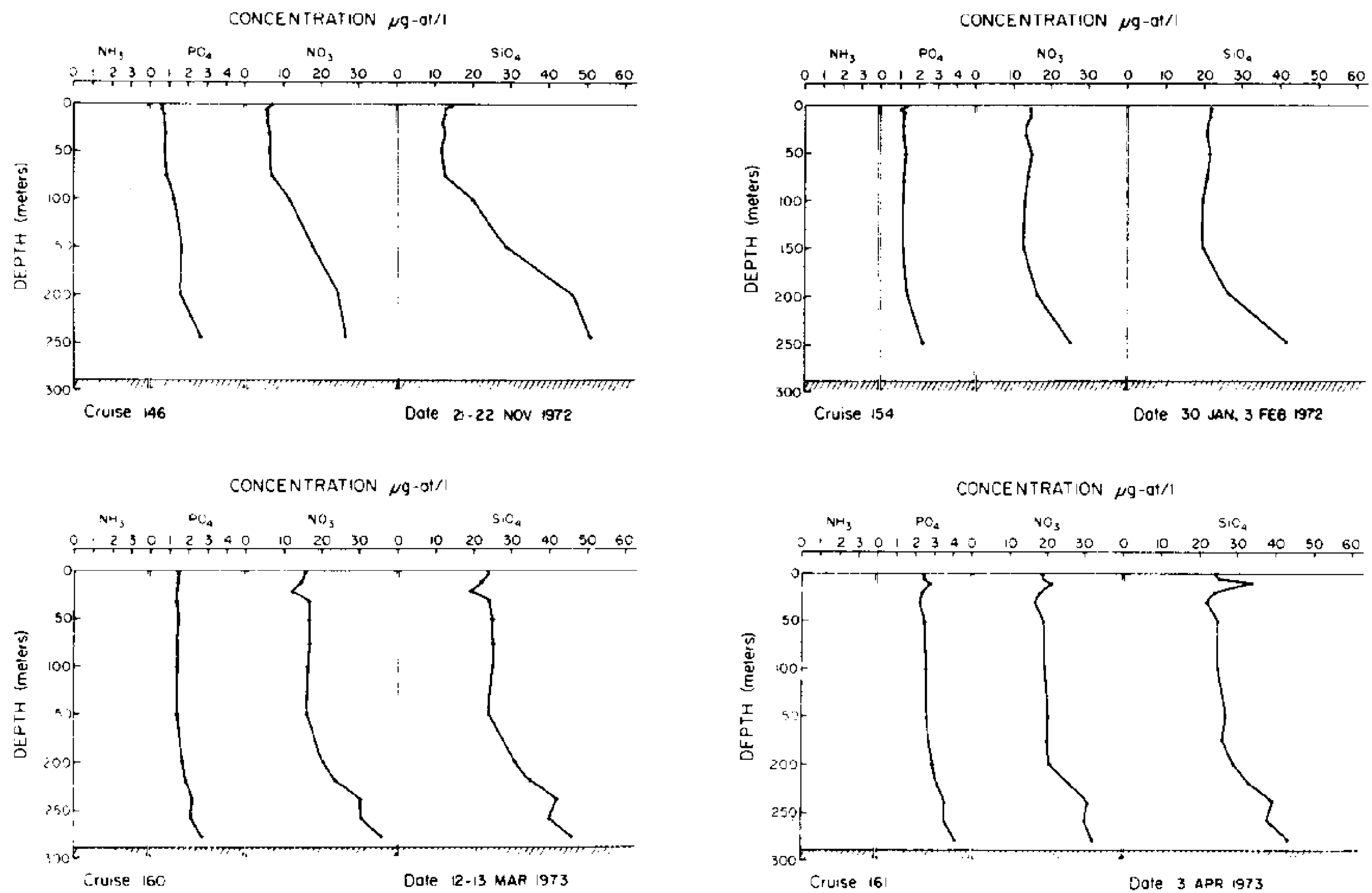

Figure 38. Vertical profiles of ammonia, phosphate, nitrate, and silicate, RES-2.5, November 1972 - April 1973.

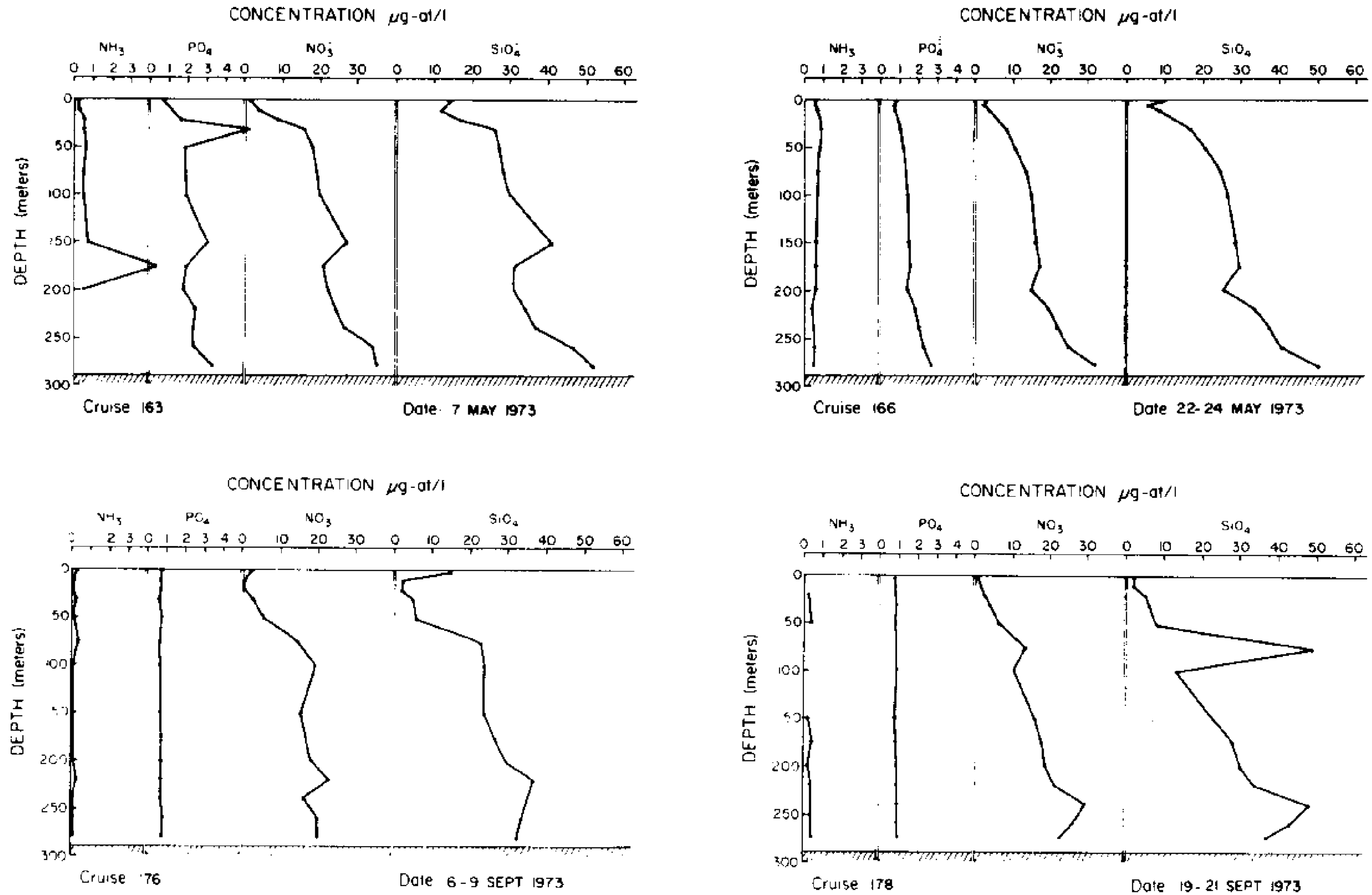

Figure 39. Vertical profiles of ammonia, phosphate, nitrate, and silicate, RES-2.5, May 1973 - September 1973.

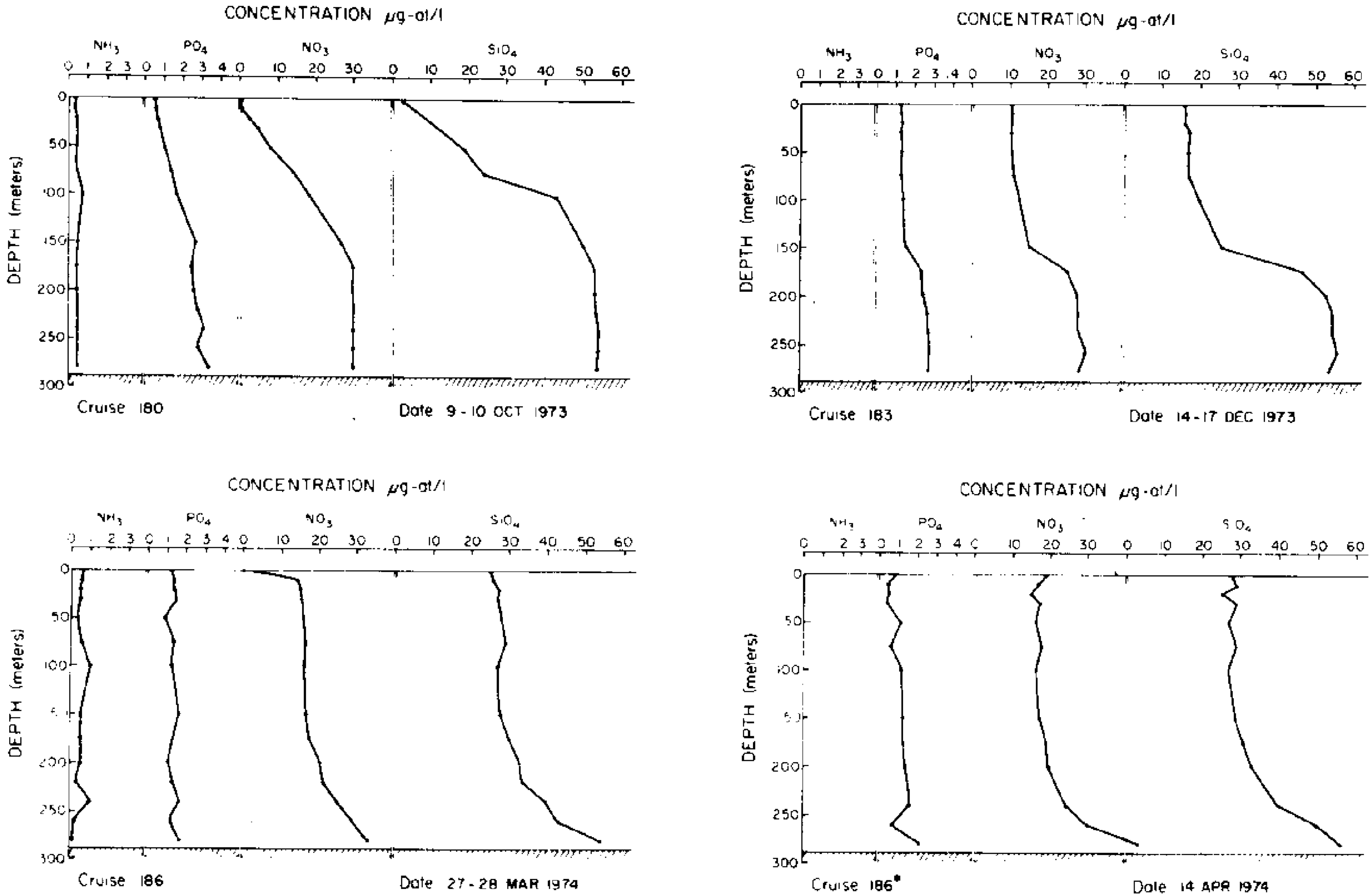

Figure 40. Vertical profiles of ammonia, phosphate, nitrate and silicate, RES-2.5, October 1973 - April 1974.

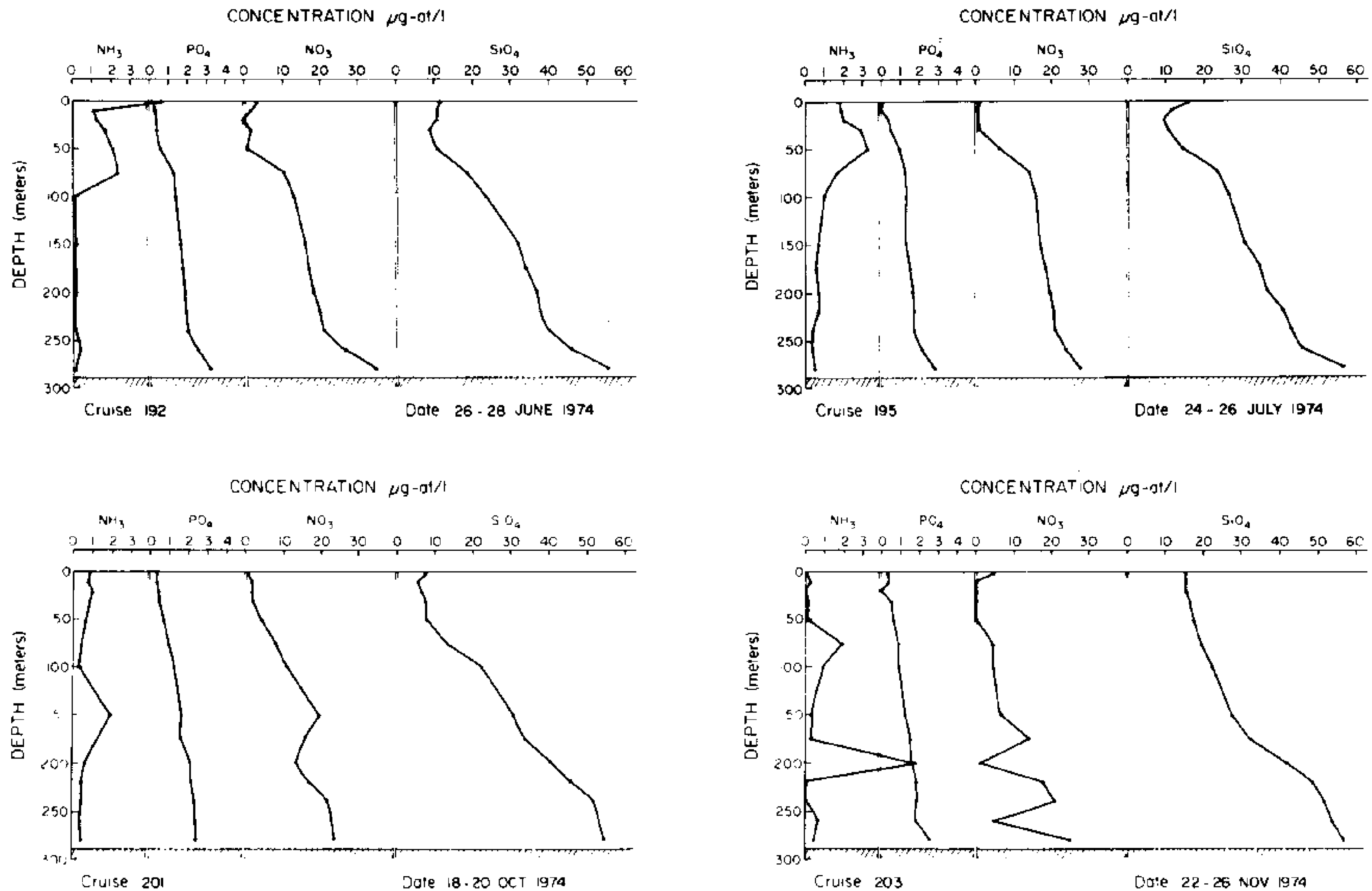

Figure 41. Vertical profiles of ammonia, phosphate, nitrate, and silicate, RES-2.5, June 1974 - November 1974.

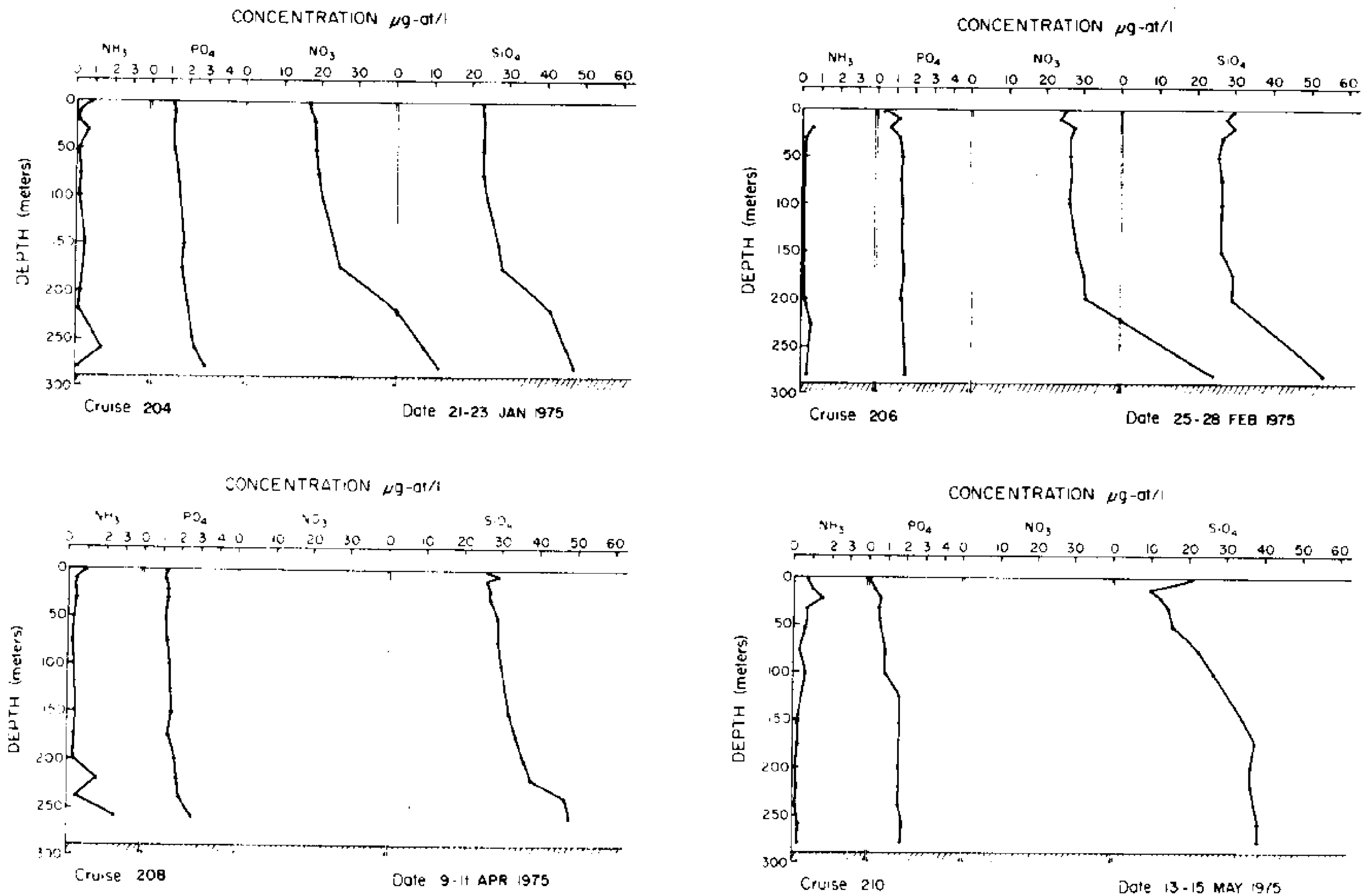

Figure 42. Vertical profiles of ammonia, phosphate, nitrate, and silicate, RES-2.5, January 1975 - May 1975.

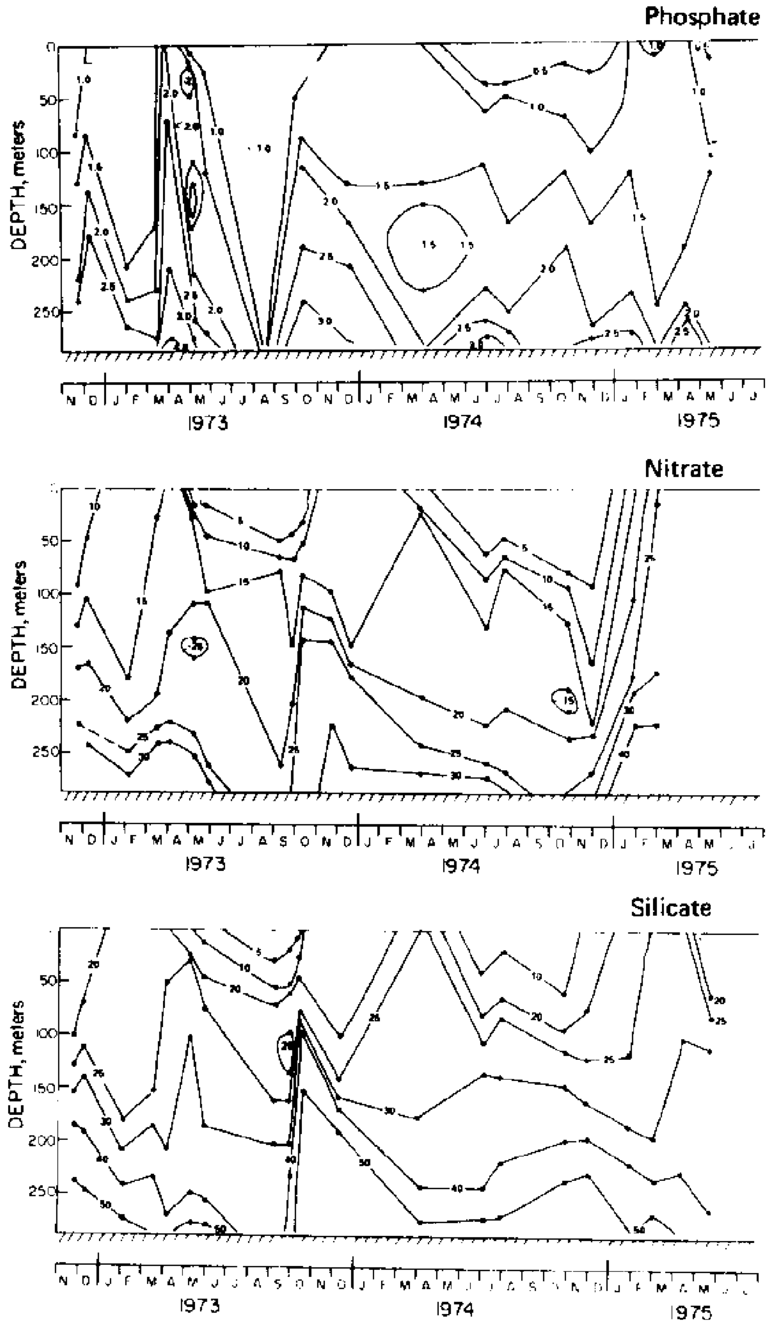

Figure 43. Seasonal variations of phosphate, nitrate, and silicate, RES-2.5.

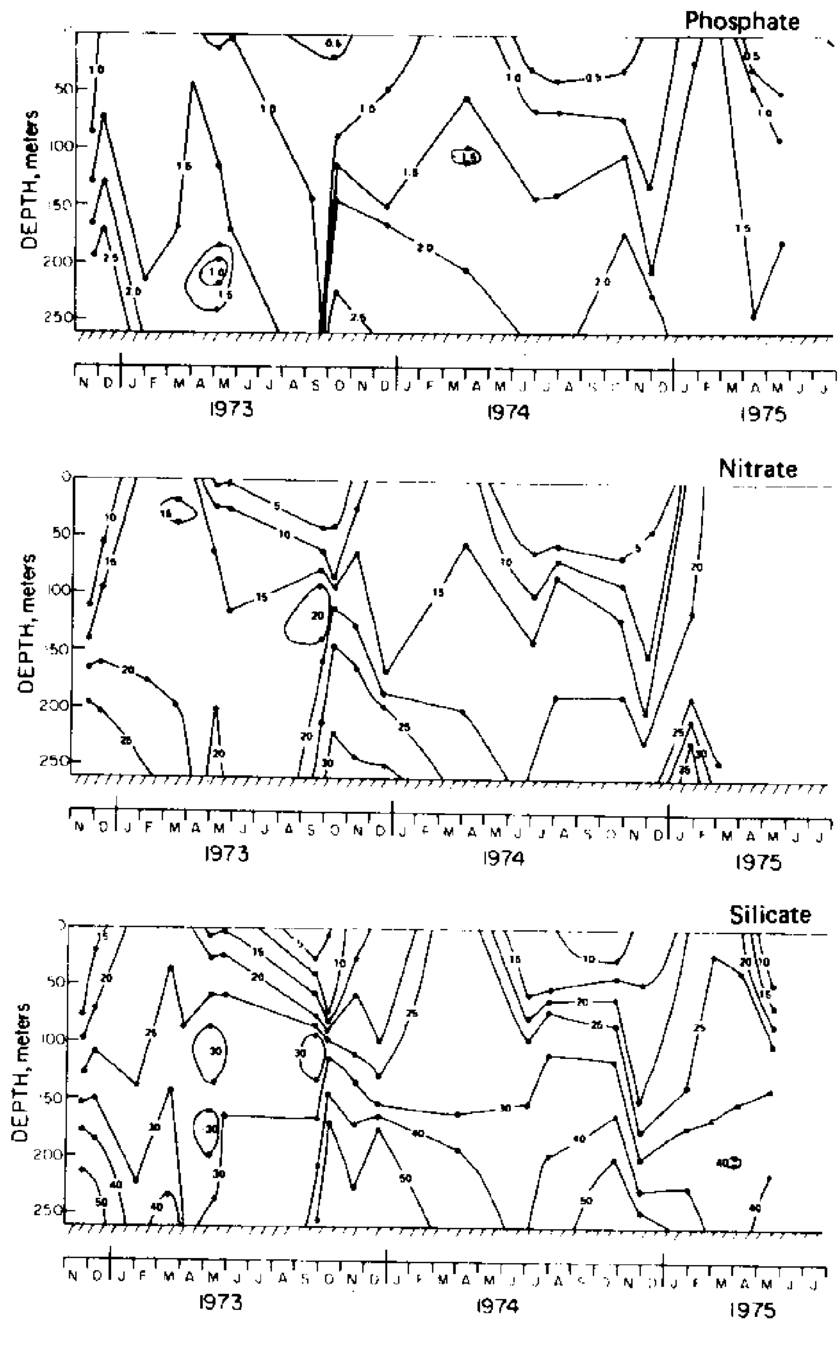

Figure 44. Seasonal variations of phosphate, nitrate, and silicate, RES-4.

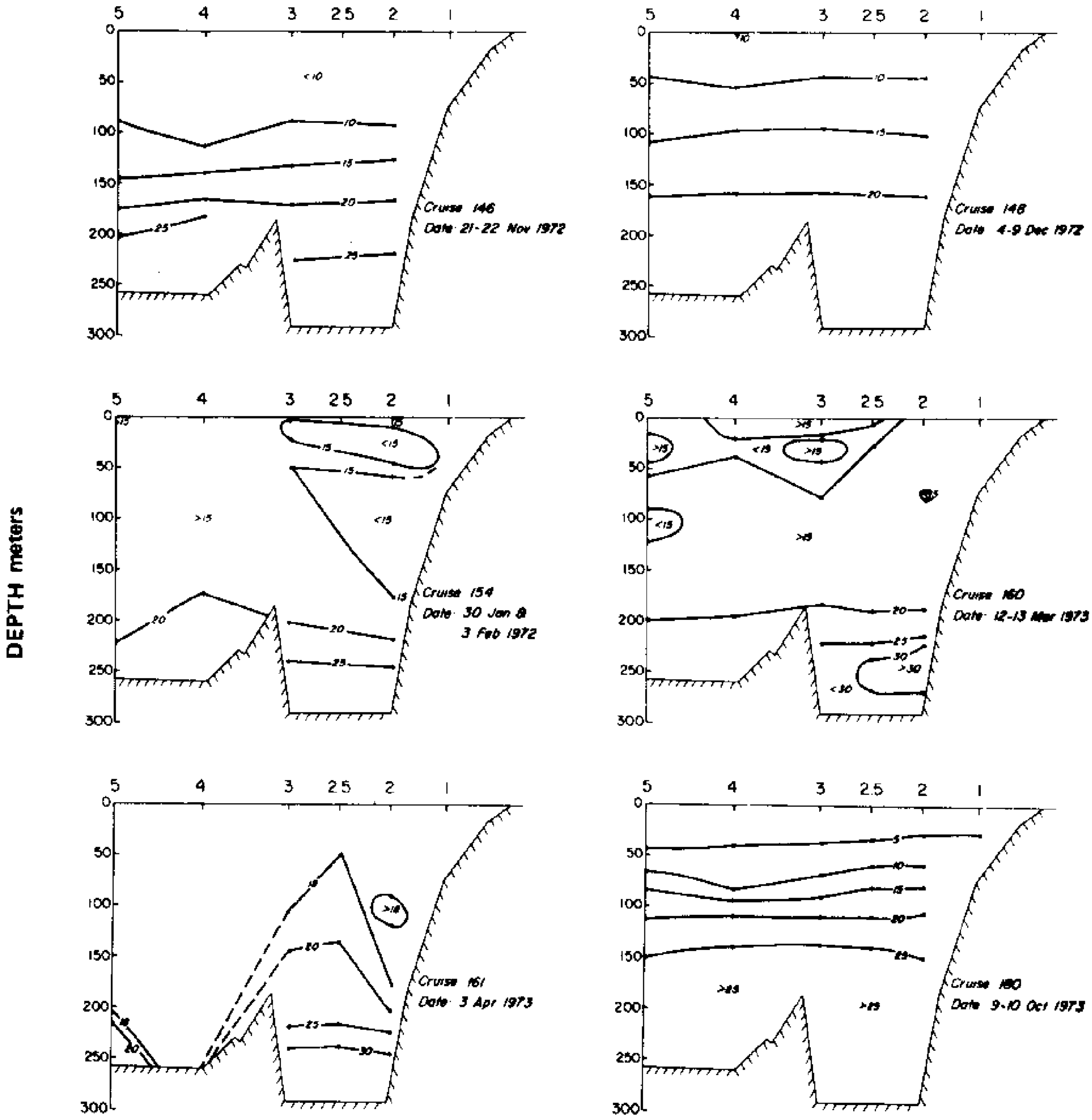

Figure 45. Fjord longitudinal profiles of nitrate, November 1972 - October 1973.

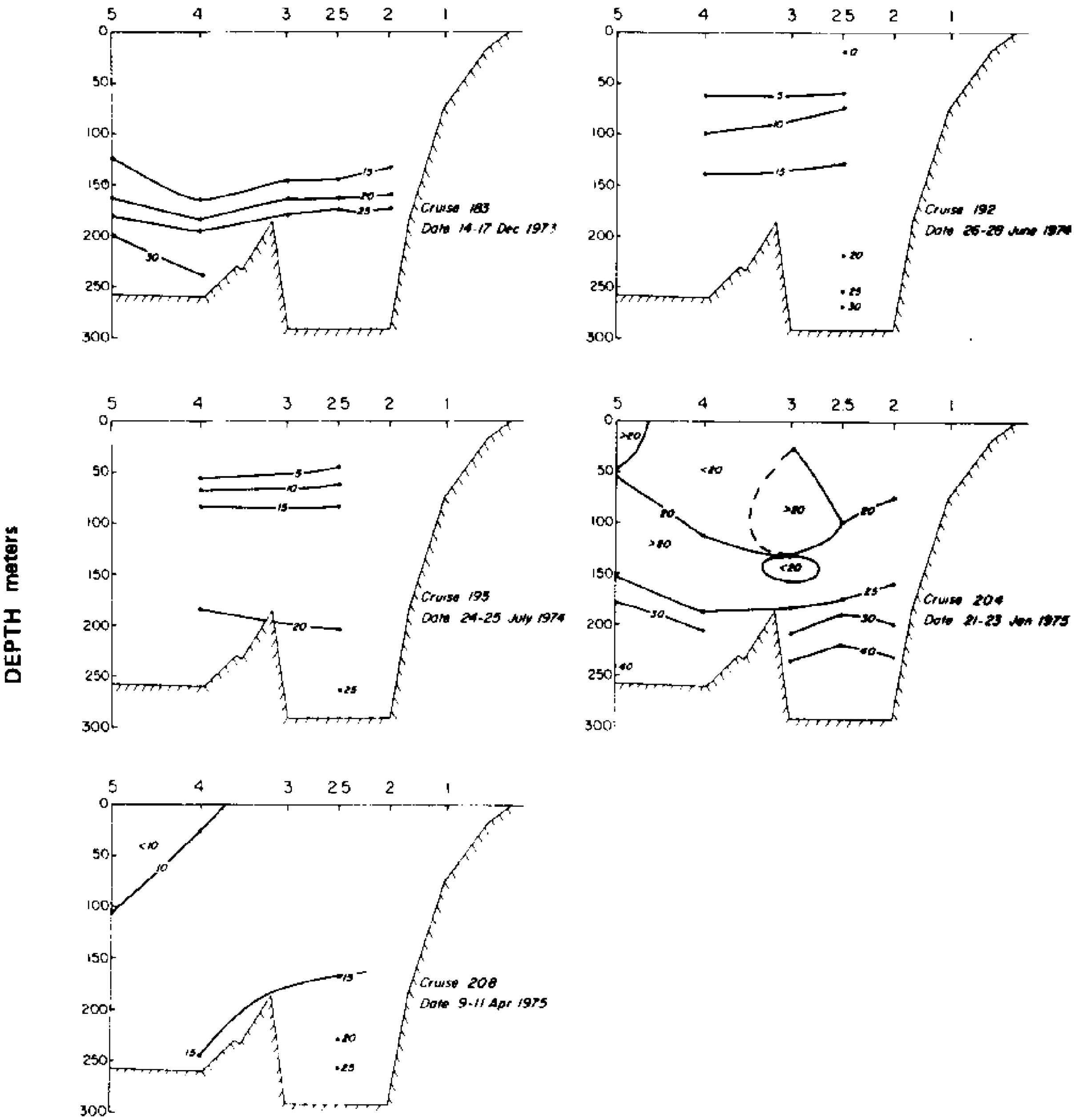

Figure 46. Fjord longitudinal profiles of nitrate, December 1973 - April 1975.

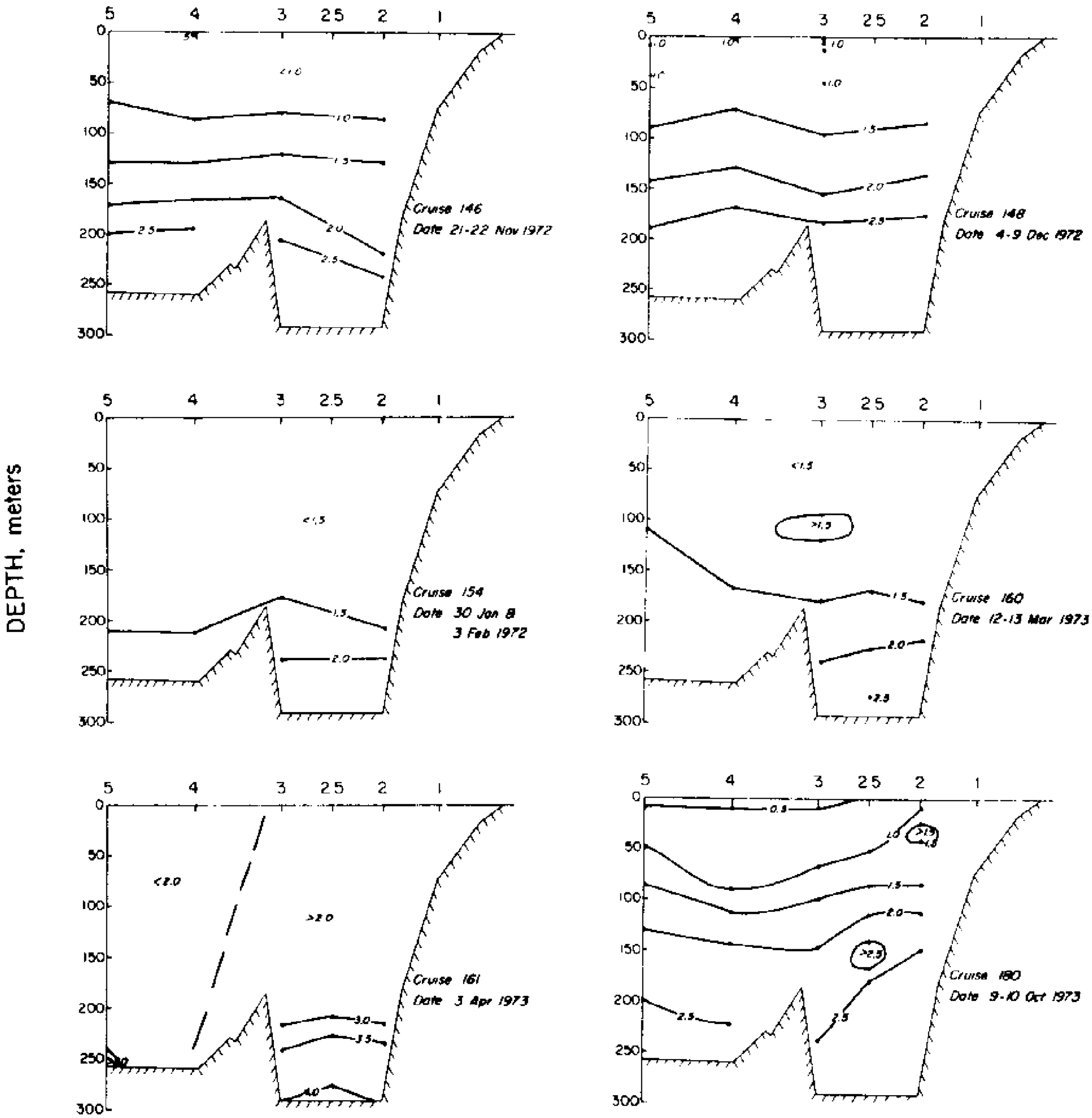

Figure 47. Fjord longitudinal profiles of phosphate, November 1972 - October 1973.

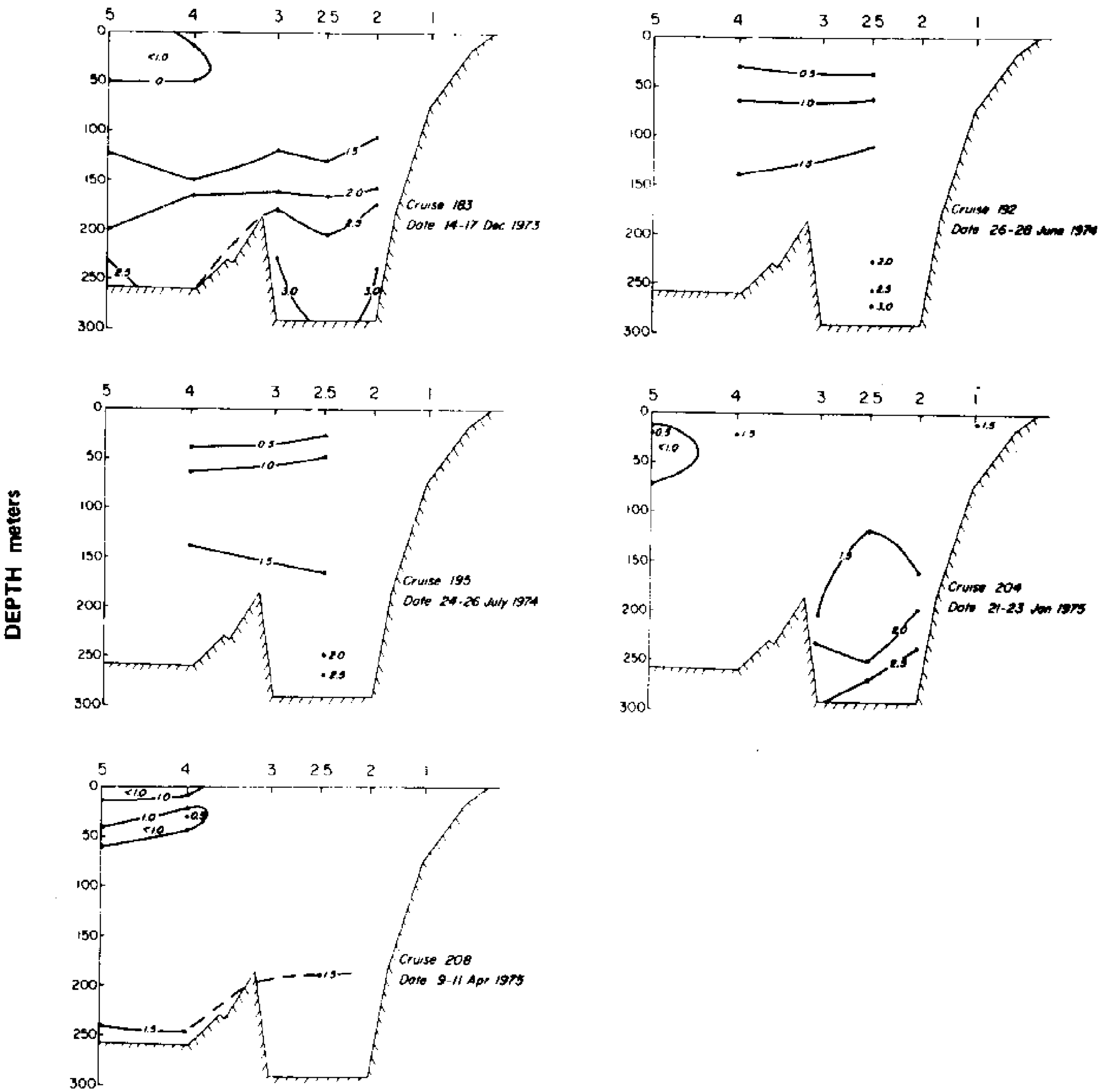

Figure 48. Fjord longitudinal profiles of phosphate, December 1973 - April 1975.

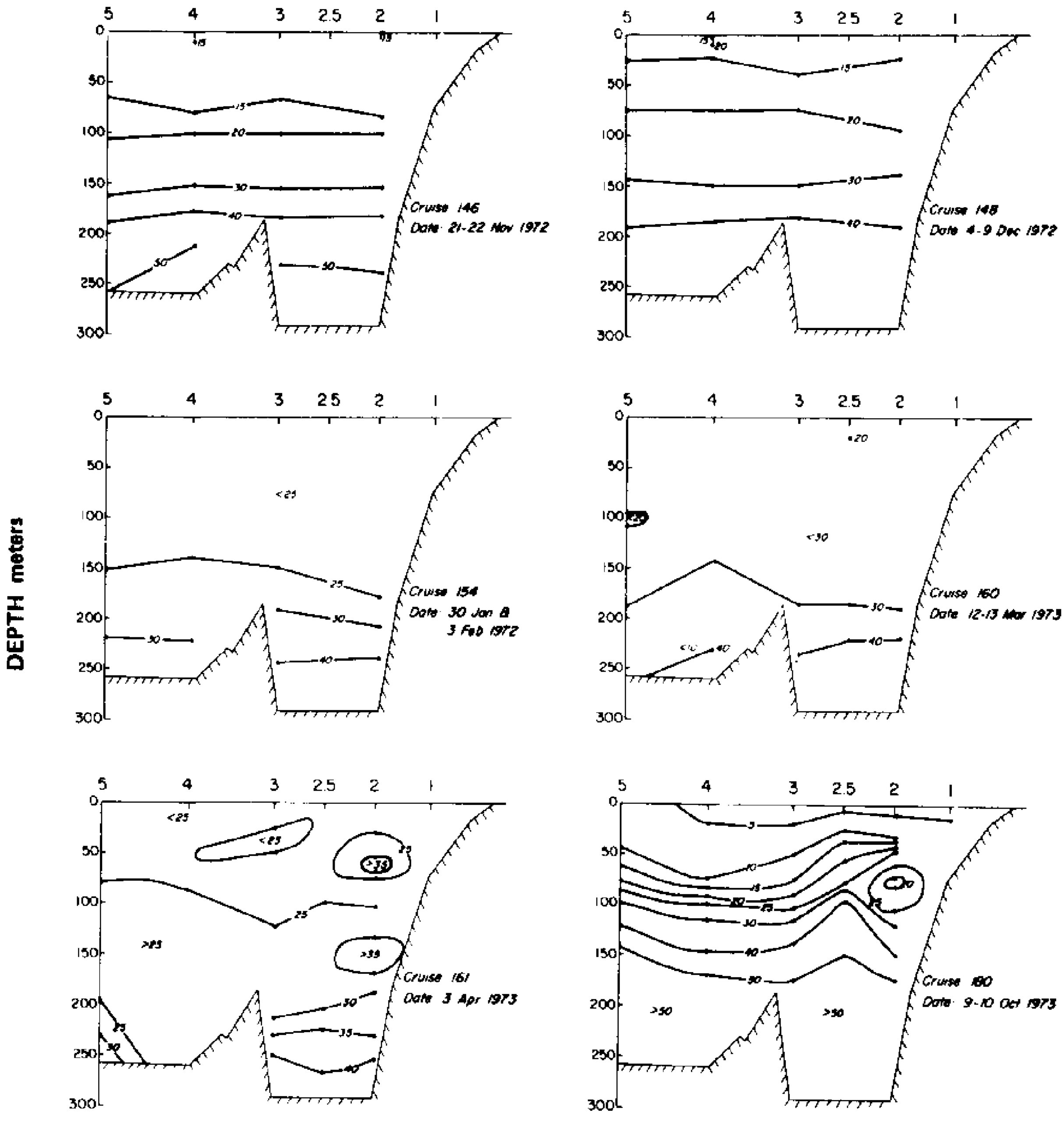

Figure 49. Fjord longitudinal profiles of silicate, November 1972 - October 1973.

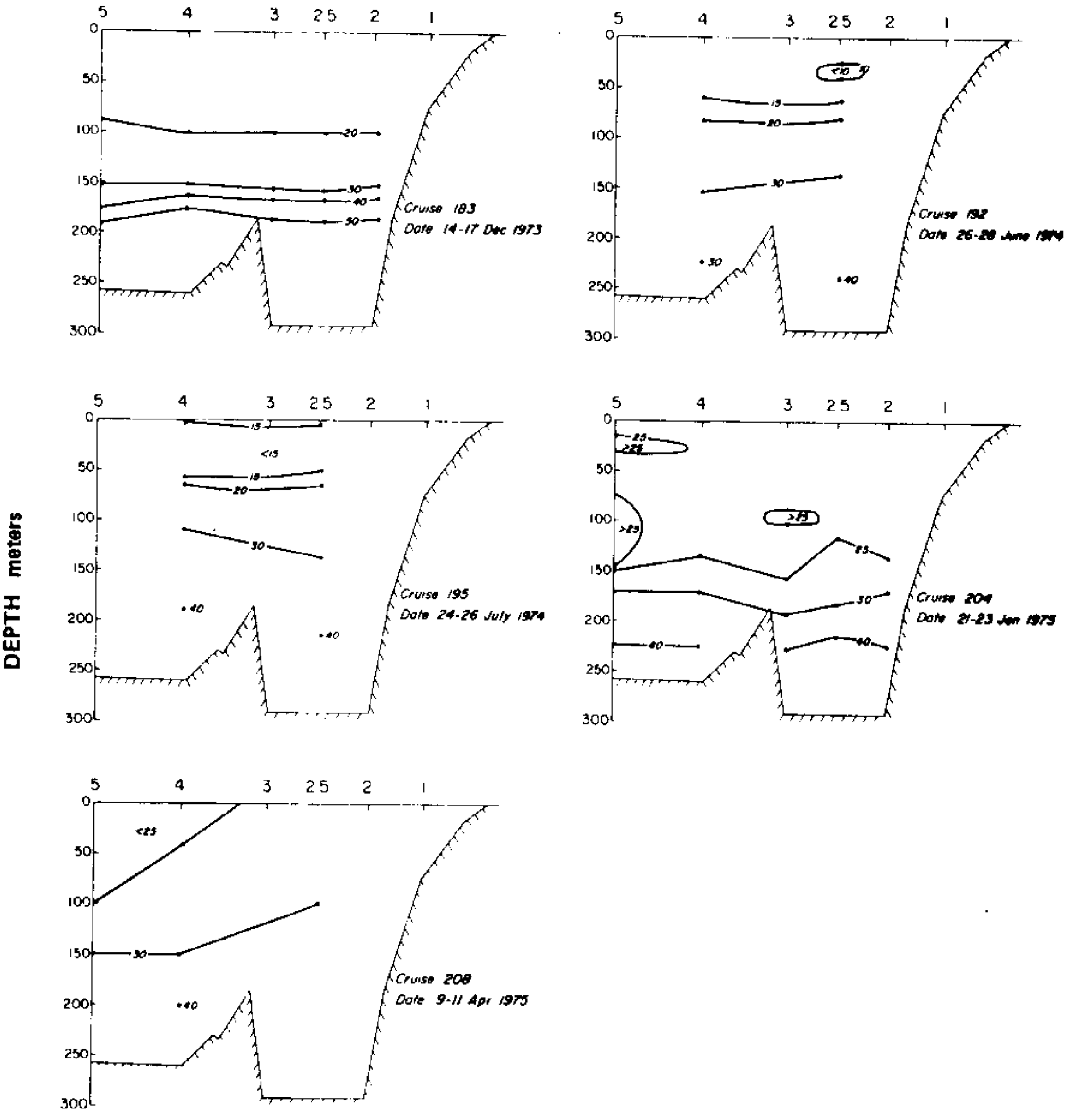

Figure 50. Fjord longitudinal profiles of silicate, December 1973 - April 1975.

months, of between about 15 and 30μ M. A general depletion of silicate was found throughout the surface waters during the summer. Concentrations always increased with depth but gradients throughout the water column were minimal during the winter. Minimum concentrations were found in the deep waters in mid-winter at the outer station RES-4. At the inner station, RES-2.5, concentrations in deep water generally decreased throughout the winter months also, but in the bottom waters of the inner basin an approximately steady state concentration (50 to 60μ M) seemed to be maintained for most of the year.

Phosphate

Phosphate concentrations in the fjord varied between about 0.2μ M in surface waters to greater than 4.0μ M in bottom waters. Throughout the surface waters a general depletion of phosphate occurred during the summer months, but concentrations increased during the winter months, when there was little plankton activity. Maximum concentrations were found in the surface waters during early spring months of about 1 to 2.0μ M. As was found with the nitrate and silicate distributions, phosphate concentrations increased with depth. Deep water concentrations generally decreased throughout the winter months, although highest concentrations were found in the bottom waters of the inner basin. Similarly to the nitrate and silicate distributions, minimum phosphate concentrations were found in the deep and bottom waters of the outer fjord reaches during the winter months.

Ammonia

Ammonia concentrations varied between about 5μ M and barely detectable levels of less than 0.1μ M. Highest concentrations generally were found during the summer months in surface and intermediate waters, and are probably related to the activities of grazing zooplankton. Minimum concentrations were found throughout most of the water column during the winter, although some relatively high (0.5μ M to 3.0μ M) concentrations were occasionally measured in the deep and bottom waters of the inner basin.

Interstitial Waters

Nutrients were determined on two occasions (October 1974 and May 1975) in pore waters squeezed from sediment cores. The data are summarized in Table 8 and Figure 51. These analyses were exploratory in nature. There is some variation in the absolute concentrations measured but this is in part probably due to the large dilution (x10 and x20) of the samples that was required for analysis, and possibly also to chemical changes that occurred in the core subsequent to coring, but prior to analysis. The most notable feature of the depth distributions is the persistent surface and near-surface maxima in the nitrate, phosphate, and silicate distributions. Nitrate concentrations are reduced to <1.0μ M below about 10 cm depth and this is probably due to denitrification (Richards, 1965) in the sediments. (Denitrification is the process, which proceeds only under anoxic conditions, whereby nitrate (NO_3^-) is reduced to molecular nitrogen (N_2) or (N_2O).) Silicate and phosphate are also depleted at depth in the sediment but not to the same extent as nitrate. More complex distributions of these nutrients would probably become evident if the sampling depth frequency were increased. Ammonia, a byproduct of anaerobic decomposition, increases with depth in the sediment from concentrations of around 100μ M in surface interstitial waters to concentrations exceeding 500μ M at around 30 cm depth.

The highest concentrations of silicate and phosphate in the surface interstitial waters are about an order of magnitude higher than the highest concentrations in the overlying waters. Nitrate concentrations in the surface 5 cm of sediments are also higher than concentrations in the overlying waters, but to a lesser extent. By way of contrast, ammonia concentrations in the top 5 cm of sediments are about two orders of magnitude greater than in the overlying water.

Titration alkalinities determined for the interstitial waters are summarized in Table 9. Alkalinities increased with depth in all cores, from concentrations of around 3 to 4 meq ℓ^{-1} in the surface segment to greater than 25 meq ℓ^{-1} at around 100 cm depth. Pore water samples were analyzed for alkalinity aboard ship, immediately following squeezing and extraction from the sediments.

TABLE 8

Interstitial Water Nutrient Concentrations

CRUISE: 180 October 1974

Depth in Sediment (cm)	Phosphate (μ M)	Ammonia (μ M)	Nitrate (μ M)	Silicate (μ M)
0-16	34.9	44.0	12.0	535
18-28	35.2	330.0	<1.0	290
29-42	31.3	516.0	<1.0	310
85-96	41.8	737.0	<1.0	460

CRUISE: 210 May 1975

Depth in Sediment (cm)	Phosphate (μ M)	Ammonia (μ M)	Nitrate (μ M)	Silicate (μ M)
0-5.5	17.5	134	94.1	310
	16.8	143	89.2	281
7-13	31.1	198	<1.0	497
	29.3	194	<1.0	488
14.7-20.5	17.5	241	<1.0	372
49-54.1	17.5	519	<1.0	339
89.5-96.5	18.5	552	<1.0	347

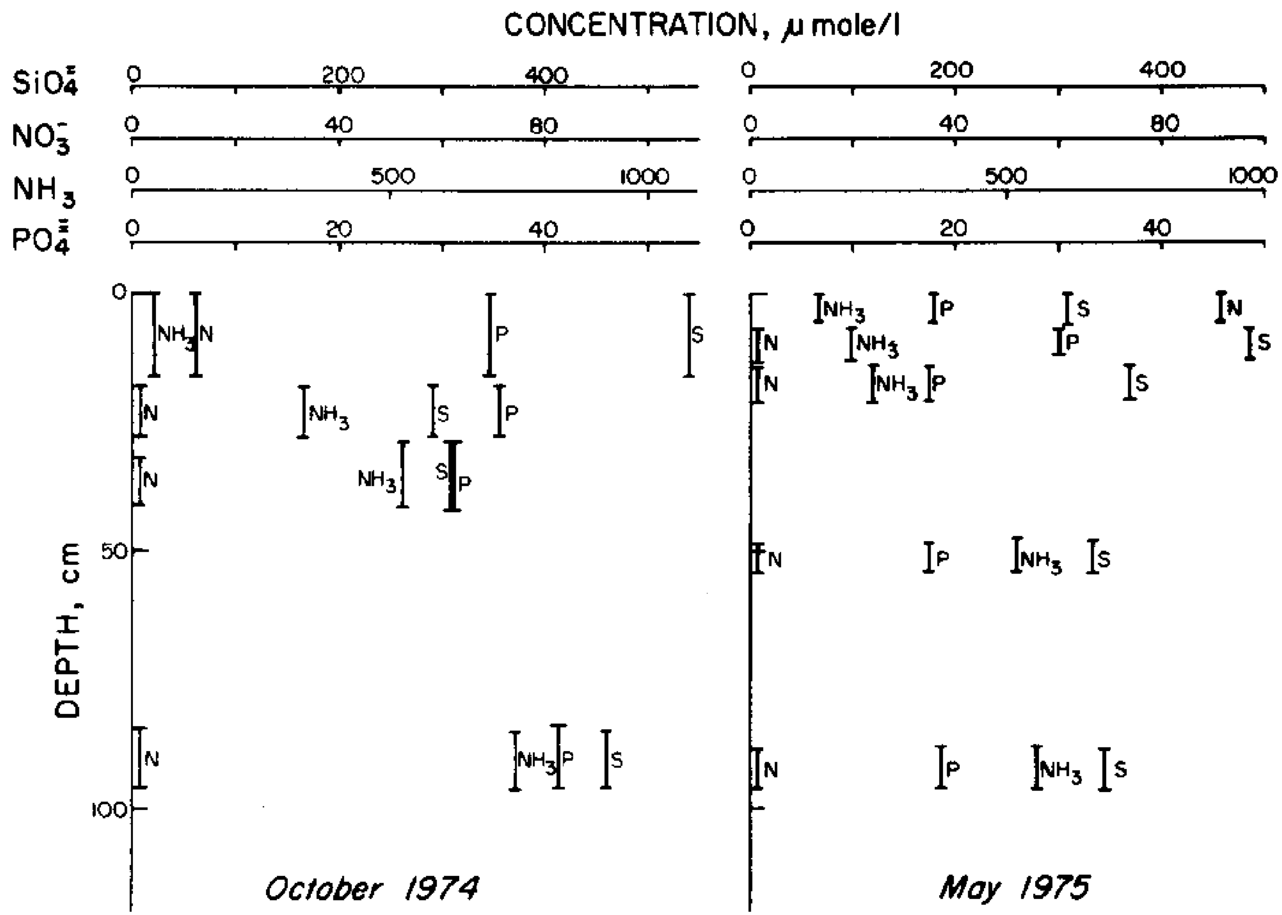

Figure 51. Vertical profiles of ammonia, phosphate, nitrate, and silicate in interstitial waters, October 1974 and May 1975.

TABLE 9

Interstitial Water Titration Alkalinities

DATE: February 1975

Depth in Sediment (cm)	Alkalinity (meq ℓ^{-1})
0 - 6.3	3.81
21.5 - 26.5	8.15
50 - 56	16.79
94.5 - 101	27.24

DATE: May 1975

Depth in Sediment (cm)	Alkalinity (meq ℓ^{-1})
0 - 5.5	3.81
7 - 13	4.80
14.7 - 20.5	6.48
49 - 54.1	16.28
89.5 - 96.5	25.16
122.5 - 129	33.84

DISCUSSION

Surface Waters

The seasonal variations of nitrate, phosphate, and silicate shown in Figures 43 and 44 reflect the general depletions of these nutrients from the water column, throughout the fjord, during the summer months. Such depletion is due to autotrophic processes in the euphotic zone, which convert dissolved inorganic nitrate, phosphate, silicate and ammonia into particulate organic material. Conversely, concentrations of nitrate, phosphate and silicate increase in the surface waters during the winter months because of decreased uptake by plants, and re-supply, by vertical mixing processes, from deeper waters of the fjord.

Deep Waters

Probably primarily because of vertical mixing, concentrations of nitrate, phosphate and silicate generally decreased throughout the fjord deep waters during the winter months. Differences between the depth and temporal profiles of these nutrients in the deep waters >150 m between the outer and inner fjord reaches should be noted however. Variations at RES-4 are quite erratic and probably reflect the rapidly changing hydrographic conditions at the coastline, and the advection through the outer fjord reaches of water masses of different nutrient concentrations. At the inner station (RES-2.5) behind the sill, the variations are generally less marked and reflect the relative isolation of these waters. Between about October and April processes controlling concentrations and vertical profiles at RES-2.5 are probably a combination of exchanges *via* vertical mixing processes across the sill depth region and remineralization in the bottom waters and at the surface sediments. Although concentrations of nitrate, phosphate and silicate generally were observed to decrease throughout the winter months in the intermediate and deep waters, concentrations in the very bottom waters increased or approximated steady state. This observation, together with that of higher concentrations of nitrate, phosphate and silicate in the surface sediments, suggests a flux of these nutrients from the sediments into the overlying waters. Since there are net decreases of these nutrients below the sill depth, the flux away from the sediments apparently cannot keep pace with the flux of nutrients out of the basin across the sill depth. It was noted previously that about 40% of the summer primary productivity escaped degradation in the water column and reached the sediment surface. This computation, together with the fact of very high nutrient concentrations in the interstitial waters, suggests that remineralization in the sediments is significant and that the sediments act as a source of nutrients for the overlying fjord waters.

Although concentrations of ammonia in the surface interstitial waters are about two orders of magnitude higher than ammonia concentrations in the water column, there is no evidence of a significant escape of ammonia from the sediments reaching high into the water column. While the ammonia gradient in the sediments indicates supply to the overlying waters, a gradient in ammonia concentrations directed away from the sediments does not persist in the water column as in the case of phosphate, nitrate and silicate. This observation indicates removal of ammonia from the very bottom fjord waters. Nitrification, the biological oxidation of ammonia to nitrite, and nitrate may be responsible, and the mechanism may be another source of nitrate for the fjord bottom waters. A measurement of the rate of nitrification (by incubation of a seawater sample with added ammonia) in the fjord bottom waters could provide a direct measure of the flux of ammonia from the sediments. The cycling of nitrogen between the sediments and overlying waters appears to be complex. Nitrate in surface sediments produced directly by remineralization from particulate organic matter and/or nitrification also serves as the source of oxygen for denitrification processes in the anoxic zone of the sediments. The various pathways and fluxes of nitrogen in sediments and across the sediment-seawater interface may be ellucidated with ^{15}N stable isotope techniques. Similarly, with isotope techniques, the relative contributions of phosphate and silicate regenerated in the water column *vs.* fluxed from the sediment may be resolved in the fjord bottom waters.

PRIMARY PRODUCTIVITY

BACKGROUND

Primary production, the photosynthetic formation of high energy organic compounds from carbon dioxide, water, sunlight and certain mineral nutrients, most notably salts of nitrogen and phosphorus, represents the basic energy source of a food chain. Heterotrophic production is ultimately dependent on the amount of organic material supplied by green plants, the greatest part of which is contributed by phytoplankton (Raymont, 1963). Phytoplankton production in turn is regulated by physical parameters which may limit or enhance growth. Sunlight, obviously, imposes a daily and a seasonal cycle on production. Nutrient concentrations within the euphotic zone limit both standing crop and productivity. Mixing and stratificating processes in the water column act to control the resupply of nutrients and the distribution of phytoplankton in the euphotic zone.

RESULTS AND DISCUSSION

Resurrection Bay exhibited a yearly cycle of productivity typical of other fjord systems in Alaska (e.g., Hood *et al.*, 1973). The bulk of production and highest rates of productivity occurred during the longer daylight hours of summer (Table 10).

At station RES-2.5 productivity ranged from 111 mg C m^{-2} hr^{-1} with a daily rate of 1776 mg C m^{-2} d^{-1} in June, 1974 (Fig. 52) to 2 mg C m^{-2} h^{-1} with a daily rate of 8 mg C m^{-2} d^{-1} in January, 1975. However, zero nitrate and ammonia concentrations throughout the euphotic zone on 28 June 1974, suggest that peak phytoplankton productivity occurred earlier in the year, late May and early June. The productivity value in late June may reflect a nitrate-nitrogen limited condition. Levels of nitrogen, regenerated in the water column as ammonia, increased slightly in the following month and ammonia may have been the nitrogen source supporting production through July and August.

Productivity at station RES-4 (Fig. 53) closely parallels the seasonal structure at RES-2.5 with integrated values ranging from 175 mg C m^{-2} h^{-1} with a daily rate of 2978 mg C m^{-2} d^{-1} in June, 1974 to 2.5 mg C m^{-2} h^{-1}

TABLE 10

Rates of Carbon Uptake and Standing Stock

Date	Cruise	Carbon Uptake				Standing Stock	
		RES-2.5		RES-4		RES-2.5	RES-4
		mg $m^{-2}h^{-1}$	mg $m^{-2}d^{-1}$	mg $m^{-2}h^{-1}$	mg $m^{-2}d^{-1}$	Chl *a* mg m^{-2}	
12 Apr 1974	186	29.1	320	28.6	315	-	4.50
26 Jun 1974	192	84.8	1441	175.2	2978	8.76	26.04
24 Jul 1974	195	111.0	1776	89.4	1430	11.29	8.91
18 Oct 1974	201	53.6	428	36.6	292	13.75	18.34
22 Nov 1974	203	2.0	8	3.2	12	1.78	2.40
22 Jan 1975	204	1.6	6	2.3	9	1.62	1.24
22 Feb 1975	206	7.6	38	5.0	25	2.24	1.33
9 Apr 1975	208	62.7	627	82.6	826	23.11	30.98

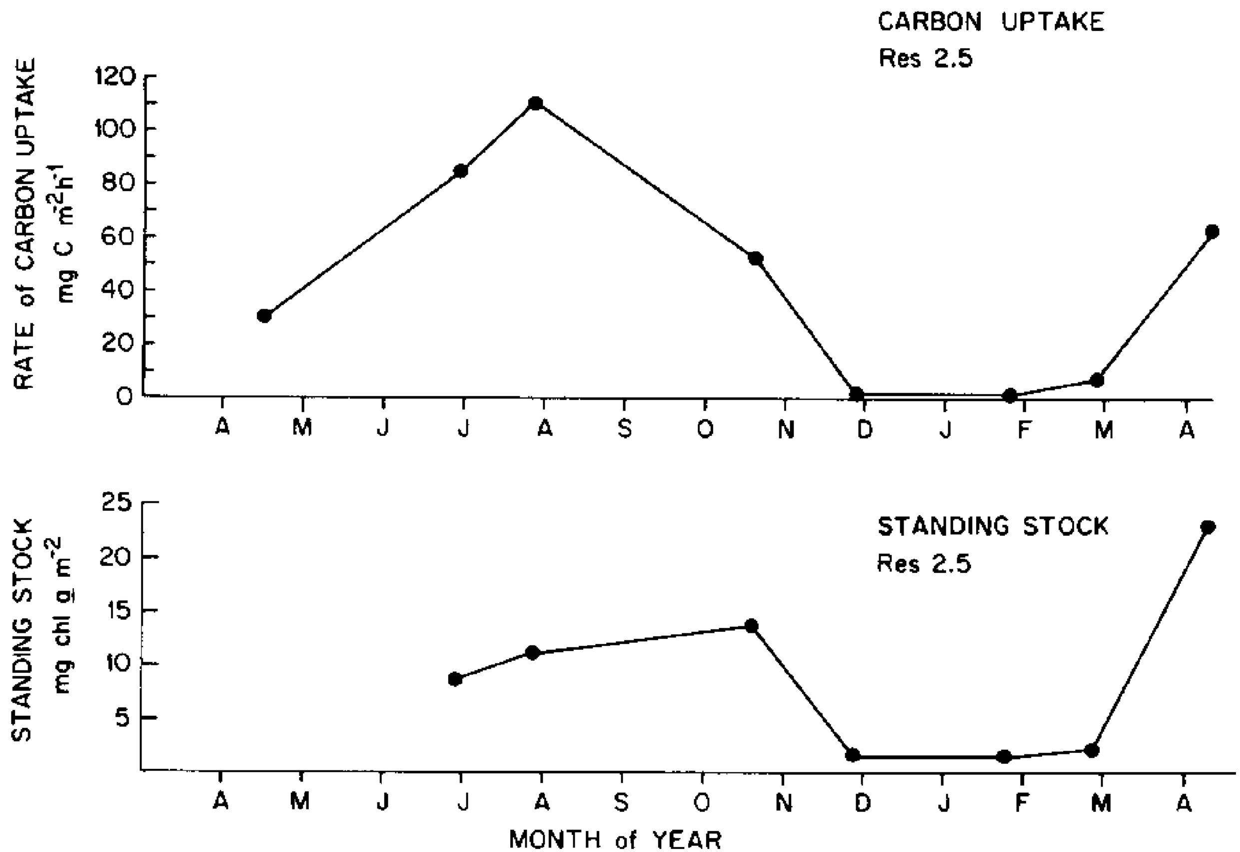

Figure 52. Carbon uptake rates and standing stock at RES-2.5, April 1974 - April 1975.

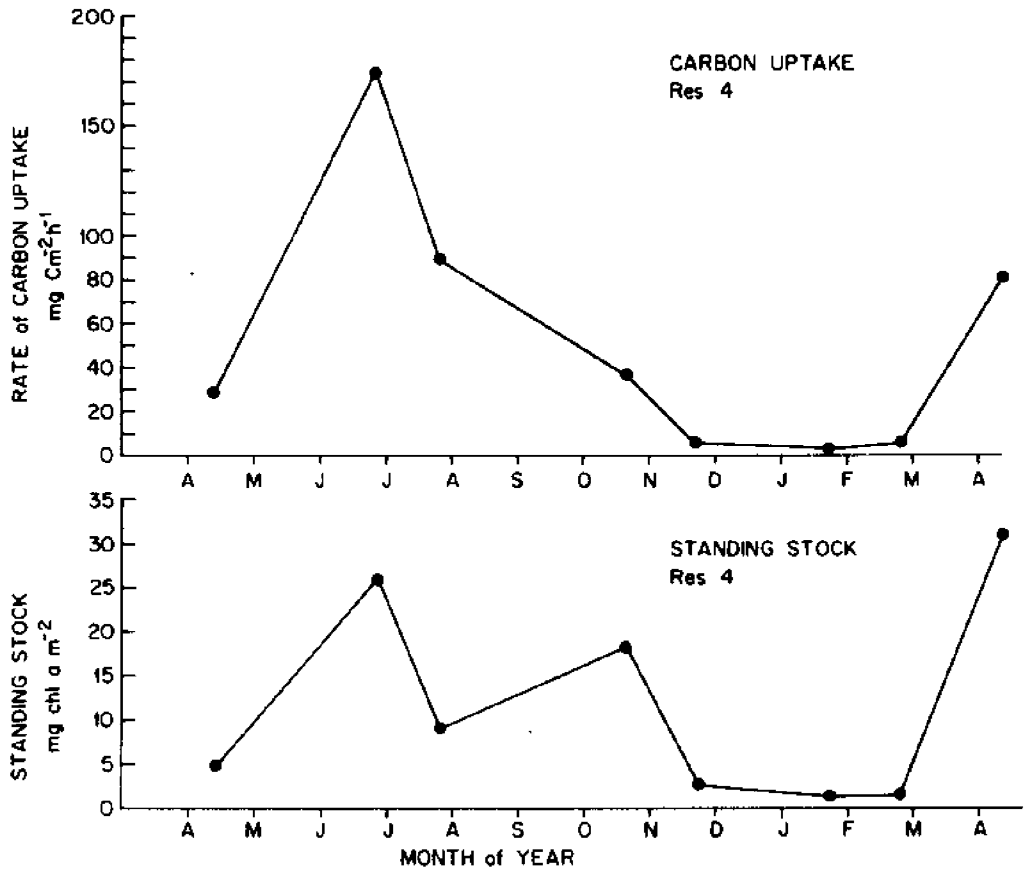

Figure 53. Carbon uptake rates and standing stocks at RES-4, April 1974 - April 1975.

and a daily rate of 10 mg C m^{-2} d^{-1} in January, 1975. Nitrate concentrations throughout the euphotic zone suggest that available nutrients may have sustained the spring bloom for a longer period at station RES-4 than at station RES-2.5.

Measurements of standing stock in mg Chl *a* at station RES-4 (Fig. 53) demonstrate a spring peak of 26 mg Chl *a* m^{-2} followed by a decline to less than half that value in mid-summer, possibly the result of grazing and nutrient limitation, followed by a lesser peak in early fall of 18 mg Chl *a* m^{-2}. The standing stock measured on 9 April 1975 is about six times (Fig. 53) greater than that obtained during the same period in 1974. Productivity measurements also support an earlier advent of the spring bloom in 1975. Unfortunately, biomass values for RES-2.5 in April 1974 were lost. However, productivity measurements are similar to those observed at RES-4.

Annual net productivity at station RES-2.5 weighted on an hours of sunlight base is estimated at approximately 228 g C m^{-2}, a value which agrees well with those reported for other fjord systems in Alaska (e.g., Hood *et al.*, 1973). At station RES-4 annual net productivity is estimated at 285 g C m^{-2}.

SUMMARY

The water column of Resurrection Bay is most stratified during the summer months because of the addition of less dense freshwater into the surface waters. The latter, to conserve volume, in part flows seaward out of the fjord, while the remainder mixes with more dense resident fjord waters. Because of decreased freshwater runoff, the water column approaches homogeneous conditions during the winter months, but surface waters probably still flow predominately seaward, due to the persistance of down-estuary (northerly) winds during this period.

The exchange of deep water between the Gulf of Alaska and Resurrection Bay occurs principally during the oceanographic summer months (June through October), and is a direct result of the advection of more dense water up onto the continental shelf. The relatively dense water (σ_t>26) is advected horizontally into the inner fjord basin and, *via* gravitational displacement, sinks to replace the resident water of the deep inner basin. Over a 35 day period during September and October 1973, the transport through the basin was sufficient to replace the topographic basin volume about five times over. The rapid change in atmospheric conditions, and hence wind field, over the Gulf of Alaska between about September and November depresses isopycnal surfaces at the coastline and drives the more dense summer water mass down and out of the outer reaches of Resurrection Bay. The water that penetrated below the sill during the summer remains isolated for the following winter period and exchanges with the less dense winter water masses above the sill predominately *via* vertical eddy mixing. Advective exchange across the sill begins again around May or June of the following year and is complete by October. This sequence of advective exchange in the summer and diffusive exchange in the winter has been observed in the inner fjord basin for three years (1972-1975) and is schematically illustrated in Figure 54. The advection of dense water into the basin during oceanographic summer probably occurs annually: it is effected by a decrease in density of the basin water during the preceeding winter and the appearance of more dense water at the sill due to the seasonal change in the water masses on the adjacent Gulf of Alaska.

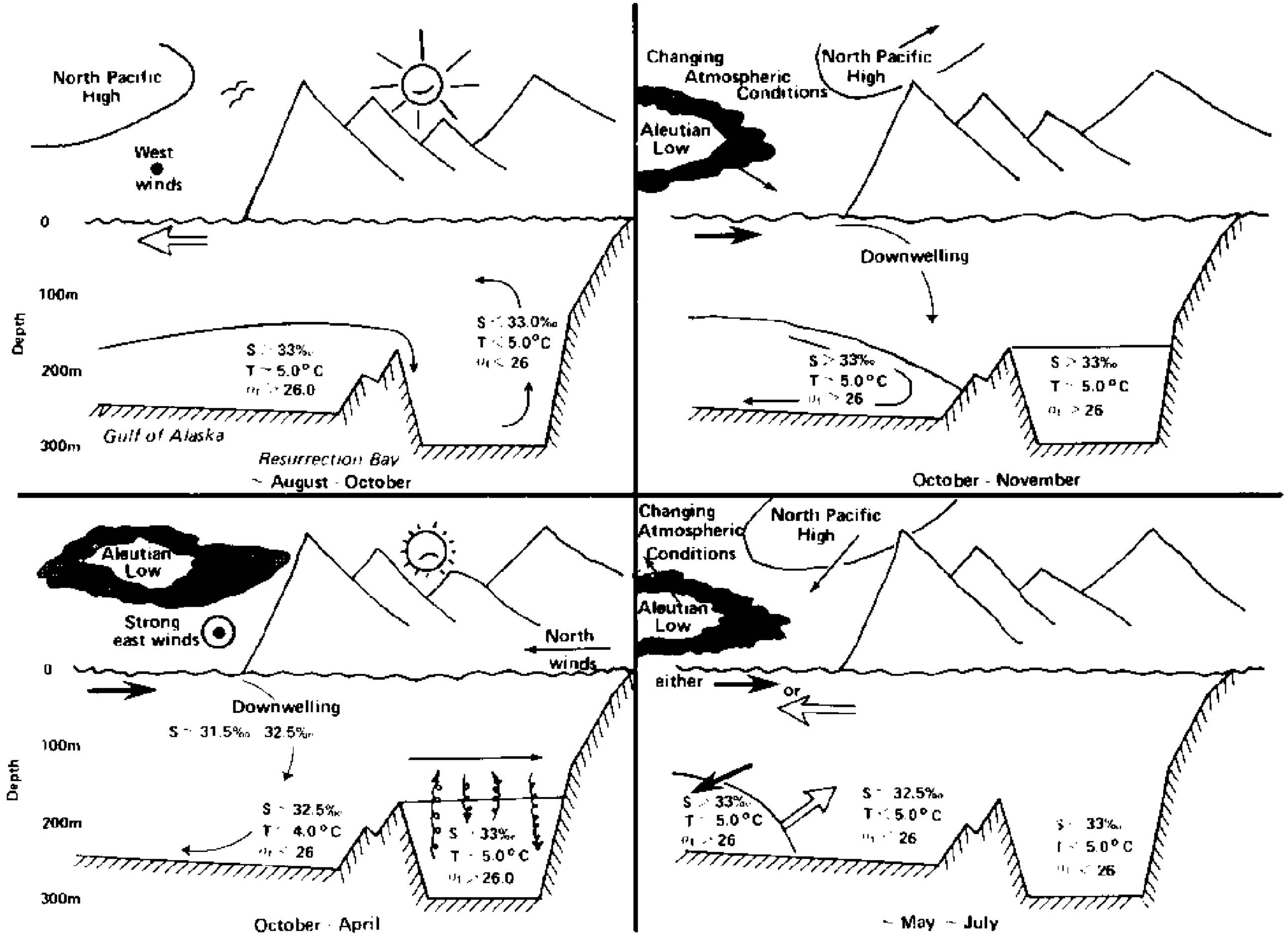

Figure 54. Schematic representations of the seasonal exchange of water between the Gulf of Alaska and Resurrection Bay.

Oxygen consumption rates in the water column were found to vary between 1.1 and 7.6 ml ℓ^{-1} yr^{-1}. The mean water column oxygen consumption rate was computed to be $\sim$3.5 ml ℓ^{-1} yr^{-1}, which, together with the frequency of renewal of the fjord bottom waters by advective and mixing processes would indicate that, under the present rate of supply of organic carbon to the fjord, the deep waters are not likely to become anoxic. Anoxic conditions however appear at shallow depths ($\sim$10 cm) in the sediments of the inner fjord basin.

Seasonal and spatial variations of concentrations of nitrate, phosphate and silicate in surface waters of Resurrection Bay appear to be controlled by uptake by phytoplankton growth during the summer, and replenishment of the depleted nutrients during the winter. The latter is a result of the combined effects of negligible uptake and resupply by vertical mixing processes. The deep water variations are controlled, during the summer and fall months, by the advection of more dense water below about 150 m from the Gulf of Alaska, and during winter by vertical mixing processes and remineralization processes in the deep and bottom waters, and surface sediments. Denitrification in sediments and nitrification in very surface (<10 cm) sediments and/or fjord bottom waters appear to be important controls on the flux of nitrogen compounds across the sediment-seawater interface.

Daily rates of primary productivity in Resurrection Bay varied between 2978 mg C m^{-2} d^{-1} in June and 8 mg C m^{-2} d^{-1} in January. Annual net productivity at two stations in the fjord varied between 228 and 285 g C m^{-2}. Primary productivity in Resurrection Bay appeared to be limited by nitrate-nitrogen supply.

REFERENCES

Bakun, A. 1973. Coastal Upwelling Indices West Coast of North America (1946-1971). NOAA Technical Report NMFS SSRF-671.

Barnes, C. A. and E. E. Collias. 1958. Some considerations of oxygen utilization rates in the Puget Sound. *J. Mar. Res.* 17:68-80.

Craig, H. 1969. Abyssal carbon and radiocarbon in the Pacific. *J. Geophysical Res.* 74:5491-5506.

Fanning, R. A. and M. E. Q. Pilson. 1972. A model for the anoxic zone of the Cariaco Trench. *Deep-Sea Res.* 19:847-863.

Hansen, D. V. and M. Rattray, Jr. 1966. New dimensions in estuary classification. *Limnology and Oceanography* 11:319-326.

Heggie, D. T. 1977. Copper in the Sea: A Physical-Chemical Study of Reservoirs, Fluxes and Pathways in an Alaskan Fjord. Ph.D. dissertation. Univ. of Alaska, Fairbanks. 222 pp.

Hood, D. W., W. E. Shiels and E. J. Kelley (eds.). 1973. *Environmental studies of Port Valdez.* Institute of Marine Science, University of Alaska, Fairbanks Occasional Publ. No. 3, Vols. I and II.

McAllister, W. B., M. Rattray, Jr. and C. A. Barnes. 1959. The dynamics of a fjord estuary: Silver Bay Alaska. Univ. of Washington. Department of Oceanography Technical Report No. 62.

Muench, R. D. and G. M. Schmidt. 1975. Variations in the hydrographic structure of Prince William Sound. Institute of Marine Science, Univ. of Alaska, Fairbanks Report No. R75-1. 133 p.

Muench, R. D. and D. T. Heggie. 1977. Deep water exchange in Alaskan sub-Arctic fjords. Presented at the 7th Belle W. Baruch Institute for Marine Biology and Coastal Research Symposium "Transport Processes in Estuarine Environments", May 19-22, 1976. Georgetown, S. Carolina. (In press).

Nebert, D. L. 1972. A proposed circulation model for Endicott Arm, an Alaskan fjord. M.Sc. Thesis, Univ. of Alaska, Fairbanks. 90 p.

Pickard, G. L. 1967. Some oceanographic characteristics of the longer inlets of southeast Alaska. *Journal of the Fisheries Research Board of Canada* 16:635-678.

Pritchard, D. W. 1967. What is an estuary: physical viewpoint. *In* C. H. Lauff (ed.), *Estuaries.* Assoc. for the Advancement of Science Publ. No. 83. Washington, D. C. pp. 3-5.

Rattray, M., Jr. 1967. Some aspects of the dynamics of circulation in fjords. *In* C. H. Lauff (ed.), *Estuaries.* American Assoc. for the Advancement of Science Publ. No. 83. Washington, D.C. pp. 52-62.

Raymont, J. G. 1963. *Plankton and Productivity in the Oceans.* Pergamon Press, Oxford. 660 p.

Redfield, A. C., B. H. Ketchum and F. A. Richards. 1963. The influence of organisms on the composition of sea water. *In* M. N. Hill (ed.), *The Sea*, Vol. 2. Composition of Seawater, Comparative and Descriptive Oceanography. John Wiley & Sons, New York. pp. 27-77.

Reeburgh, W. S. 1967. An improved interstitial water sampled. *Limnology and Oceanography* 12:163-165.

Reeburgh, W. S., R. D. Muench and R. T. Cooney. 1976. Oceanographic conditions during 1973 in Russell Fjord, Alaska. *Estuarine and Coastal Marine Science* 4:129-145.

Richards, F. A. 1965. Anoxic basins and fjords. *In* J. P. Riley and G. Skirrow (eds.), *Chemical Oceanography*, Vol. 1. Academic Press, London. pp. 611-645.

Royer, T. C. 1975. Seasonal variations of waters in the northern Gulf of Alaska. *Deep-Sea Res.* 22:403-416.

Schmidt, G. M. 1977. The exchange of water between Prince William Sound and the Gulf of Alaska. M.Sc. Thesis, Univ. of Alaska, Fairbanks. 116 p.

Sholkovitz, E. R. and J. M. Geiskes. 1971. A physical-chemical study of the flushing of the Santa Barbara Basin. *Limnology and Oceanography* 16:479-489.

Spencer, D. W. and P. G. Brewer. 1971. Vertical advection diffusion and redox potentials as controls on the distribution of manganese and other trace metals dissolved in waters of the Black Sea. *J. Geophysical Res.* 76:5877-5892.

Steeman-Nielson, E. 1962. Use of radioactive carbon (C^{14}) for measuring organic production in the sea. *J. Cons. Perm. Int. Explor. Mer* 18: 117-140.

Strickland, J. D. H. and T. R. Parsons. 1968. A practical Handbook of Seawater Analysis. Queens Printers, Ottawa, 311 pp.

Sverdrup, H. V., M. W. Johnson and R. H. Fleming. 1942. *The Oceans*, Prentice Hall, Inc., Englewood Cliffs, N. J. 1087 pp.

Winter, D. F. 1973. A similarity solution for steady-state gravitational circulation in fjords. *Estuarine and Coastal Marine Science* 1:387-400.

APPENDIX

Depth profiles of salinity within the inner basin of Resurrection Bay (stations RES-2, RES-2.5 and RES-3) from September 1972 through May 1975 are shown in Figures 1-3. Corresponding data for temperature distributions are given in Figures 4-6. The general longitudinal homogeneity below sill depth (the latter marked by the horizontal dashed line), through the oceanographic winter, should be noted.

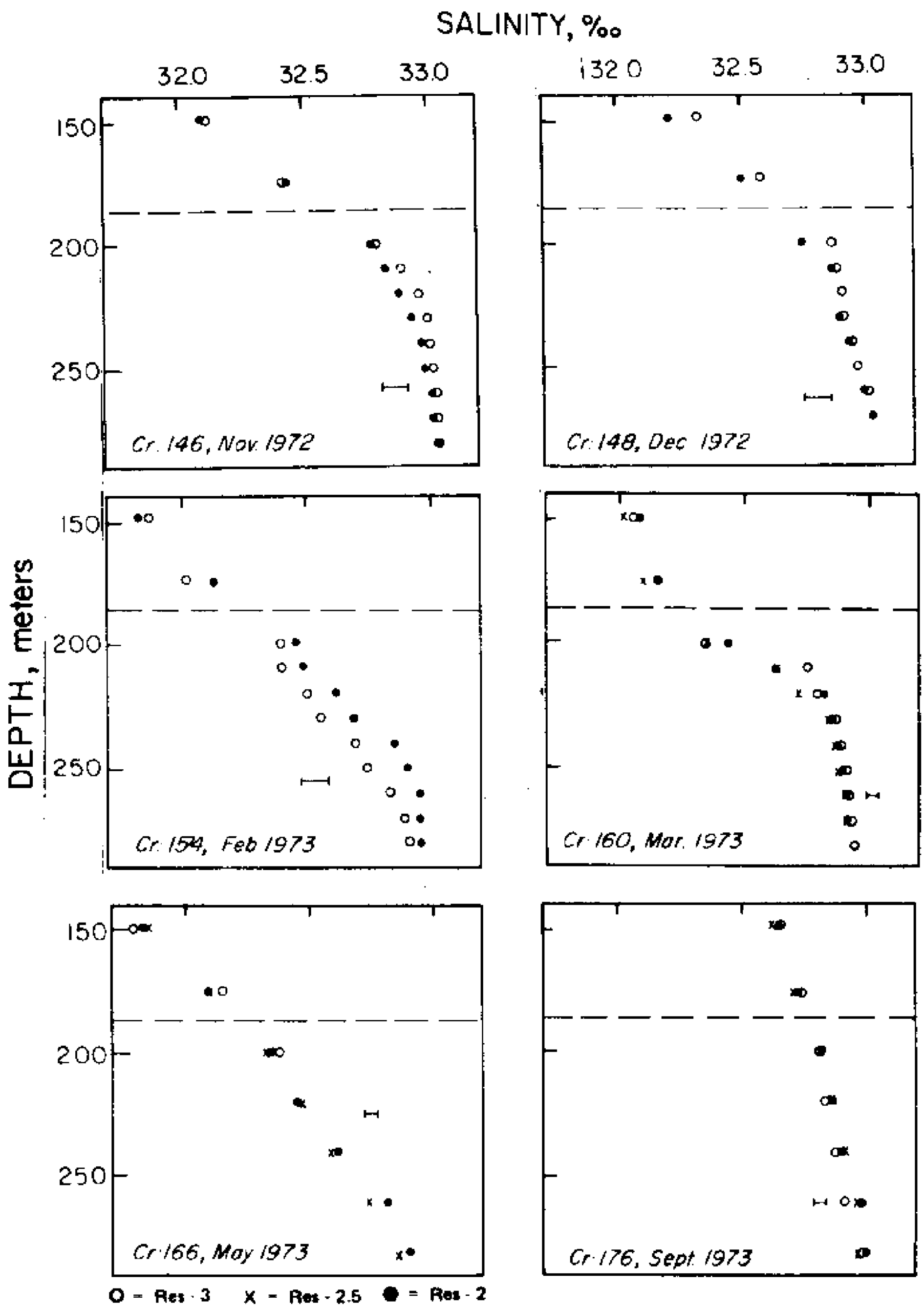

Appendix Figure 1. Vertical salinity profiles for the inner basin, November 1972 - September 1973.

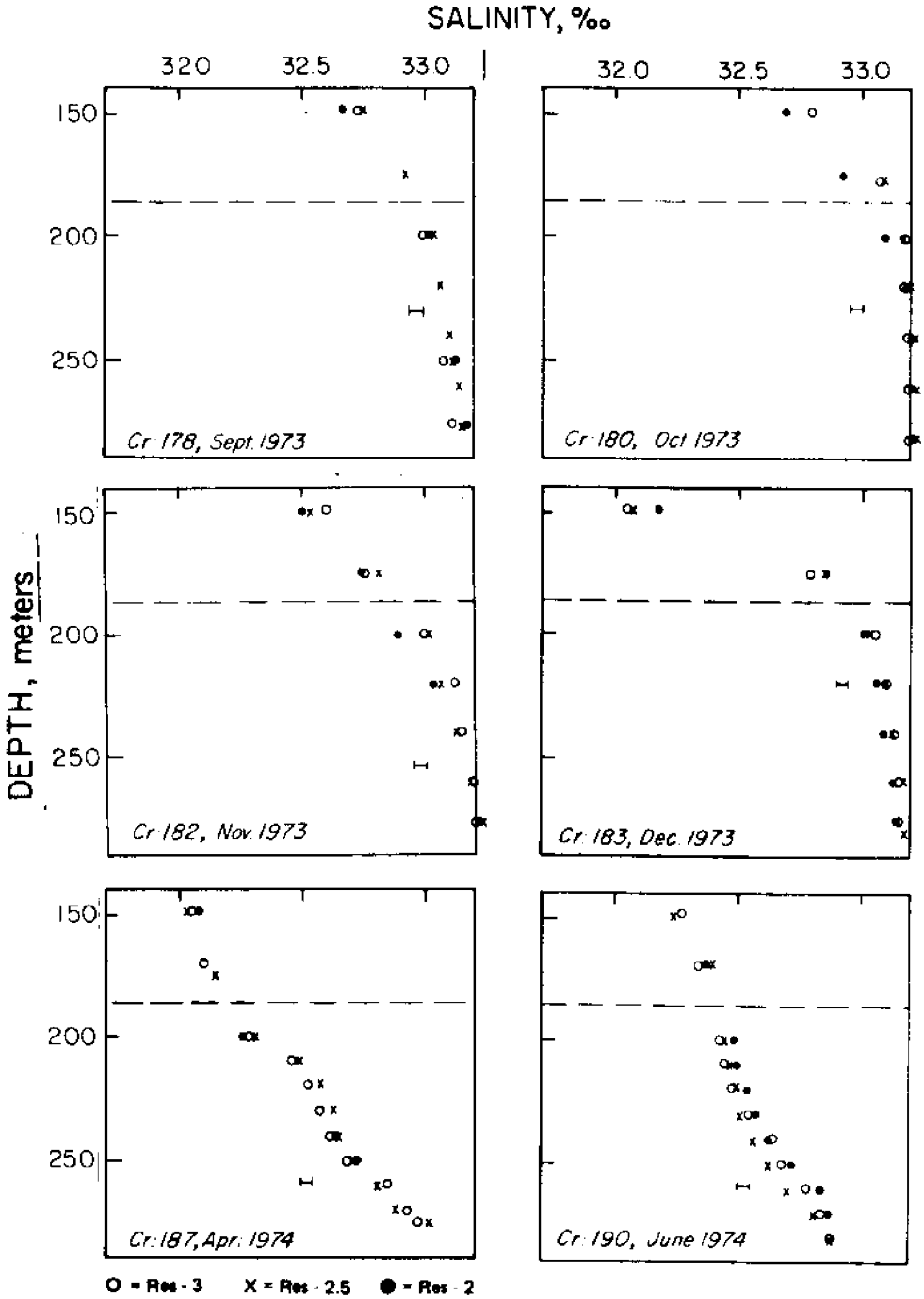

Appendix Figure 2. Vertical salinity profiles for the inner basin, September 1973 - June 1974.

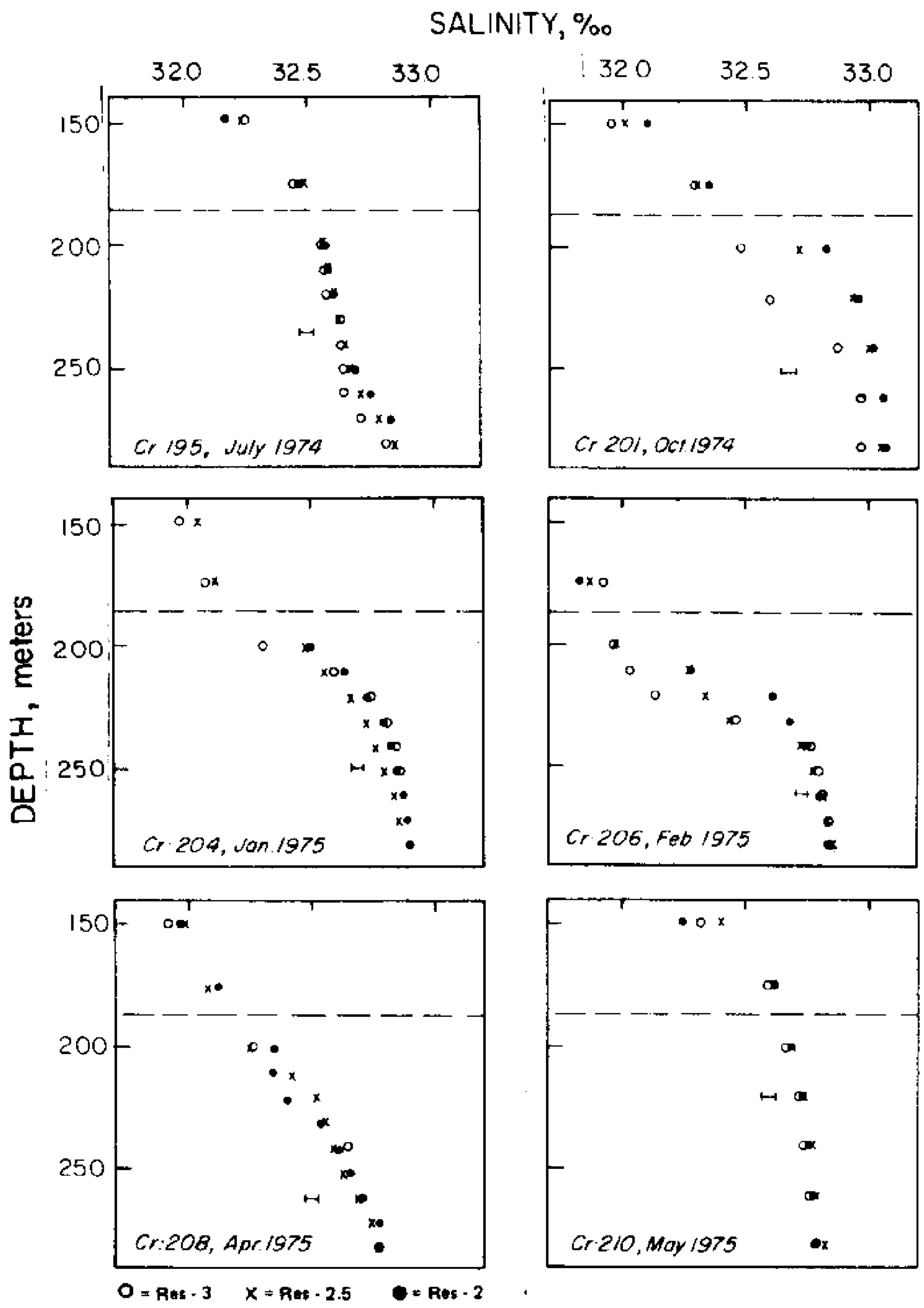

Appendix Figure 3. Vertical salinity profiles for the inner basin, July 1974 - May 1975.

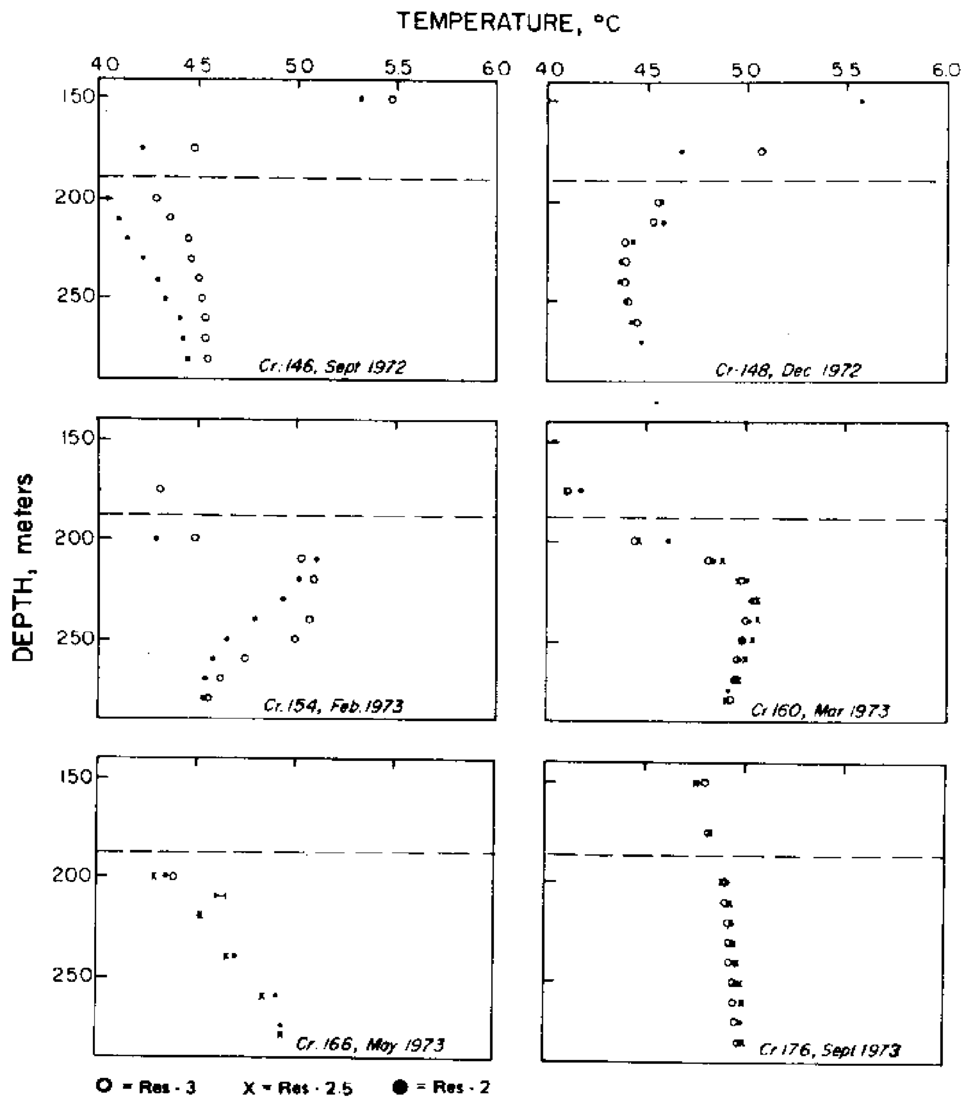

Appendix Figure 4. Vertical temperature profiles for the inner basin, September 1972 - September 1973.

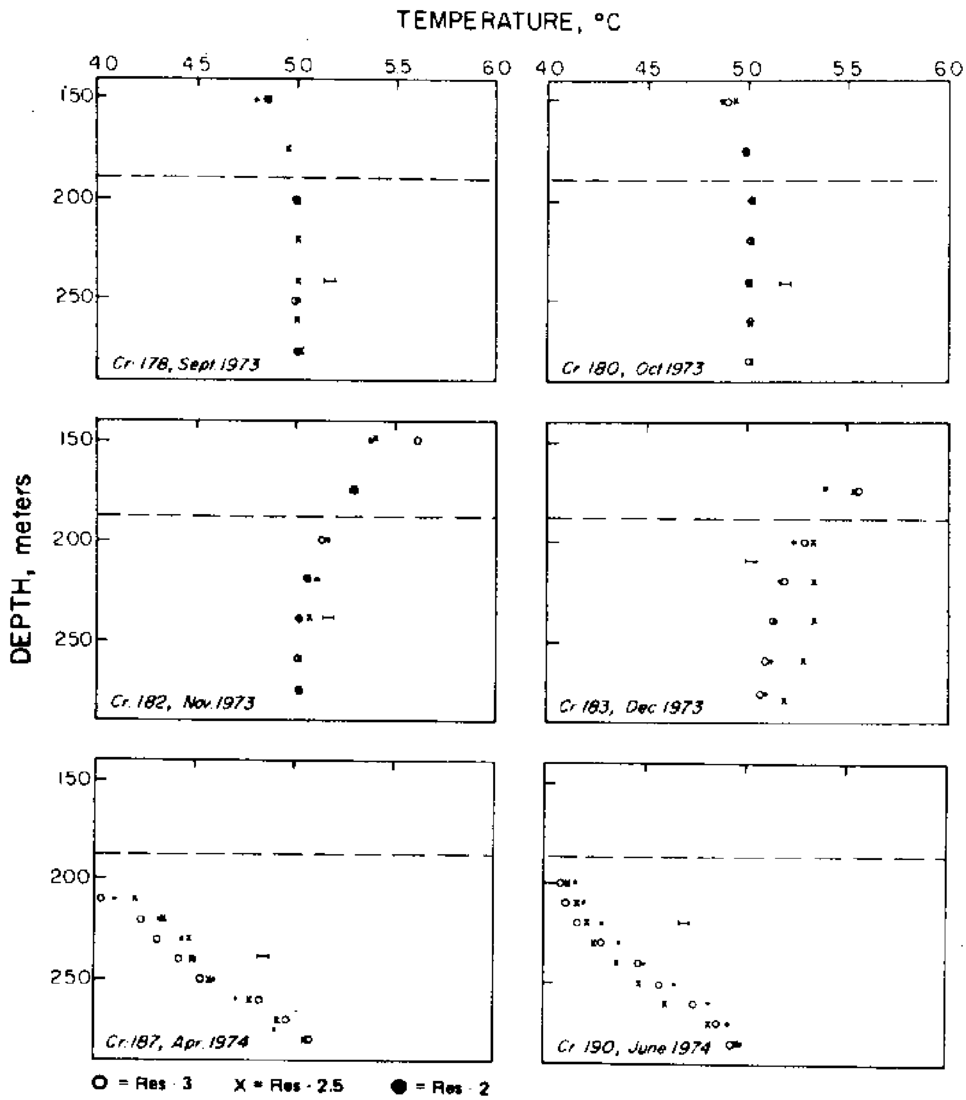

Appendix Figure 5. Vertical temperature profiles for the inner basin, September 1973 - June 1974.

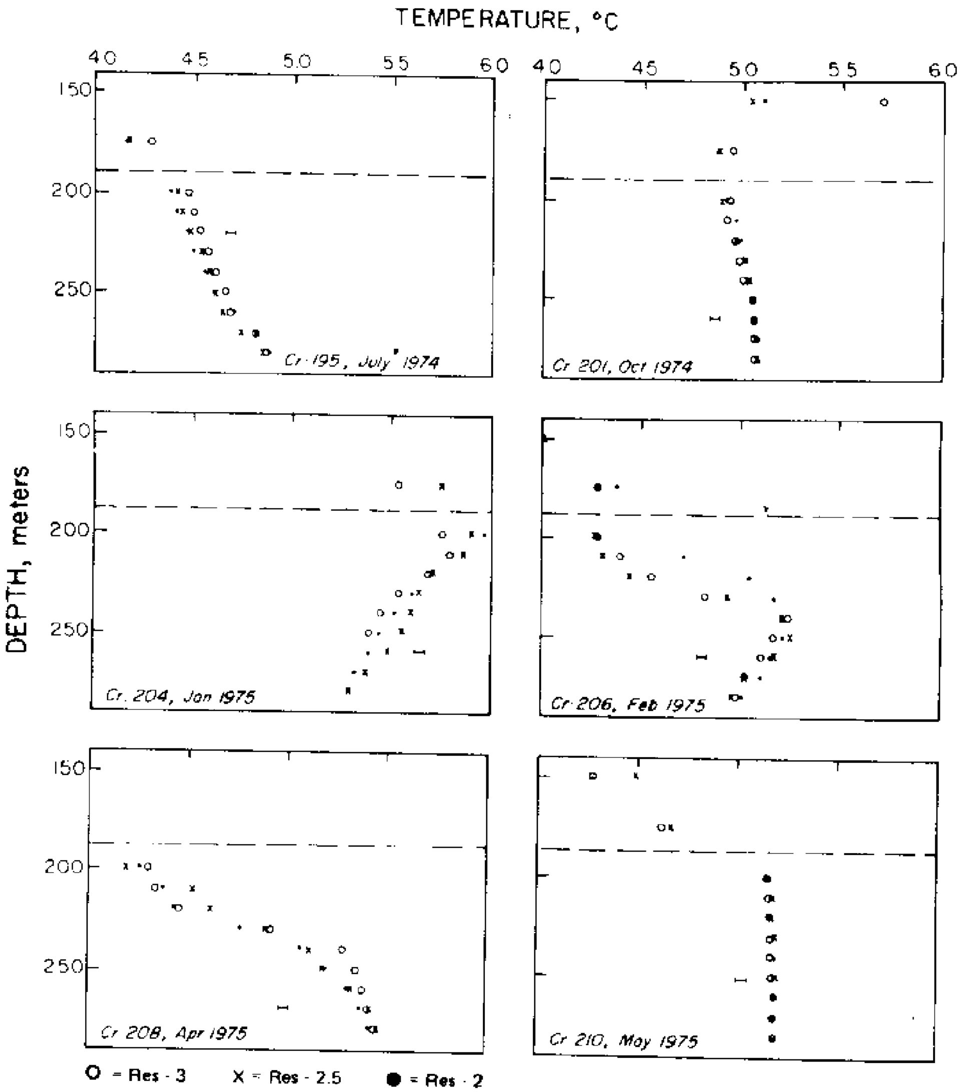

Appendix Figure 6. Vertical temperature profiles for the inner basin, July 1974 - May 1975.